KAUNAS UNIVERSITY OF TECHNOLOGY

JULIUS DENAFAS

PHOTOVOLTAIC DEVICE MANUFACTURING ENVIRONMENTAL IMPACT REDUCTION BY SILICON RECYCLING AND TECHNOLOGICAL PROCESS MODIFICATION OF INDUSTRIAL C-SI SOLAR CELLS

Doctoral dissertation

Technological Sciences, Environmental Engineering (T 004)

Kaunas, 2021

This dissertation was prepared in 2016–2020 at the Environmental Engineering Institute of Kaunas University of Technology.

Scientific supervisor:
Professor, senior researcher Dr. Jolita KRUOPIENĖ (Kaunas University of Technology, Technological Sciences, Environmental Engineering, T 004).

Website address where the dissertation is published:
http://ktu.edu

Editor: Armandas Rumšas (Publishing House "Technologija")

KAUNO TECHNOLOGIJOS UNIVERSITETAS

JULIUS DENAFAS

FOTOELEKTRINĖS ĮRANGOS GAMYBOS POVEIKIO APLINKAI MAŽINIMAS TAIKANT SILICIO PERDIRBIMĄ IR SAULĖS ELEMENTŲ PRAMONINĖS GAMYBOS PROCESŲ MODIFIKAVIMĄ

Daktaro disertacija

Technologijos mokslai, aplinkos inžinerija (T 004)

Kaunas, 2021

Disertacija buvo rengta 2016–2020 m. Kauno technologijos universiteto Aplinkos inžinerijos institute.

Mokslinis vadovas:
Prof. dr. Jolita KRUOPIENĖ, (Kauno technologijos universitetas, technologijos mokslai, aplinkos inžinerija, T 004).

Interneto svetainės, kurioje skelbiama disertacija, adresas:
http://ktu.edu

Redagavo: Armandas Rumšas (Leidykla „Technologija“)

CONTENTS

LIST OF FIGURES

LIST OF TABLES

LIST OF ABBREVIATIONS

abs – absolute
AC – alternating current
Al BSF – aluminum back surface field
AR – antireflective layer
CCZ – continuous Czochralski
Cz – Czochralski
CoO – costs of ownership
COP24 – 24th Conference of the Parties to the United Nations Framework Convention on Climate Change
DC – Direct Current
DI – deionized
DS – direct solidification
DW – diamond wire
EDS – energy dispersive X-ray spectroscopy
EG – electronic grade
EPBT – energy payback time
EoL – end of life
FBR – Fluidized Bed Reactor
GW – gigawatt
ITRPV – International Technology Roadmap for Photovoltaic
I-V – Current – Voltage
KPI – Key Performance Indicator
kWp – kilowatt peak
LBIC – light beam induced current
LCA – life cycle assessment
MG – metallurgical grade
MW – megawatt
O&M – operation and maintenance
Pcs – pieces
PECVD – Plasma Enhanced Chemical Vapor Deposition
PERC – passivated emitter and rear cell
PSG – phosphorus silicate glass
PV – photovoltaics
QSSPC – quasi steady state photoconductance
RoHS – restriction of Hazardous Substances
RSCW – recycled solar cell waste
SCW – solar cell waste
SEM – scanning electron microscope
SG – solar grade

SiNx – silicon nitride
TW – terawatt
UMG-Si – upgraded metallurgical grade silicon
XRD – X-Ray diffraction

INTRODUCTION

Motivation for the research topic

Solar energy is a great way to ensure that your power needs are satisfied at any time. It is the cleanest and most abundant renewable energy source available on our planet Earth. With the help of recent technological developments, energy coming from the sun can be harnessed for a variety of uses, including generation of electricity to provide light and power, as well as heating water for domestic, commercial, or industrial use. The photovoltaic effect which was discovered by Mr. Alexandre Edmond Becquerel in 1839 explains how such a conversion from solar to electrical energy can happen. Becquerel discovered that the conductance of electrodes and electrolytes can be increased by illumination. However, it took as long as up to 1958 when first commercial solar cells were manufactured by *Hoffman Electronics* for space applications. When the oil crisis began in 1973, interest in photovoltaic devices started to rise again; however, the real expansion of the PV industry started only in 2008.

The cumulative global photovoltaic (PV) manufacturing capacity was reported to be about 140 GW by the end of 2018 [1]. This allowed for the first time in the history of solar industry to reach 0.5 TW of installed power. It is estimated that, until the end of 2023, an additional 500–700 GW will be installed globally. Taking into account these massive figures which reflect the rapid development of the solar energy sector, there is no doubt that this industry will be playing a crucial role in achieving the targets of COP24 and Paris Agreements stating that not more than 65 g CO_2/kWh of electricity is allowed in European Union [2].

The reduction of the carbon footprint has recently become an important topic in the photovoltaic equipment manufacturing sector. Low CO_2 photovoltaic devices are becoming a unique selling point for European solar manufacturing companies, and it is also one of the ways to support and protect the European PV industry against unfair competition with the low cost Asian products. Currently, there is an action ongoing at the European Commission level which has initiated a study to prepare a policy which includes PV modules and other PV devices demanding that they meet the requirements of Eco-design, Energy labeling, EU Ecolabel and GPP directives. There is a particular focus on the device quality, durability and circularity.

The circular economy in the solar photovoltaic industry has recently become an important research topic with a particular focus on the end-of-life (EoL) phase of the PV equipment. EoL PV volumes remain relatively small; however, the treatment of PV waste is becoming a serious concern, and ways to manage the upcoming rise of the waste volume in the solar industry still has to be developed. Many research groups are focusing on finding feasible methods how to recycle and recover materials from solar panels, which is usually still not economically feasible. Moreover, the

development of recycling technologies is still immature. Thus, the ongoing researches into this topic are highly relevant. These are the main barriers in the way towards the proper recycling of solar panels and the recovery of high-purity materials.

The average lifetime of a solar module is about 25–30 years, which is the typical power degradation and product warranty given by manufacturers. As long as there is no physical damage because of a storm, vandalism or other *force majeure* situations, PV panels will continue generating electrical energy even longer. Nevertheless, a significant amount of the installed PV modules reach their end-of-life phase sooner. The reasons for that can be manufacturing defects, damage during transportation and installation, severe weather conditions, etc. It has been stated that 1,600 tons of end-of-life photovoltaic modules were collected in Europe as early as in 2016. This amount was essentially made up of waste from solar modules in such countries as Germany, Italy and France which are the largest European solar energy markets. The aforementioned amount is still small compared to a prediction that the globally accumulated volume will exceed 1 million tons by 2030, and Europe alone will contribute with approximately 600,000 tons of PV waste [3].

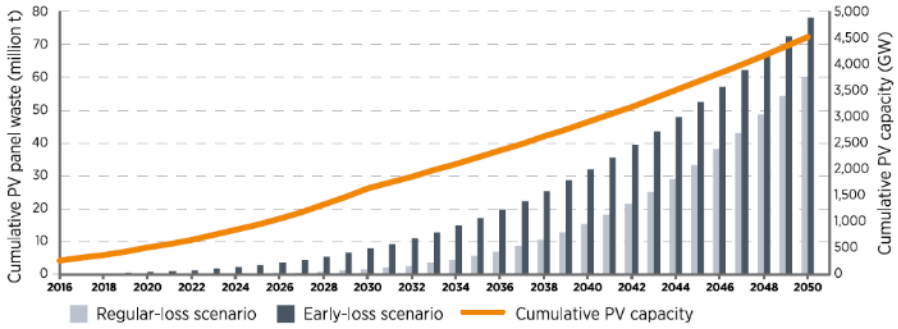

Figure 1. Photovoltaic waste generation forecast [3]

Beside end-of-life PV modules, it is highly important to consider another source of waste associated with the solar energy – waste generation during the production phase of solar cells and modules. Such a type of waste can be further divided into several groups, such as production scrap (broken silicon wafers), loss of consumables (chemicals, silver and aluminum pastes) or emissions of hazardous substances to water and air. So far, circular models have only been tested on the R&D level, but little has been done in order to adapt scientific knowledge of sustainable production and eco design thinking to mass production. All the production waste generated during the manufacturing stage simply turns into losses of the production yield, finances and negative environmental impact. A simple example can be given to illustrate this in practice. The standard capacity of a single production line in the PV sector is about 100 MW per year, which is equivalent to about 2,000,000 pcs of solar cells and

330,000 pcs of solar modules per month. If the production yield loss is around 2–2.5%, then ≈ 833 solar panels, or ≈ 50,000 pcs of solar cells, become waste every month. At today's prices, this would amount to about 30,000 Eur/month. It is worth noting that most of defective solar cells and modules are not returned back to the manufacturing processes nowadays. In other words, the typical linear economic model prevails.

The International Energy Agency presented a typical lifecycle of PV systems in its 2015 report [4]. As shown in Figure 2, there are six main phases starting from raw material acquisition and ending with the disposal stage of the end of life PV products.

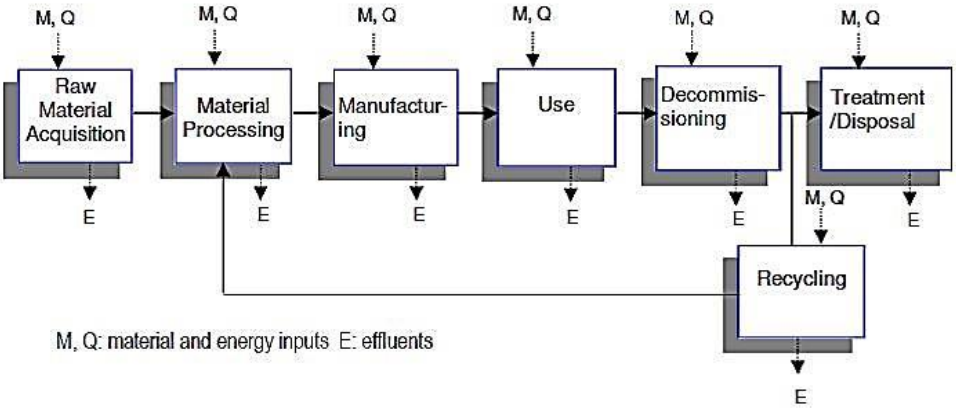

Figure 2. Lifecycle stages, flow of materials, energy and effluents of a typical photovoltaics system [4]

This thesis is focusing mainly on the manufacturing stage and proposes how environmental challenges can be tackled by implementing and testing industrial ecology principles on the mass production level of c-Si solar cells. A fully installed and operating solar power plant typically consists of several main components. These are: the PV array with solar modules, mounting systems, connectors and cables. Then, an inverter is needed which transforms DC to AC and distributes energy by feeding it to the grid or for direct use at households (Figure 3).

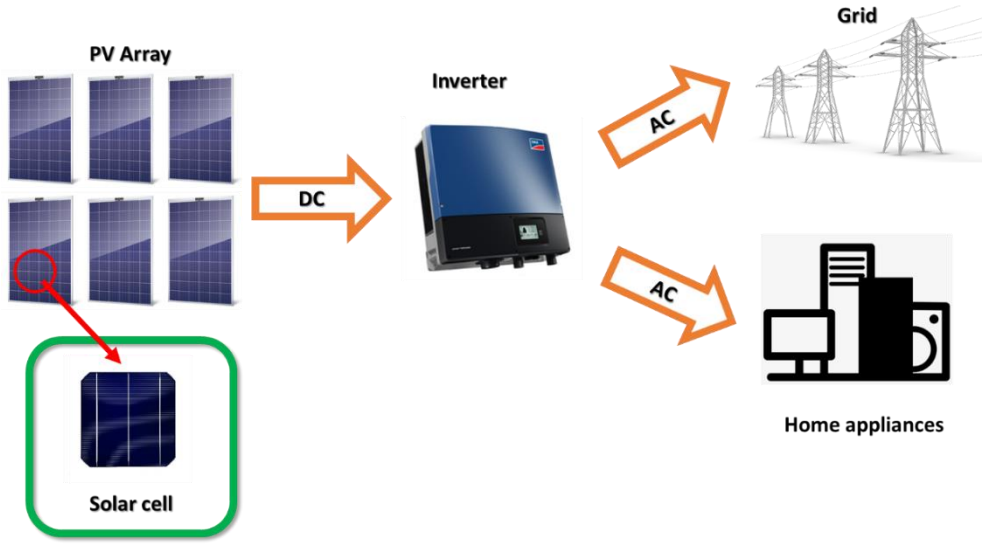

Figure 3. Schematics of a basic solar power system and its main components

However, the heart of every PV system lies inside the solar module, and it is a single solar cell. It is the main component because it is responsible for the conversion of light into electrical energy. The research of this thesis is particularly focusing on this component

In order to fulfill this goal, possibilities to recycle and reuse silicon wafers, reduce the consumption of water, chemical materials and electricity in the solar cell production were demonstrated by implementing two methods of industrial ecology:

1. Recycling and reuse – by evaluating and demonstrating recycling and re-use of silicon wafers for the production of Al-BSF mc-Si solar cells. Even though a solar module is not emitting any CO_2 during the operation phase, there is still a significant contribution coming from the manufacturing, the transportation to the installation site, and the end-of-life phases. It has been reported that a roof system which is operating in Germany is responsible for 50–67 g CO_2 eq./KWh of electricity generated [1]. The majority of this amount is the contribution of Si ingot and Si wafer [2], and therefore it is important to understand and propose methods how it can be minimized.
2. Process modification by implementing a modified technological process in order to reduce material and energy consumption, the reduction of production waste generation while at the same time ensuring that there is no negative impact on the product quality and durability. To be more specific, the emitter formation (phosphorous diffusion) process has to be modified in

the way so that it would become possible to utilize benefits of an in-situ grown SiOx layer along with the benefits of the elimination of the phosphorus silicate glass (PSG) removal step.

Aim of the research

The aim of this research was to demonstrate and evaluate the application of the innovative environmental impact reduction methods in a real manufacturing environment of multicrystalline silicon solar cells.

Objectives

I. To conduct literature review of the trends related to technological developments in manufacturing and the environmental impact reduction activities for c-Si solar cells and modules.
II. To analyze the main factors related to the environmental impact of photovoltaic devices during their lifecycle, specifically:
    a. The production stage of c-Si solar cells, and to identify processes that generate the highest negative environmental impact;
    b. End-of-life management methods of photovoltaic equipment.
III. To create and execute an experimental plan based on reviewed and selected environmental impact reduction methods so that to verify recycling, pollution reduction and technology modification possibilities in the mass production of c-Si solar cells.
IV. To evaluate the impact of the proposed options on the environment, the performance quality and manufacturing costs related KPIs of a chosen functional unit: LCA analysis and GHG emissions, energy payback time (EPBT), solar cell efficiency (%) and manufacturing costs (Eur/Wp).

Research object

A research object of this thesis is the manufacturing process of multi crystalline silicon solar cells and modules.

Key thesis

By implementing specific industrial ecology methods (silicon recycling and process modification), it is possible to reduce the environmental impact of c-Si solar cell manufacturing without any loss in the quality parameters and without any negative impact incurred on the manufacturing costs. A modified manufacturing technology can be developed and applied on the industrial level. To be more precise, a separate key thesis can be distinguished for every method:

a. Solar cell production scrap which is collected after various stages of the manufacturing process, such as incoming wafer inspection, texture and metallization, can be recycled and is suitable for reuse in c-Si solar cell mass manufacturing in a technically and economically feasible way.

b. By applying a certain phosphorous diffusion process recipe modification, it is possible to shorten the manufacturing chain of c-Si solar cells (the PSG cleaning process step can be eliminated, the PECVD process step can be shortened), thus allowing savings in the consumption of materials and electrical energy comparing to the standard mc-Si production process.

Scientific novelty

The main scientific novelty of this study is the development of a modified c-Si solar cell manufacturing technology which enables significant reduction of the environmental impact at the manufacturing stage. The new process is unique because it combines two principles of sustainable production – recycling and process modification.

Recycling of broken solar cells and recovery of materials, mainly silicon, is not a novelty by itself; however, a detailed study of quality-related issues when different grade solar cell production scrap (as-cut, partially processed, and fully processed) is involved has not been presented yet to the best of the author's knowledge.

The second innovation related to process modification is a full-scale novelty because reduction of materials consumption has been achieved by implementing the modified emitter formation process which enables in-situ oxidation of the silicon surface. This eliminates the need for the subsequent PSG cleaning step which is an important production step of c-SI solar cells. The strategy of the new diffusion process has been applied for the manufacturing of mc-Si Al-BSF solar cells, which has not been reported by any other researchers.

Practical value

Solar grade silicon material due to very energy intensive purification processes has the maximum share of cumulative energy demand in the whole value chain of PV equipment. This indicates the importance and practical value of implementing sustainable production and eco-design principles in the PV manufacturing chain with the focus on the recycling and reuse of silicon wafers. The technology which has been developed and demonstrated in this research is able to contribute to these goals because it allows PV manufacturers to bring a significant share of their production scrap back to the manufacturing process thus saving the value of materials which is otherwise lost.

A second innovation, which is dematerialization, offers good practical value since process modification allows significant material and electrical energy savings, as well as reduction of the volume of the process waste water.

It is highly important to mention that the developments presented in this research have cost advantages as well because silicon wafer is responsible for about 47% of the total cost of a solar cell. By implementing the dematerialization principle in the manufacturing chain (in-situ growth of SiOx and elimination of the PSG cleaning step), additional manufacturing cost savings are also coming from the reduction of materials and electricity consumption.

The solar cell and panel production sector is a relatively low margin business area where manufacturing companies are able to obtain only single digit margins from their products. In the PV industry, the true revenue is generated at the system level where the owners of a PV plant are able to generate income from the sales of electricity. Not all companies are fully vertically integrated; therefore, every fraction of percentage which can be saved at the manufacturing level is fundamentally important for component manufacturers in the harsh competition battle against Asian products.

To conclude, the developed technological innovations can increase the competitive advantage of the European PV industry by the reduction of the environmental impact and manufacturing costs while keeping the quality level as high as in the standard processes.

Scientific approval of the dissertation

The scientific results of the dissertation and related additional activities in the field of circular economy in the PV sector have been presented in five publications, with four of which presented in peer reviewed journals referred in the *Clarivate Analytics-Web of Science* database with the impact factor, and in two conferences (one oral presentation and one poster).

1. Sleiniute Agne, Urbelyte Liucija, **Denafas Julius**, Kosheleva Arina, Denafas Gintaras. Feasibilities for silicon recovery from solar cells waste by treatment with nitric acid. CHEMIJA. 2020. Vol. 31. No. 3. P. 137–145, ISSN 0235-7216, DOI: 10.6001/chemija.v31i3.4287

2. M.P. Bellmann, G. Stokkan, A. Ciftja, **J. Denafas**, T. Kaden. Crystallization of multicrystalline silicon from reusable silicon nitride crucibles: Material properties and solar cell efficiency. Journal of Crystal Growth, Volume 504, 2018, Pages 51-55, ISSN 0022-0248, DOI: 10.1016/j.jcrysgro.2018.09.026.

3. John A. Tsanakas, Arvid van der Heide, Tadas Radavičius, **Julius Denafas**, Elisabeth Lemaire, Ke Wang, Jef Poortmans, Eszter Voroshazi. Towards a circular supply chain for PV modules: Review of today's challenges in PV recycling, refurbishment and re-certification. Volume 28, Issue 6, Special Issue: EU PVSEC, June 2020, Pages 454-464. DOI: 10.1002/pip.3193.

4. Bendikiene, Regita; Baltusnikas, Arunas; Ciuplys, Antanas; Lukošiūtė, Irena; Juzenas, Kazimieras; Kalpokaite-Dickuviene, Regina; Sertvytis, Rolandas; **Denafas, Julius**. Utilization of industrial solar cells' scrap as the base material to form coatings // Waste and biomass valorization. Dordrecht: Springer. ISSN 1877-2641. eISSN 1877-265X. 2021, vol. 12, iss. 5, p. 2757-2767. DOI: 10.1007/s12649-020-01153-8

5. Samy Yousef, Maksym Tatariants, **Julius Denafas**, Vidas Makarevicius, Stasė-Irena Lukošiūtė, Jolita Kruopienė. Sustainable industrial technology for recovery of Al nanocrystals, Si micro-particles and Ag from solar cell wafer production waste. Solar Energy Materials and Solar Cells, Volume 191, 2019, Pages 493-501, ISSN 0927-0248, DOI: 10.1016/j.solmat.2018.12.008

Structure and content of the dissertation

The dissertation consists of the following main chapters: introduction, literature review, methodology description of technological experiments, results and conclusions.

The literature review section focuses on such areas as the operational principle of PV equipment, technological and market development trends and the implementation of environmental impact reduction methods in the PV industry.

The methodological chapter analyzes the main loss mechanisms which are manifested in solar cells, as well as the characterization and evaluation approaches which were applied in the experimental part of this thesis. In addition, it explains the purpose and implementation of all the activities related to recycling and dematerialization methods applied for the manufacturing of mc-Si solar cells.

The results section presents evaluation of how the three groups of KPIs (environmental, quality and costs) were affected by the technological experiments performed in this thesis.

Conclusions of the results and all work performed by the author are written in Chapter 4.

The dissertation is presented in 120 pages, 77 figures and 13 tables. The dissertation refers to 75 literature sources.

1. LITERATURE REVIEW

This chapter presents the trends and technological developments related to photovoltaic equipment. Firstly, an overview of the manufacturing processes and the photovoltaic market development is given. The two final sections evaluate the methods and the latest achievements of the circular economy model implementation and environmental impact reduction during the manufacturing and EOL stages of PV equipment. The political aspect and the relation to the research topic is also presented in the final sections of this chapter.

1.1 Operational principle of PV devices, analysis of various available technologies

Solar cell operation can be explained by taking a look into the fundamental mechanism of the photo current generation in semiconductor materials and the charge carrier transport across the p-n junction. This mechanism applies to all p-n semiconductor devices. Much of the theory which is applicable for solar cells these days was being worked on as early as in the middle of the 20th century (1940–1950s). As explained by L. McEvoy *et al*. [5], there are three main parameters to mention when talking about the operation of solar cells:

- Band gap
- Concentration of charge carriers available for current conduction
- Generation and recombination of charge carriers.

The band gap is the minimum energy which is needed for an electron to leave the so-called steady state and reach the free state where it participates in the current conduction. It is a property which depends on the material and, in the case of silicon solar cells, if the energy of an absorbed photon is equal or greater than the band gap of the silicon material (E_{gap} =1.12eV), then, the electron is excited from valence to the conduction band and can move across the p-n junction. In such a way, photocurrent is created which is proportional to the level of sunlight coming into the solar cell [5].

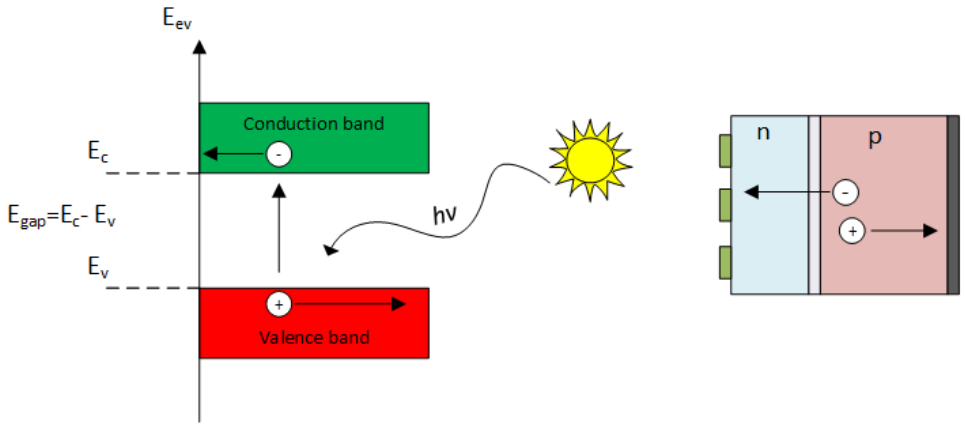

Figure 4. Explanation of a band gap, photon absorption and electron excitation from valence to the conduction band. Separation of charge carriers at the p-n junction. This image was created based on explanations given in ebook: *Solar Cells: Materials, Manufacture and Operation* [5]

As illustrated in Figure 4, a free electron is created when a photon coming from the sun is absorbed by the semiconductor material. If the photon energy is equal to the band gap energy of the semiconductor material, then its energy is absorbed and consumed to excite the valence band electrons to the conductive band thus leaving an empty space (the positive charge carrier 'hole') in the valence band. Free electrons and holes are then separated by the built-in electrical field at the p-n junction. Electrons generated in the p region move towards the p-n junction and are pushed through it towards the negative contact terminal, while holes move towards the positive electrode. This movement of charge carriers generates an electrical current which can be transmitted to the end user. Concentration of intrinsic carriers (electrons and holes) that participate in conduction depends on the semiconductor material bandgap and the temperature. It can also be tuned by changing the concentration of impurities in the semiconductor material. In the electronic industry, silicon is usually doped by adding such impurities as Ga, B or P in order to adapt the carrier concentration for device fabrication [5].

After light absorption and generation, electrical charge carriers (electrons) do not stay in the conductive band for some indefinite amount of time. Electrons eventually stabilize again into a lower energy position in the valence band. This phenomenon is called the recombination effect, and, for c-Si solar cells, there are three main recombination mechanisms: radiative, Augier and Shockley-Read-Hall. Obviously, the lower is the recombination speed, the higher efficiency of solar cells can be achieved. Recombination effects are important for the research of this thesis and, especially, for the experimental part of it [5].

A single solar cell is not able to generate enough power for the final use, and it must also be protected from such negative environmental impacts as UV radiation, moisture or mechanical stress. Due to this requirement, in practice, solar cells are

connected into strings and assembled into panels, which can later be installed in a photovoltaic system on a roof or on the ground [5].

.

1.2 Technology and manufacturing process overview

All photovoltaic equipment is currently grouped into three main generations depending on what kind of technology is used [6].

- 1st generation: crystalline silicon based solar cells and modules: mono, mono-like and multi.
- 2nd generation: thin film technology based solar modules. The most popular of them are: a-Si, CdTe, CIS and CIGS.
- 3rd generation: concentrated PV (CPV), dye-sensitized solar cells (DSSC), organic, tandem, quantum dot, up-conversion, down-conversion and other exotic and emerging PV technologies.

The global production capacity of solar cells and modules, including all the three generations, was about 200 GW at the end of 2019. The market share of crystalline silicon was about 95% of the total volume, and 5% was taken by thin film technologies as reported by S. Phillips *et al*. in *Photovoltaic Report* of *Fraunhofer ISE* [7].

IEA (International Energy Association) in its 2016 report gave a very simple, yet explanatory chart of the manufacturing chain of the 1st generation PV devices [3]. According to Figure 5, it all starts with sand, which is then turned into silicon feedstock material to be used as a raw material for silicon ingot production.

Figure 5. Production chain of silicon based photovoltaic devices (Image adapted by using information received from Soli Tek R&D)

Ingots are then sliced into wafers which are used as the raw material for the solar cell production. Once solar cells are ready, they are transported downstream towards the PV module, where solar cells are inspected, interconnected into strings and laminated under a sheet of glass and polymer encapsulant materials. PV modules are then shipped to the installer which builds a PV system. Power electronic devices, such as inverters and/or storage systems, are another part of power plants which can be of various sizes ranging from several kWs to hundreds of MWs [3].

1.2.1 Manufacturing process – from sand to silicon wafer

The value chain of photovoltaic devices starts from turning quartz sand into a metallurgical grade silicon material. Xakalashe and Tangstad reviewed this process in their publication [8]. Silicon is the second most abundant element on earth (after oxygen) and is found in the nature as quartz sand. This sand is introduced into an electric-arc furnace with carbon where the temperature reaches 2000 °C, which leads to the total energy consumption to be estimated at around 11–13 MWh per production of 1 ton of silicon material. The chemical reaction which explains the transition of sand to silicon is written as [8]:

$$SiO_2 + 2C = Si + 2CO \qquad (1)$$

Silicon in its liquid form is accumulated at the bottom of the furnace and is extracted and cooled after the process. The purity of MG grade silicon is 98–99% (≈100 ppm) with impurities, like carbon, transition metals, boron and phosphorus which are present in the composition of this material. Impurities play a vital role in the performance quality of solar cells and modules. Therefore, their concentration has to be controlled precisely. As explained further in this research, such impurities as boron or phosphorus (small amounts of it) are needed for the formation of the p-n junction, but other types of elements can reduce the efficiency of solar cells dramatically by inducing material defects and recombination centers in the structure of the solar cells. Therefore, further refining of MG silicon is an important next step in the value chain of c-Si PV devices [8].

A very detailed overview of the silicon feedstock preparation and ingot growth technologies is given by M. Green [9]. Solar grade (SG) silicon material is produced from lower quality metallurgical grade (MG) polysilicon by Siemens or FBR (fluidized bed reactor) processes. The Siemens process was initially developed to produce electronic grade polysilicon (EG Si) which has the purity of at least 99.9999999%, or 9N. This is the purity level needed in the micro-electronics industry, although the requirements in the solar PV industry may be less demanding [6]. The most widely used (over 90%) and market dominant technology for polysilicon purification is the Siemens process.

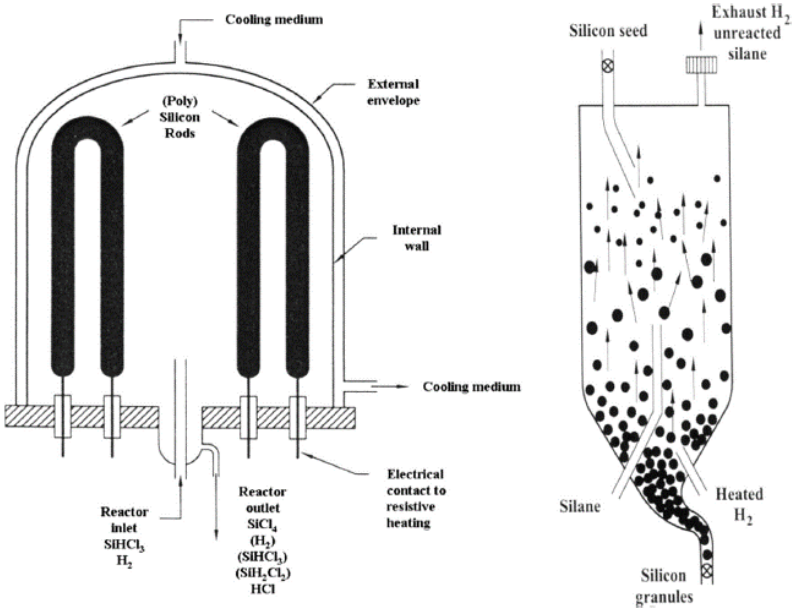

Figure 6. Comparison of Siemens (Left) and FBR (right) processes for polysilicon purification [10]

As shown in Figure 6, the process occurs inside a bell-shaped thermal chemical vapor deposition (CVD) reactor containing heated silicon seed rods in the reactive gas atmosphere. The reactive gas, which is highly pure trichlorosilane (TCS), is vaporized and introduced in the reactor. The gas is decomposed onto the surface of electrically heated (typically, 1100–1150 °C) silicon seed rods thus building large rods of high purity silicon according to the main equilibrium equations [10] as given below:

$$2SiHCl_3 = SiH_2Cl_2 + SiCl_4 \quad (2)$$

$$SiH_2Cl_2 = Si + 2HCl \quad (3)$$

$$SiHCl_3 + H_2 = Si + 3HCL \quad (4)$$

$$SiHCl_3 + HCl = SiCl_4 + H_2 \quad (5)$$

The initial diameter of the seed rods is less than 1 cm, and the deposition process runs until the rods' diameters are in the range of 13–20 cm. Recent technological developments allow having 36–48 inverted U rods fitting into the industrial reactors with the annual capacity between 450–600 t and with energy consumption being 50 kWh/kg of polysilicon [10].

Less than 10% of polysilicon is produced by the alternative fluidized bed reactor (FBR) using silane as the feed-gas. FBR offers a strong reduction of energy consumption comparing to the Siemens technology; therefore, it has the potential to reduce significantly the environmental impact on the polysilicon production level. During the FBR process, seeds in the form of fine particles are fed from the top, while silane and hydrogen are introduced near the bottom of the reactor. Chemical vapor deposition is responsible for the growth of particles. The process runs in such a way that it is necessary to have a constant and continuous flow of seeds and likewise to remove the largest particles ('beads') so that to compensate for the growth. A simple equation explains the formation of Si in a FBR reactor where hydrogen is the only byproduct:

$$SiH_4 = Si + 2H_2 \qquad (6)$$

The currently used industrial FBR reactors have a 1,000 t annual capacity, and the typical energy consumption is as low as 5–10 kW h/kg of polysilicon [10].

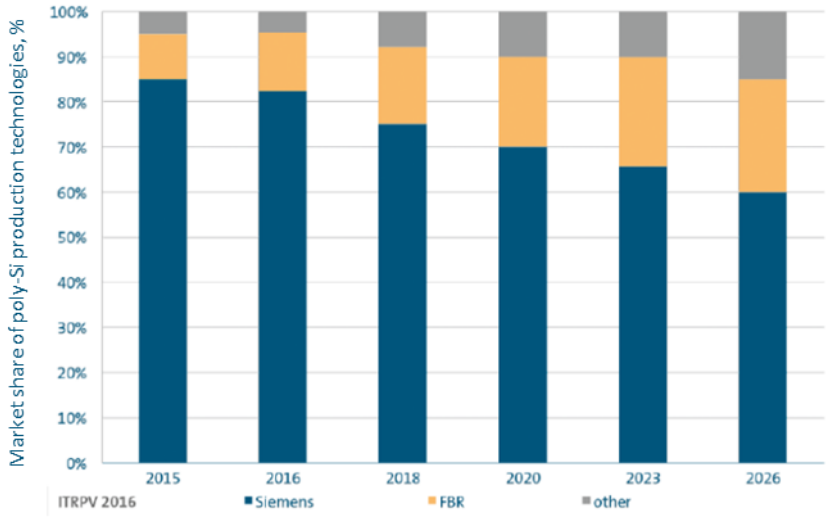

Figure 7. Estimation of poly-Si production technologies distribution for the period of 2015–2026 [11]

A forecast given by the ITRPV report (Figure 7) tells that the market share of the Siemens process will decline from 85% down to 60% until 2026, while the share of the FBR technology is likely to increase from around 10% in 2015 up to 25%. Such a change is expected to happen due to the upcoming investments in the industry which will be dedicated to the low cash cost and more environmentally-friendly technologies. Other – UMG-Si and epitaxial growth – technologies will be available

in the market, but are not yet expected to provide significant cost advantages; therefore, no market share increase is foreseen for them [11].

The next step in the production chain of PV components is the conversion of the feedstock material into single (sc-Si) or multi crystalline (mc-Si) ingots. The ingot in other words is a block of silicon which is later sliced into thin wafer substrates. As shown by ITRPV 2020 report [12], the weights of multi and mono silicon ingots are about 400 kg for mono and 800 kg for multi crystalline silicon ingots. Future trends are that the weight of Cz ingots will approach the 600 kg value, while multi is expected to grow up to 1600 kg/ingot before 2031. The higher weight trend stems from the fact that manufacturing companies are trying to increase the production capacity which is directly linked to lowering the costs and the usage of resources in the manufacturing of silicon substrates.

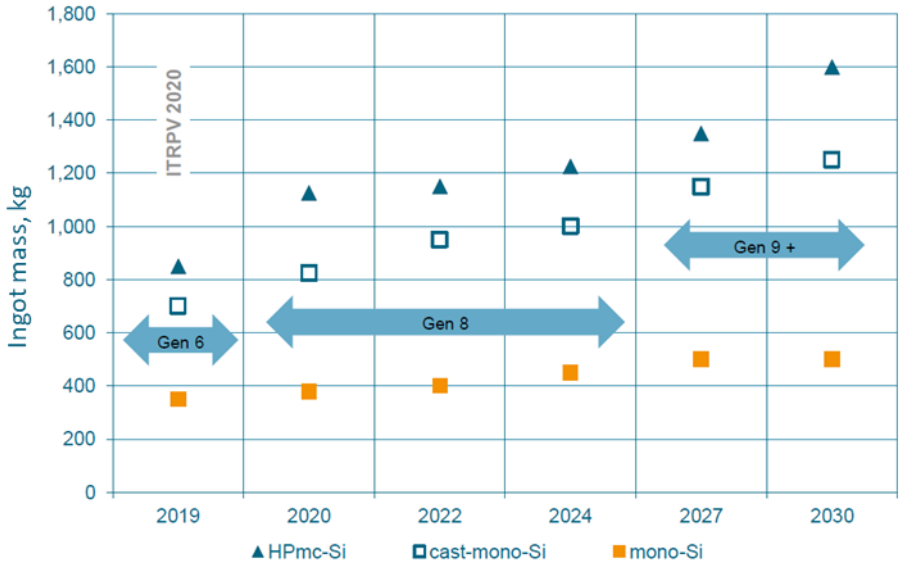

Figure 8. Trends of mc-Si and mono-Si ingot mass development [12]

There are two main methods used industrially for single crystal ingot growth: Czochralski (Cz) and Continuous Czochralski (CCz) processes. As reported by ITRPV, the standard Cz method is dominating the market these days and is predicted to be the main technology for the next 10 years. Despite the fact that the share of the CCZ technology remains below 20%, it will drive the trend of ingot mass growth from 200 kg to more than 400 kg. A very informative comparison between the two processes was given by H. Seigneur *et al*. [13] where the differences between Cz and

CCz are explained. The main difference from the traditional CZ is the continuous supply of fresh polysilicon and dopant during the growth process, which results in the long-body crystals with uniform resistivity and an increased productivity. Nevertheless, the CCz technique has some limitations which are worth mentioning. To name a few, these are the process complexity, the longer run time, the need for good purity feedstock, and the low lifetime of quartz crucibles (a limit of 2 pulls).

Multicrystalline ingots are typically produced by the direct solidification (DS) process. As given by H. Seigneur *et al*. [13], the Bridgman DS method is primarily used for the production of multi-Si material and is widely adopted by the PV industry. The main advantages of the DS process are the low costs and the relatively simple process technology. In contrast to the Cz type ingot, multi-Si material has typical defects which reduce its quality: dislocations and grain boundaries. Depending on the size of the grain boundaries, multi-Si material is sorted into the so-called 'standard' and 'high performance' categories. As given by [14], HP (High Performance) multi-Si ingots and wafers with a small grain size exhibit a much lower dislocation density compared to the normal multi-Si ingot, which leads to significantly (up to 0.3–0.5% abs) higher cell efficiencies. Fused silica based crucibles are typically used for multi ingot production. Because of the high price and only single use possibilities, these crucibles contribute with up to 30% of the conversion costs from silicon-feedstock to the as-grown ingot. To solve these problems, some initiatives have already started within the frame of the H2020 Eco-Solar project where a new material – silicon nitride – was introduced for the manufacturing of crucibles, and multi-use for ingot casting has been successfully demonstrated [15].

When talking about the wafering process, two dominant technologies have to be mentioned: slurry and diamond wire saw cutting. Slurry based wafer sawing has been the dominant technology for poly type ingots for many years, but recent material and technological developments have changed the status quo, and the diamond wire cutting process has been the mainstream for mono already since 2016, whereas, for poly, the same trend can be observed (Figure 9) [16].

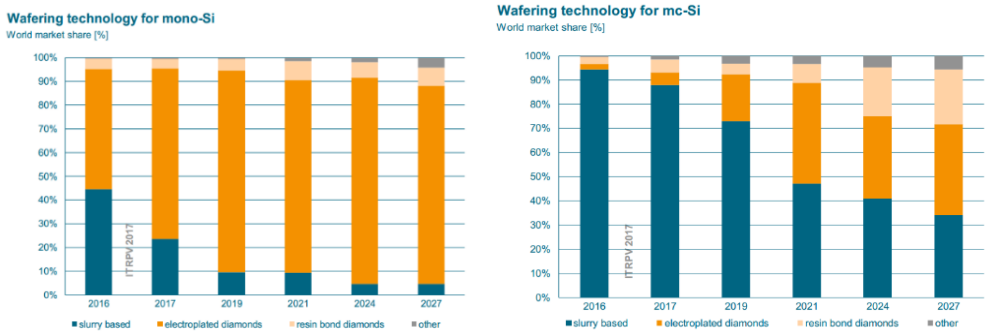

Figure 9. Market share of wafering technologies for mono and poly silicon ingots [16]

The key differences between the slurry and diamond cut technologies are that the first one relies on sawing induced by moving steel wires and a slurry consisting of loose abrasive particles (SiC) and a carrier fluid (polyethylene glycol or oil).

Meanwhile, the second strategy relies on diamond particles fixed on the wire by the electroplating method (Figure 10).

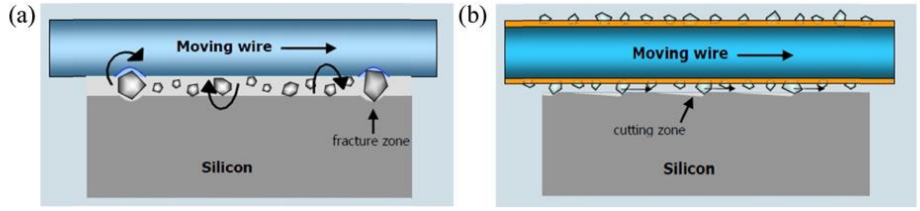

Figure 10. Schematics of the cutting mechanisms: slurry sawing (a) and diamond wire sawing (b) [17]

The environmental impact comparison for these two wafering processes has been reported by some authors where the advantages of the DW technology were clearly described. To name a few, these are: higher material removal rate, higher quality wafers with fewer crack defects, the reduction of the kerf loss and the use of less toxic cutting fluids [18].

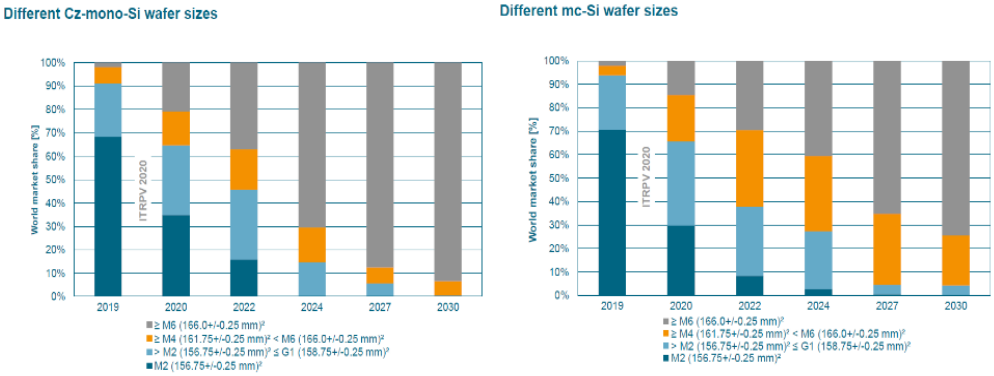

Figure 11. Trends of mc-Si and Cz-mono-Si wafer sizes [12]

As shown in Figure 11, the thickness range for as-cut silicon wafer is between 180–200 µm for poly and 160–170 um for mono. It is predicted that mono wafers will reduce the thickness faster than multi and will reach the 150 um range already in 2021 [16]. Another important aspect to mention about silicon wafers is the trends of the new dimensions formats. Since 2019, the wafer and ingot manufacturing industry has invested a lot into the upgrade of equipment, which translates into increasing the wafer size. The increasing ingot diameters allow this industrial shift towards larger wafer formats. In addition, full square-shaped wafers have started to increase their market share due to this technological trend initiated by major wafer manufacturing companies [12].

From the environmental point of view, it is very important to mention that both wafering steps generate huge silicon material losses (called silicon kerf) which can

reach even up to 40% of the total ingot mass as reported by [19]. Despite the fact that this problem is not yet solved on the industrial level, researchers are looking into ways to reuse silicon kerf for the production of new silicon feedstock and ingots or to find a place for this type of material to be used in other industries As an example, there are efforts reported to investigate the potential of using it as an anode material for Li-Ion batteries [20]. Kerfless wafer production technologies is another option to avoid the loss of silicon during manufacturing, and small scale production of such substrates has already reached the industrial production level [21].

1.2.2 Manufacturing processes – from silicon wafer to solar module

The oldest and still one of the most common c-Si cell types in the industry is the Al-BSF (aluminum back surface field) cell structure. It was first presented by COMSAT in 1974 [22]. The highest average efficiencies achieved on the BSF cell structure in the industrial production are up to 19% for p type multi, and about 20% for p-type mono. Because of the high pressure from the market to reduce the costs and improve the efficiency, the BSF structure was used as a base for further developments of higher efficiency c-Si solar cells. The BSF cells structure is limited for higher efficiencies because of the high rear side recombination. In order to overcome this problem, a solar cell with rear side passivation was developed and originally presented by M. Green in 1983 [22].

However, it took as long as until 2012, when the PERC process was introduced into industrial production, and, starting from 2015/2016, PERC-based solar cells started to gain the larger portion of the market share.

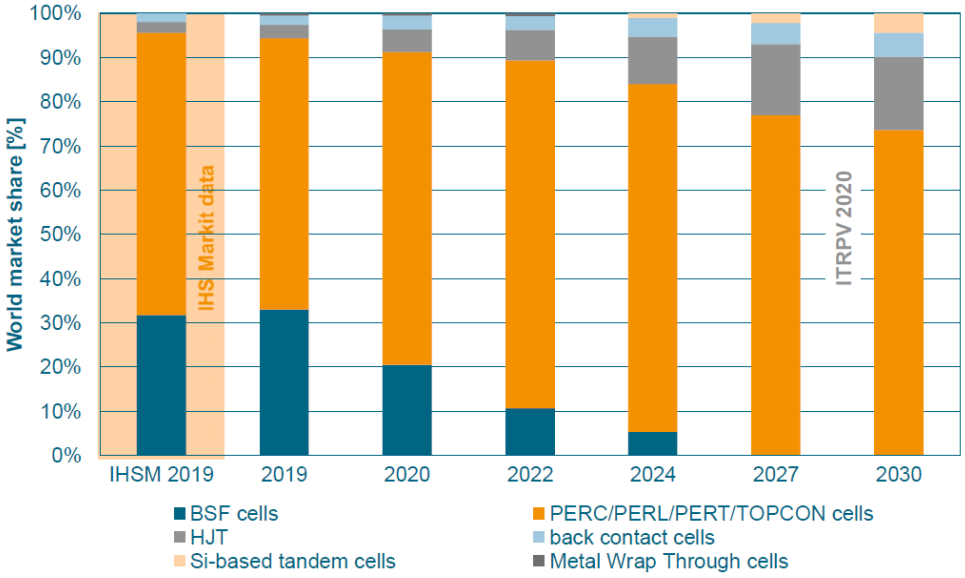

Figure 12. Market share of different c-Si solar cell technologies [12]

According to the ITRPV roadmap (Figure 12), the two dominant industrial solar cell technologies PERC and BSF are covering together more than 70% of the global market. It has been predicted that cell structures with rear side passivation, such as PERC/PERT/PERL, will continue to take over more market share and will become the mainstream during the next 5 to 7 years, while BSF cell structures are expected to be phased out completely. Furthermore, it is expected that the share of the two side light sensitive solar cell structures (bifacial) will continue to increase and will reach 30% by 2027 [12].

An overview of the manufacturing process flow for both Al-BSF and PERC type solar cells was described by J. Denafas *et al*. [23]. The two processing technologies are very similar, but PERC cells need additional rear side polishing, coating and local laser opening processes. The contact formation is also different because, for PERC type solar cells, modified Al and Ag pastes are needed. The average solar efficiencies of different cell technologies in mass production were reported in the latest edition of the ITRPV roadmap in Figure 13 [12].

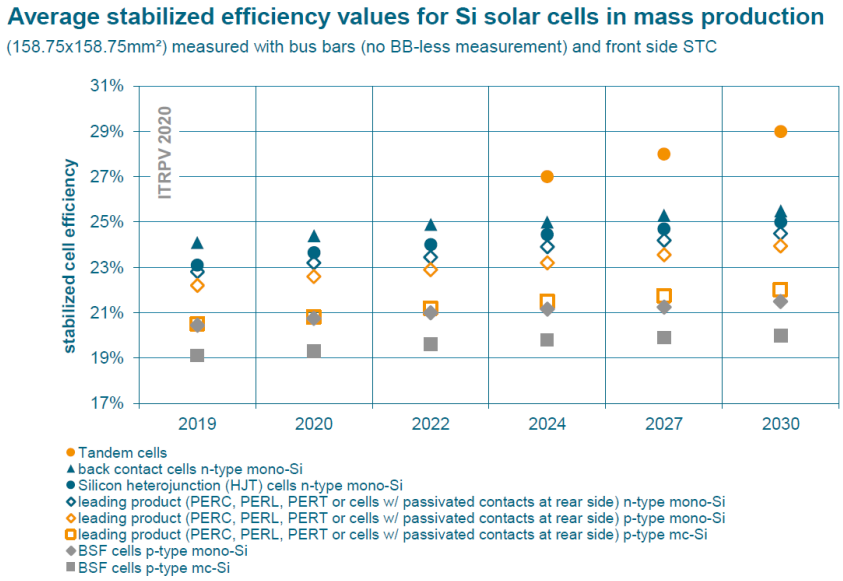

Figure 13. Average cell efficiency trends for different types of solar cell structures [12]

For this research, only the Al-BSF solar cell technology was further analyzed according to the process sequence description in Figure 14. Other types of cell technological processes are excluded since it is not relevant for the experimental work carried out in this thesis.

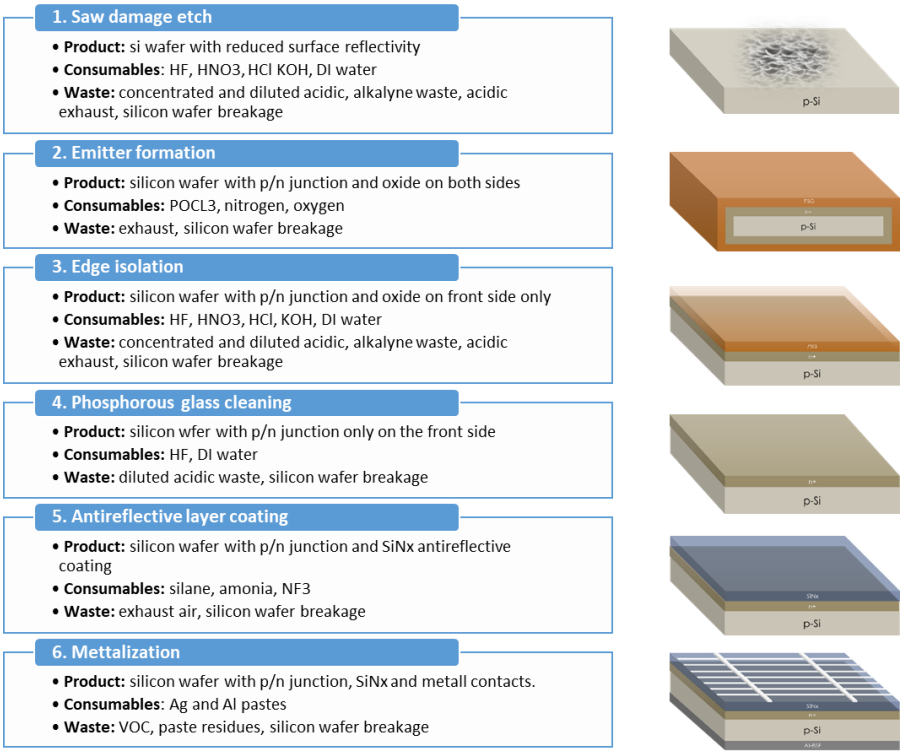

Figure 14. Process steps of Al-BSF solar cell production and corresponding solar cell structures (products). (This image was created based on the information provided by *Soli Tek R&D*)

The surface of as-cut wafers contains physical damage and organic/inorganic contaminants which are left after the sawing step. If not cleaned and removed, such a wafer surface will lead to low cell efficiencies and to the increased wafer breakage during the cell manufacturing process. Alkaline texturing has been widely used as a standard process for monocrystalline silicon wafers. It typically requires an alkaline etchant like KOH. A random pyramid surface is created because of the anisotropic etching process which has a much faster etching rate along the specific crystalline structure planes and allows exposing crystal planes which have much slower etching rates. The surface after etching looks different on the mc-Si material due to its random crystal orientation. For it, the isotropic etching process is needed in order to provide homogenous etching over the whole wafer surface. An etchant solution of nitric acid (HNO_3) and hydrofluoric acid (HF) is typically used. The complete process for the isotropic etching process can be written by using chemical reaction equation [24]:

$$3Si + 4HNO_3 + 18HF \rightarrow 3H_2SiF_6 + 4NO + 8H_2O \quad (7)$$

which can be split into partial equations for better explanation:

a) Oxidation: $3Si + 4HNO_3 \rightarrow 3SiO_2 + 4NO + 2H_2O$ (8)
b) Oxide dissolution: $SiO_2 + 4HF \rightarrow SiF_4 + 2H_2O$ (9)
c) Water soluble complex: $SiF_4 + 2HF \rightarrow H_2SiF_6$F6 (10)

The texturing process is controlled mainly by three steps:

- Control of the etching depth by adjusting the bath concentration, time and temperature;
- Process quality control by measuring the weight and reflectance of the silicon wafer surface.

It is important to note that formation of not only NO, but also of NO_2, N_2O, etc. (NO_x) occurs during this process step because oxidation is a very intense exothermal reaction. KOH is used for cleaning the porous surface layer after the etching process, and HF/HCL treatment is needed for the pre-diffusion cleaning of metallic impurities from the wafer surface. The saw damage etching and isotexture process also generates chemical waste which can be divided in two categories: concentrated and diluted. Concentrated acidic waste is collected after the process and treated in an external dedicated waste treatment center. Meanwhile, the diluted type of waste is collected and cleaned in internal waste treatment facilities.

Emitter formation is usually the 2nd production step in the standard c-Si solar cell process technology, such as Al-BSF or PERC. The emitter is a region formed in the upper part (the front surface) of a solar cell and is usually marked as the n+ layer, which means that it is doped with atoms having an extra free electron as shown in Figure 15.

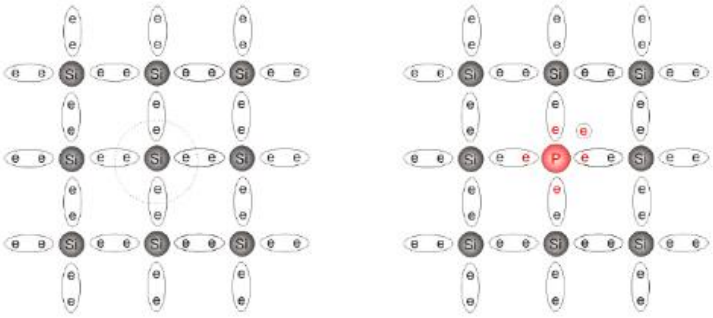

Figure 15. Illustration of doping a silicon material with phosphorus, an element having an extra free electron (This image was created based on the information provided by *Soli Tek R&D*)

Phosphorus diffusion is one of the key processes related to the experimental part of this research; therefore, slightly deeper analysis of the emitter formation principle is given comparing to all other processes which can be explained with the following chemical equations [25]:

$$4\,POCl_3 + 3O_2 \rightarrow 2P_2O_5 + 6Cl_2 \quad (11)$$

$$2P_2O_5 + 5Si \rightarrow 4P + 5SiO_2 \quad (12)$$

First, evaporation of liquid $POCL_3$ and transport via carrier gas into Quartz tube furnace takes part. During the deposition step, $POCL_3$ reacts with oxygen, thus forming P_2O_5 and chlorine gas. Then, the temperature is raised above 800 °C in order to initiate a drive in the mechanism. In this step, P_2O_5 acts as an unlimited dopant source and allows enough phosphorus to diffuse into silicon up to about 400–500 nm deep. In parallel, a phosphorus-rich silicon oxide layer is formed on the wafer surface. The whole process and the principle of the equipment – a low pressure quartz tube furnace – is shown in Figure 16. A dopant source ($POCL_3$) and process gasses (oxygen and nitrogen) are supplied into a quartz tube filled with textured silicon wafers. In the standard industrial diffusion equipment, one tube can process from 500 to 1,000 wafers per one load. The diffusion process depends on several main parameters, specifically, the duration, temperature, the $POCL_3$-N_2 and oxygen gas flow.

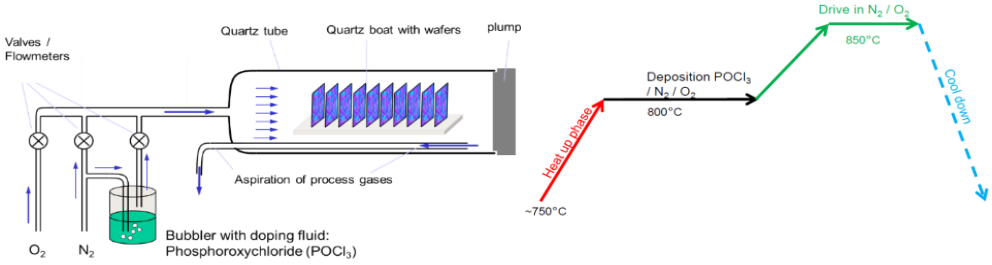

Figure 16. Structure of the phosphorous diffusion furnace (left) and the process sequence (right) [The image was provided by Soli Tek R&D]

All these parameters control the growth of the highly doped phosphosilicate glass (PSG) layer acting as a dopant source during the diffusion process. When forming a homogeneous emitter during the $POCL_3$ diffusion process, it is important to find the perfect balance between low emitter recombination, low contact resistance,

and high lateral conductivity. Phosphorus is the most common choice as a doping material, and such a type of emitters can be formed by several different process techniques, as reported by the ITRPV 2018 report in Figure 17 [12].

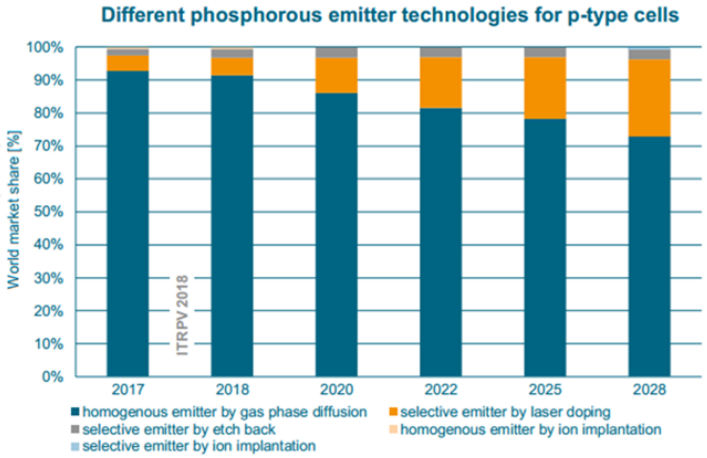

Figure 17. Overview of the emitter formation processes and trends [12]

Gas phase diffusion, or the commonly called $POCL_3$ diffusion, has been and will continue to be the dominating technology to form the n+ layers in the solar cell manufacturing process. In combination with this step, the selective emitter by laser doping is also expected to gain a significant part of the market share. The N type emitter region together with the intrinsically doped p type wafer bulk forms the p-n junction in a solar cell [12].

The schematic mechanisms of this process are shown in Figure 18. As a result of the n and p type regions being in contact, excess electrons from the n-type layer diffuse to the p-type side, and excess holes from the p-type region diffuse to the n-type side. Because of this movement, positive ions are exposed on the n type side, and negative ions are exposed on the p type region, which results in the buildup of an electrical field inside the silicon wafer, and also a depletion region.

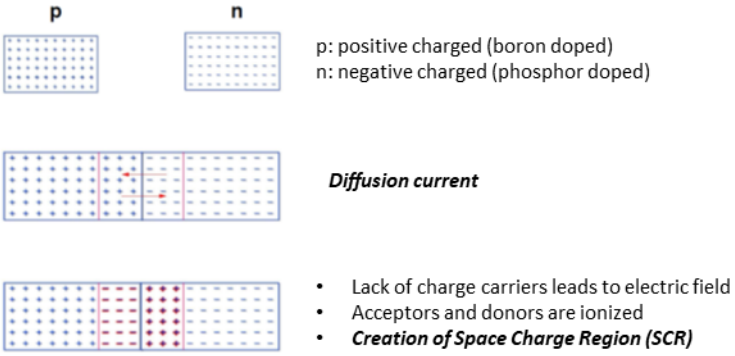

Figure 18. Explanation of the emitter formation process and the creation of electrical field inside a solar cell. (The image was provided by *Soli Tek R&D*)

Another function of the n type region is to ensure good passivation of material defects and to make sure that there is enough concentration of electrically active phosphorus atoms in order to provide low contact resistance properties for the formation of metal contacts. The so-called 'back to back' loading position of wafers is needed in order to have the n type doping material diffused only on the front side of wafer. However, this still does not prevent completely from the diffusion on the edges and on the rear side. For the normal solar cell operation, an n type region is needed only on the front side, therefore, doping on the unnecessary areas has to be removed. As reported by Kristopher O. Davis *et al*. [25], there are a few techniques to perform edge isolation, with chemical etching being the most applicable in the industry today. Other edge isolation methods mentioned in literature are based on plasma and laser processes.

During the diffusion process, a PSG layer is formed on the silicon wafer surface. It is not useful for the solar cell because it acts as a recombination center; therefore, it has to be removed. The PSG cleaning process is achieved by using a diluted HF solution. This process is relatively simple to control since only the oxide layer is etched selectively, and the reaction slows down when the underneath layers are exposed [25]. The typical thickness of the PSG layer is about 30–50 nm. After the removal, the wafer surface becomes hydrophobic, which enhances the adhesion of the antireflective layer.

The next step of the Al-BSF cell manufacturing is the front side antireflective layer coating. Various dielectric films are used, but hydrogenated amorphous silicon nitride (a-SiNx:H or SiNx) is primarily used by the industry. It is deposited by the PECVD process which uses silane and ammonia gasses as process consumables. The typical thickness of this layer is about 80 nm, and the refractive index is about 2.1. The SiNx layer has two functions in order to improve the performance of a solar cell: the reduction of light reflection, the passivation by the hydrogenation of dangling

bonds, and the field effect created by the fixed positive charge carriers at the interface of the semiconductor/dielectric materials [25].

The refractive index can be easily tuned by changing the ratio of gases in the process chamber. The process control is performed by using a laser ellipsometer and light reflection measurements.

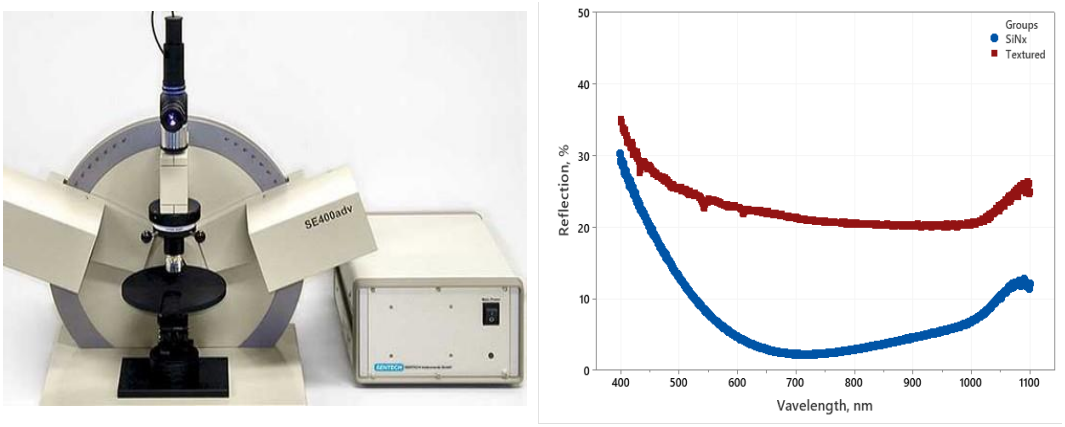

Figure 19. Left – SiNx deposition process control: *Sentech SE400* advanced ellipsometer for thickness and refractive index measurements [73]. Right – light reflection measurements for the optimization of minimum surface reflectivity

The final solar cell manufacturing step is contact formation by the screen printing and fast firing processes. The purpose of screen printing is to deposit metal pastes on the front and the rear sides of a solar cell. These pastes are later cured in a firing oven, and metal contacts are formed which are essential for the performance of a solar cell by acting as a path to extract light generated electrons out of the device [25]. For the Al-BSF type solar cell, the H-pattern contact layout is used (Figure 20).

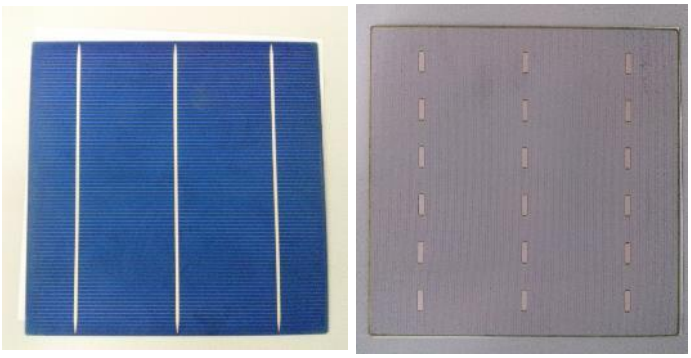

Figure 20. 3BB contact pattern of Al-BSF solar cell. Left – front side view, right – back side view of a solar cell (image taken by the author)

Cell designs with more bus bars (from 5 to 12 and more) allow for higher module power outputs and are also typically used in the industry these days.

During the contact formation step, the organic components of the metal pastes are burned out first. Then, during firing at the 850–880 °C peak temperature range, the pastes are etched through the SiNx antireflective layer thus allowing to directly contact the n type emitter region. On the rear side of the solar cell, an Al-Si eutective layer is formed which is highly p^+ doped by Al atoms and acts as a back surface field. The metallization process step is controlled by optical and electrical measurements which ensure the good printing quality of the contact lines thus ensuring that there are no interruptions and/or any other printing defects, while electrical measurements ensure low contact and line resistivity of the silver and aluminum contacts. These parameters are extracted from the I-V (current and voltage) testing step which is performed at the very end of the solar cell manufacturing process [25].

Solar cells are inspected by using special testing equipment – a solar simulator. Measurements have to be performed at the standard test conditions (STC) which correspond to: solar spectral irradiance Air Mass 1.5 at intensity 1000 W/m^2 and ambient temperature of 25 °C. IEC 61215 and 61646 standards describe precisely the testing conditions of photovoltaic devices [25].

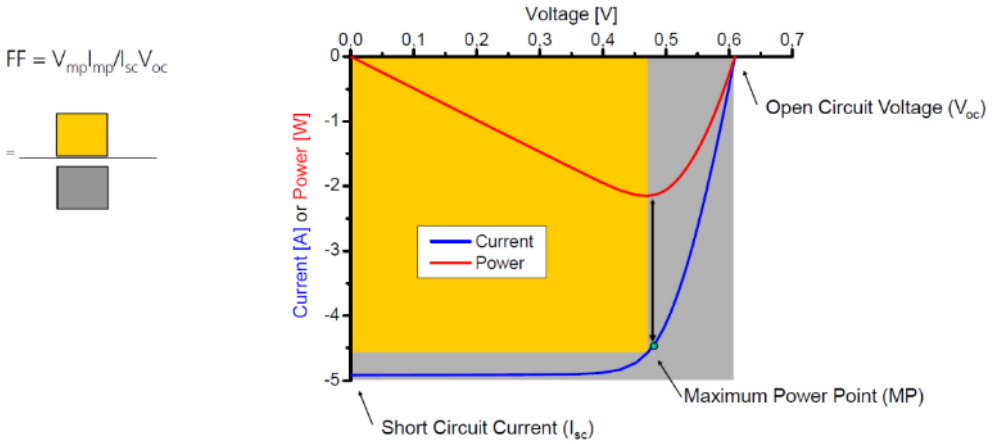

Figure 21. Typical I-V curve of a solar cell with the corresponding parameters: Isc, Pmpp, Voc, FF. (The image was provided by *Solitek R&D*)

When a solar cell is measured at STC, the I-V characteristic curve (Figure 21) is generated and shows the current and voltage (I-V) of a specific device. From the same characteristic, it is possible to extract such parameters as the maximum power (P_{max}), short circuit current (I_{sc}), Open Circuit Voltage (V_{oc}) and Filling factor (FF) [26].

Eric J. Schneller *et al.* [27] made an overview of the c-Si PV module fabrication process which can be divided into several main stages which are (1) stringing and tabbing, (2) lamination, and (3) integration of the junction box and bypass diodes. Similar to the solar cell production, the inspection of the optical and electrical quality of PV panels is performed at the end of the manufacturing process. During the first process step, tin/lead coated copper ribbons are soldered on the front and on the rear side of the solar cell. Individual solar cells are connected in series to form a string of 10 solar cells. One typical solar panel has 6 strings in total interconnected according to the electrical scheme shown in Figure 22 below.

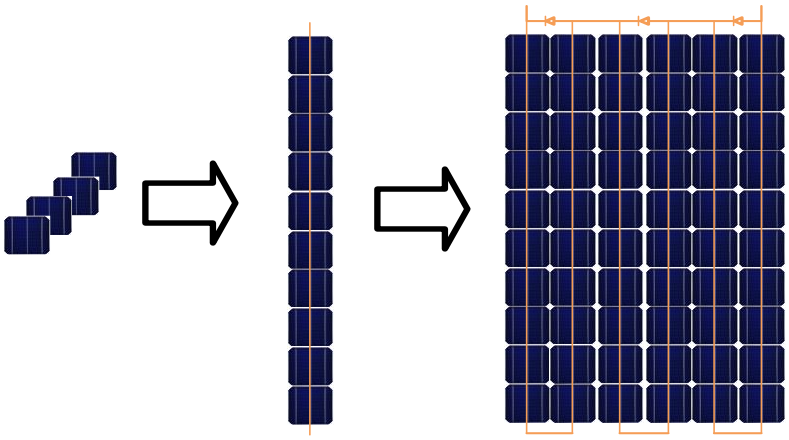

Figure 22. A simplified scheme of the solar cell interconnection process flow

Strings of solar cells have to be protected from the environment in order to achieve the 25+ years lifetime. This becomes possible with the lamination process where two encapsulant sheets are placed above and below the solar cells [27].

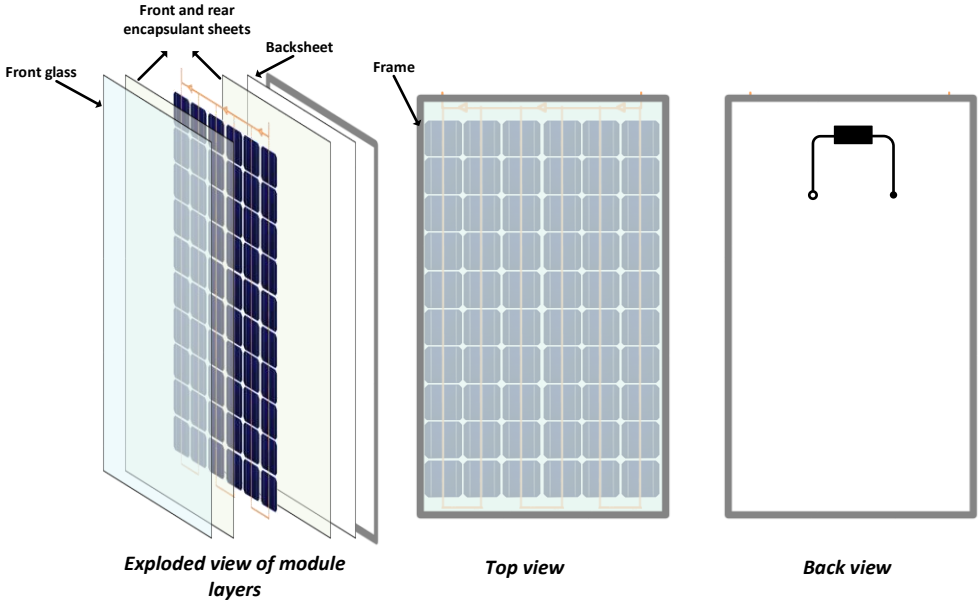

Figure 23. Schematic explanation of the solar module laminate structure: layers, top and back view

In addition, a front sheet (solar grade glass) and a back sheet (polymer or glass) is used to provide protection against the environment and also to ensure the structural rigidity for the solar module. All the front and rear side layers are sealed in vacuum laminator equipment. During the last manufacturing process step, negative and positive electrical terminals are attached to the rear side of a solar panel (Figure 23).

An important part of the two terminal connection is a junction box with bypass diodes which ensure the module reliability and contribute to maintaining energy generation during non-ideal conditions, e.g., shading, accumulation of dirt, defected single solar cells and similar factors [27].

The same as in the case of solar cells manufacturing, the modules are also measured under STC conditions at the very end of production. Moreover, PV panels have to be certified according to several IEC standards (61215, 61730, 61701) before they can be sold in the market. This ensures the top quality, a long lifetime of the PV modules, and reliable energy generation for the end users [27].

1.3 Market development in PV sector

When talking about the market trends in the solar energy sector, there are a few main factors which can best describe its development and future trends. Those are: the cumulated shipped and installed power, the cumulative global production capacity, the market share between different technologies, the efficiency and costs of PV devices, and the levelized cost of electricity. A brief overview of each of these parameters is given in this chapter.

In the photovoltaic sector, the amount of solar modules produced and installed worldwide is typically calculated not in units, but simply by the installed power in watts. Actually, solar energy has been spread so widely that it is already on the hundreds of gigawatt level and is rapidly approaching the terawatt scale. In 2019, the cumulated PV-module shipments surpassed 650 GWp, and the installed power at the end of 2019 was at the 628 GWp level. 580 GW of this was already connected to the grid [28]. As reported by the ITRPV roadmap 11th edition, the global PV production capacity reached the 200 GW level by end of 2019. 95% of this was c-Si based technologies, while 5% only was taken by thin film PV.

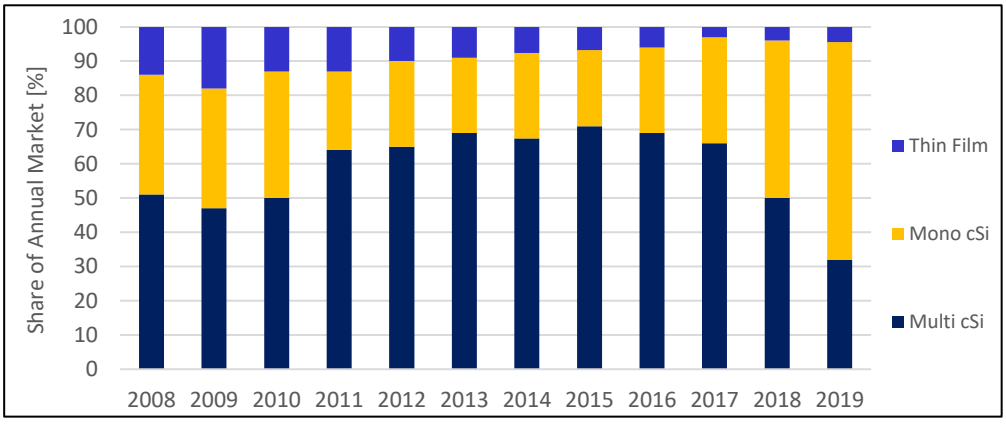

Figure 24. Share of PV technologies on the annual installed capacity (Adapted by Becquerel Institute from *Fraunhofer ISE, RTS Corporation, PV InfoLink*)

The market share development for the last 11 years is shown in Figure 24. Almost for a decade, multi c-Si technology was dominating, but it started to lose its position in favor of the mono crystalline silicon due to the recent developments which lead to significant cost reductions and high efficiency levels. It is expected that the multi c-Si material will be phased out completely during the next 10 years [12].

Silicon solar modules are not only taking the major share of the solar energy market, but are also the most powerful and reliable technology in this sector. The latest average solar module power output rating has been reported, and the future trends have been predicted by ITRPV (Figure 25) [12].

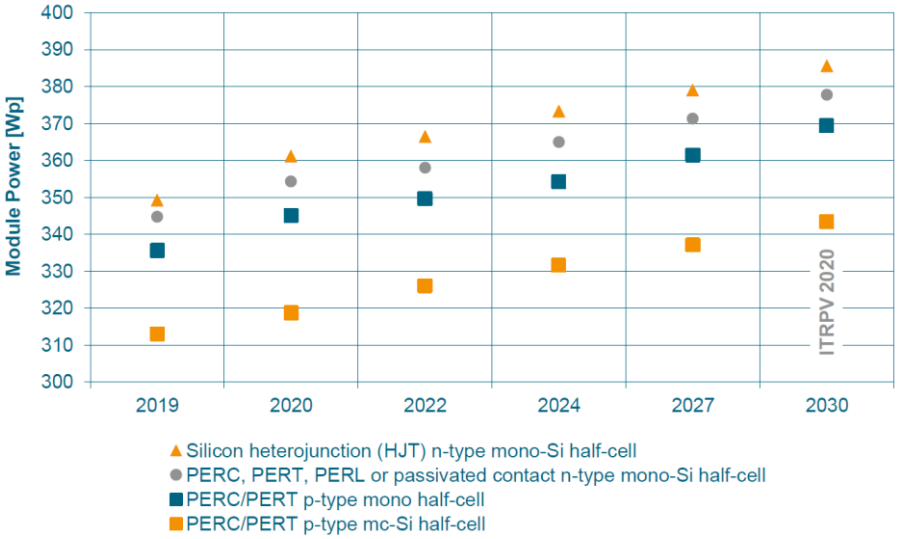

Figure 25. c-Si PV module average power output status and trends for different technologies [12]

The spread in the power ratings is quite significant between different technologies and is in the range from 310–320 to 350–360 Wp level. Following the prediction of the future trends, it is interesting to see that no matter which type of panel, but a 5–10 Wp yearly module power increase is clearly visible. This is obviously an outcome of a very intensive and rapid technological development ongoing in PV sector because the global market strongly demands high quality products [12].

What concerns the costs, the so-called ‘PV learning curve’ is a key graph to explain it, and it is well known among experts in the solar industry (Figure 26). It tells

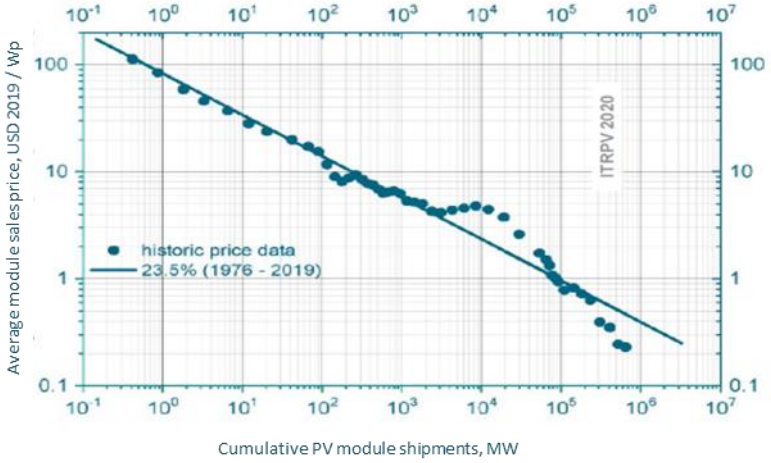

Figure 26. PV price learning curve (left) and cost developement for main technologies in PV [12]

to what extent the prices of PV modules drop down with every doubling of cumulative installed capacity worldwide. ITRPV’s recent update includes all data points starting from 1976, which gives a learning rate of 23.5% as shown in Figure 26. The constant reduction in prices of PV equipment makes this source of energy more affordable for the society and definitely one of the main factors why the solar energy is developing and expanding so rapidly [12].

The *level cost of electricity* (LCOE) is another important parameter which explains the price of solar energy in different regions because it takes into account factors like the solar irradiation level, investment conditions of PV power plants, as well as the quality, performance, warranties and lifetime of a system.

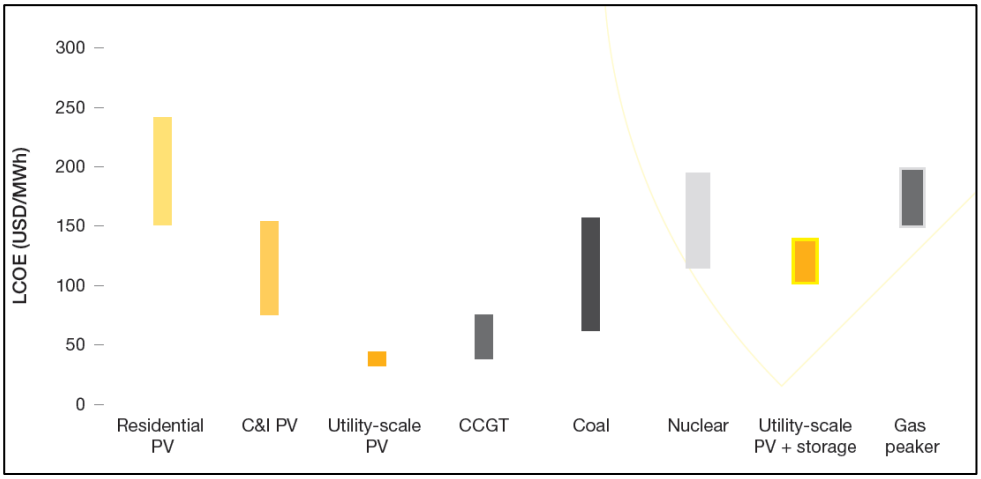

Figure 27. Solar LCOE price costs in comparison with other energy sources [29]

What is important to conclude from Figure 27 is that solar energy has achieved a cost level which is already competitive, and, in sunny regions, it is even below the cost level of the traditional energy sources [29].

Solar Power Europe reported that the global levelized cost of electricity (LCOE) for utility-scale solar power dropped by more than 90% over a recent decade: from 0.32 Eur/kWh in 2009 to less than 0.02 EUR/kWh in 2019 [29]. The drop was mainly driven by the decline of system components prices, technological improvements and contract standardization. At the same time, the cost of the conventional energy sources remained the same or even increased. As a result, today, large-scale solar power is cheaper than any fossil fuel or nuclear source power. As shown in Figure 27, solar energy is bound to experience a further drive down of the electricity costs.

Another important topic to mention while analyzing the solar energy sector is the regulations and the political strategy. It has been set by the EU 2030 Climate Target plan that Europe must reduce its GHG emission levels until 2030 by 55% comparing to the emission levels of year 1990 [30]. This ambitious plan will further stimulate expansion of renewable energy and photovoltaic, especially because 32% of energy will have to be produced by using renewable sources. It has been estimated that, in order to achieve this goal, the EU PV market will have to reach well above 400 GW. This brings an opportunity for the re-birth of the solar manufacturing industry in Europe, but it also brings environmental challenges regarding the EOL phase.

Photovoltaic module waste has been assigned to the category of e-waste in Europe under the *Waste Electrical & Electronic Equipment* (WEEE) directive. This regulation has a direct impact on manufacturing companies which want to sell their products in the EU market because it says that the producer is legally responsible for the end of life management of their products [3]. This responsibility includes several aspects:

- financing the EOL treatment procedures,
- reporting about the volumes related to production and take back of products,
- availability of information including materials, treatment methods, instructions how to handle EOL panels and similar.

It has been reported by the IRENA that EU member countries are adapting the WEEE directive individually. Therefore, different methods and schemes of PV module EOL treatment can be found across the continent [3].

In order to tackle the challenges of PV EOL management, a PV Cycle take back and recycling scheme has been established in Germany, France, Belgium, the United Kingdom, Japan and the USA. This organization basically provides all kinds of waste management solutions (including collection, recycling and legal compliance) for PV manufacturing companies [31].

PV modules must also be compliant with the RoHS regulation [32], and, especially, the following six materials have restricted usage in the manufacturing of PV equipment:

Table 1. List of substances which have restricted use in PV modules [32]

Substance	Maximum limit (ppm)
1. Cadmium (Cd)	100
2. Hexavalent chromium (Cr^{6+})	1000
3. Lead (Pb)	1000
4. Mercury (Hg)	1000
5. Polybrominated biphenyls (PBB)	1000
6. Polybrominated diphenyl ether (PBDE)	1000

The only substance which can still be found in c-Si modules from this list is lead. It is still being used nowadays in silver screen printing pastes and cell interconnection ribbons. However, the quantity is very small and is well below the limit.

1.4 Implementation of environmental impact reduction methods at manufacturing stage

Apart from the technological developments, the reduction of the environmental impact is another key aspect for successful further expansion of the photovoltaic industry and especially at the manufacturing stage of PV equipment. As reported by Erik A. Alsema *et al*. [33], there are a few areas where the impact on the environment can be minimized, including:

- reduction of materials consumption
- increased power generation efficiency
- reduction of energy consumption
- reduction of emissions
- design for life and design for recycling of PV products.

Reduction of silicon consumption is possible in a few ways. To mention several industrially feasible ones, these would be:

- improved crystallization with lower material loss
- thinner wafers
- lower kerf loss
- reduced wafer breakage.

In addition, the recycling of silicon waste from production scrap like ingot cut-offs, broken wafers or kerf loss are options to reduce the silicon consumption problem. Alternative technologies, such as casting or pulling wafers directly from liquid Si (ribbon technologies), can be found in literature, but, unfortunately, it has not been widely accepted by the industry yet.

Reduction of kerf loss is possible by implementing more advanced wafering technologies (like diamond cutting, as mentioned in Chapter 1.2). Alternatively, there are research groups which have demonstrated the potential of the recycling kerf loss and reusing it for various applications, e.g., lithium ion batteries [20] or crucibles for ingot casting [34].

One step further has been made by the company *NexWafe* which has recently introduced a kerf-less wafer technology suitable for the manufacturing of high efficiency solar cells thus offering significant savings in energy, materials consumption and costs [21].

ITRPV has reported that the average polysilicon consumption per wafer was about 15–16 g in 2019, and it is expected to go down to 12–13 g/wafer by 2030 [12]. Another parameter which reflects an increase in material efficiency while taking quality into account as well is g/Wp (mass per power unit). The usage of silicon measured in this way went down by 75% from 16 g/Wp in 2004 to 4 g/Wp in 2017.

The reduction of silicon wafer thickness is another factor which is a potential area of further improvements in terms of silicon consumption. ITRPV has reported

that wafer thickness is expected to go down from 175 μm (the average standard today) to 150 μm in 10 years [12].

In a similar way to silicon, there is a significant trend of silver reduction in PV cells and modules. Silver is mainly used in metallization pastes for contact formation, and 100 mg/cell is the median value today being reported by the industry. It is predicted that the reduction down to 50 mg/cell will be possible until 2030. [12].

The manufacturing of PV devices is a highly energy intensive technology, with feedstock, ingot and wafering having the biggest share in the total energy consumed per area of a single solar module (kWh/m^2). As suggested by Erik A. Alsema *et al*. [33], the method to reduce energy consumption on the silicon material production level is the implementation of new crystallization methods like FBR. Attempts to reduce power consumption for monocrystalline silicon ingot growth have been reported by Nam *et al*. [35] where a reduction by 1.8 kW was demonstrated by optimizing the ingot growth process. On the cell and module level, most of the energy is consumed in the clean room climate control, DI water preparation and lamination steps. Improvements are possible with focusing on the process recipe optimization and the usage of faster curing materials as in the case of lamination.

Most of the emissions are related to energy consumption at the manufacturing level. This problem is worse especially when the conventional electricity supply system is used in factories. One of the leaders among European PV manufacturers in the field of replacing fossil fuels with renewable energy is the *SoliTek* company from Vilnius, Lithuania, which is powering its production by a renewable energy mix using both solar and geothermal power [36].

Changing the design of a solar module is another way to reduce the environmental impact at the manufacturing stage. However, this is a real challenge because the design for easy recycling and the design for a long lifetime are essentially incompatible objectives. To the best of the author's knowledge, the only truly industrially applicable technology which is capable to deliver 100% recyclable and reusable components has been introduced by the French company *Apollon Solar* with their N.I.C.E. (New Industrial Cell Encapsulation) technology. It offers a PV module structure which does not require any encapsulant materials like EVA or POE, and no soldering, either, and therefore it offers a possibility to have easy access to all the components of PV modules in case something needs to be fixed, replaced or recycled [37].

1.5 Implementation of environmental impact reduction methods at EOL stage

An overview of the environmental impact reduction methods at the End-of-life (EOL) stages is given in this chapter.

Solar or photovoltaic modules have been an important part of the electronic equipment industry because these devices allow generating clean and affordable electrical energy. Due to the relatively long lifespan reaching 25–30 years of service

and above, the question of what to do with the end-of-life PV modules has been a lower priority issue. However, in reality, a significant volume of PV modules have to be discarded within first 5–7 years after being deployed outside. As given by a report by IRENA [3], there are several reasons for that, specifically, damage during the transportation and installation stages, initial failures after start-up operations, or technical and physical failures during operation caused by severe environmental conditions (hail, storm) (Figure 28).

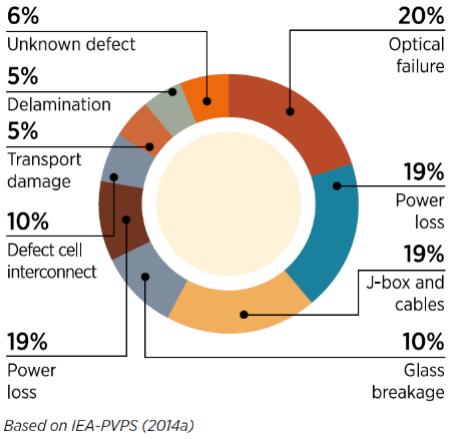

Figure 28. Failure types of EOL modules [3]

As forecasted in the same IRENA report, the high annual volumes of end-of-life modules are expected to appear only in 2030, but the global PV industry has already been working on the development of circular business at all stages of the PV module life cycle including the raw materials manufacturing, use and end-of-life phases. That is mainly influenced by the WEEE (Waste Electrical and Electronic Equipment) Directive 2012/19/EU which provides a legislative framework for extended producer responsibility of PV modules at the European scale. It says that, from 14 February 2014, the collection, transport and treatment (recycling) of photovoltaic panels is regulated in every single country of the European Union (EU) [38]. In addition, it is predicted that, once the volumes of EOL solar modules start becoming reasonable, their recycling will offer new business opportunities by creating a multi-billion market of secondary raw materials and services [39].

At the end of the PV module usage phase, they are usually dismantled and then can be treated in several ways: re-used in other application or markets, repaired, or recycled. In order to be able to choose one of these approaches, it is important to perform an inspection of solar modules. Quality inspection of end-of-life PV panels can be done visually and/or by applying electrical measurement techniques. An EOL PV module treatment sequence has been proposed by the industry leader in PV testing and recycling equipment, *PV Techno Cycle Inc.* from Japan [40].

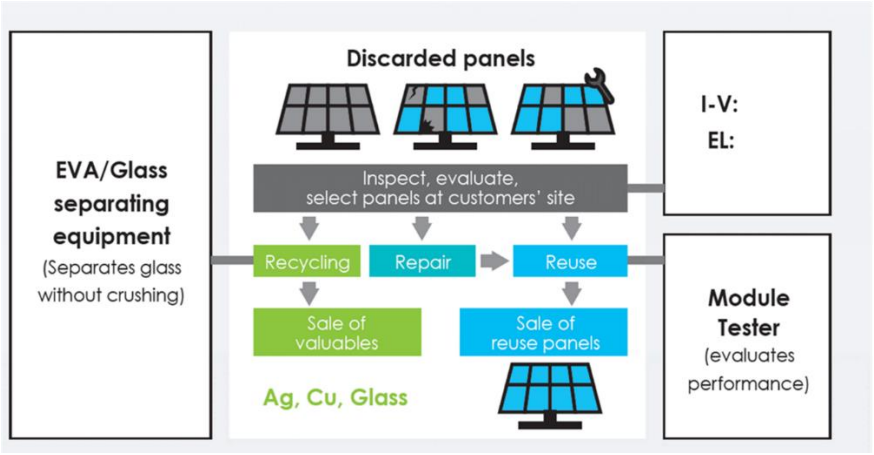

Figure 29. Scheme of end-of-life PV panel treatment including inspection, sorting, recycling and reuse [40]

As explained in Figure 29, the following defects can be detected by simple visual inspection: broken glass, delamination of bus bars or encapsulant materials, broken or deformed frames, brownish color caused by hot spots, a charred electrical connection box, defects in connectors, environmentally altered surfaces and other similar failures. Electrical inspection is typically performed by applying I-V and EL measurements. These measurements can give the most important information about the electrical condition of PV panels and provide enough data for a dedicated service provider to decide what next steps to make [40].

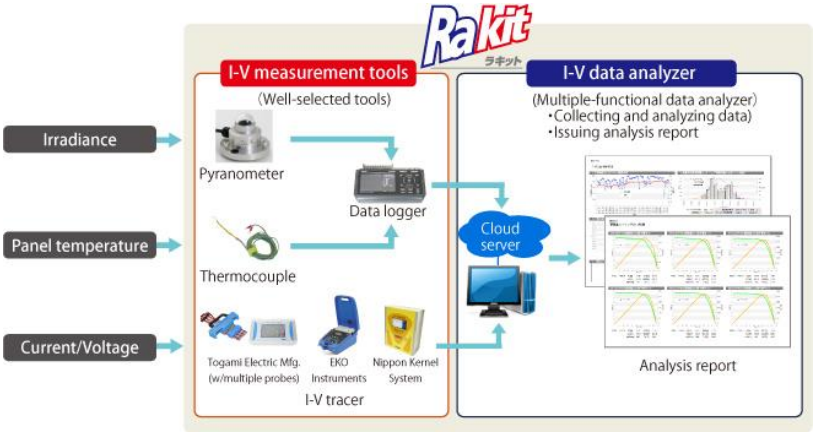

Figure 30. Multi-functional High-speed I-V Measurement System *Rakit* [40]

With the systems like *Rakit* by NPC, PV module inspection can be done onsite in a PV field, and bad panels can be identified and sorted out (see Figure 30). On the other hand, I-V measurements can be done at a manufacturing or recycling factory/facility with a dedicated PV module I-V flasher, like the one shown in Figure 31 [41].

Figure 31. CetisPV-IUCT-Q ready-to-operate high-precision pulsed xenon flasher solution for I-V classification measurements of photovoltaic modules [41]

Another set of 'must-have' equipment in PV module inspection is the electroluminescence (EL) and photoluminescence (PL) measurement tools. During the EL inspection process, electric current is applied to PV panels, and, because of that, they emit light at a certain frequency. The emitted light is captured by IR camera and then visualized [40].

Figure 32. On-site EL/PL Inspection Machine *EPTiF* [40]

As an example, a solution developed by *NPC Group* is given in Figure 32 [40]. With such an on-site inspection machine, it is possible to detect crystal or contact defects, degradation caused by PID, cracks, etc. An example of good versus defected

solar modules is given in Figure 33, where it is possible to see cracked and PID affected solar cells as the dark areas in the EL image.

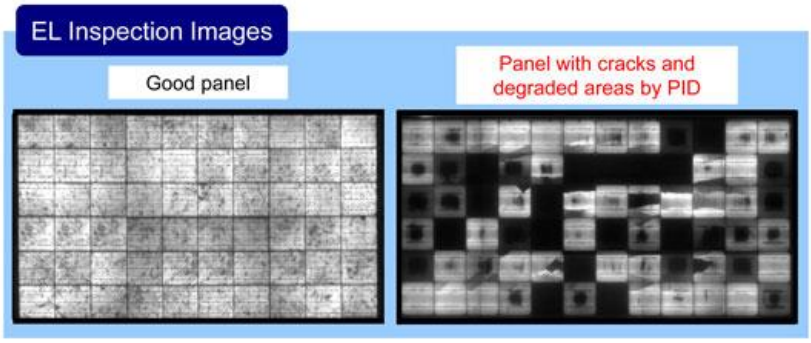

Figure 33. Example of EL images of solar modules [40]

Additional information about the degradation and homogeneity of solar cells can be collected by applying the photoluminescence (PL) method. During the PL procedure, laser light is irradiated onto PV cells, and the emitted light is captured and evaluated. The proposed inspection method is suitable for investigations on the power loss, inspections of any impact to panel performance after harsh climatic events, such as typhoons, heavy snowfall, hail, etc. [40].

With the valuable data gathered during the inspection of PV modules, it is possible for PV system owners, manufacturing companies and dedicated waste treatment facilities decide in which way defected solar modules should be treated – either sent for repairs or straight to recycling centers.

1.5.1 End of Life PV recycling processes: c-Si modules

As reported by the International Energy Association (IEA), ordinary electronic equipment waste (WEEE) recycling companies have to change only the configuration but not the process in order to recycle silicon-based PV panels [42]. Several options for recycling of c-Si solar models are shown in Figure 34, which tells that there are three main ways how to recycle silicon-based panels: thermal (combustion including pyrolysis), mechanical (scraping non-glass layers, cutting the encapsulation layer, crushing/grinding and scraping glass) and chemical (solvent treatment including ultrasound).

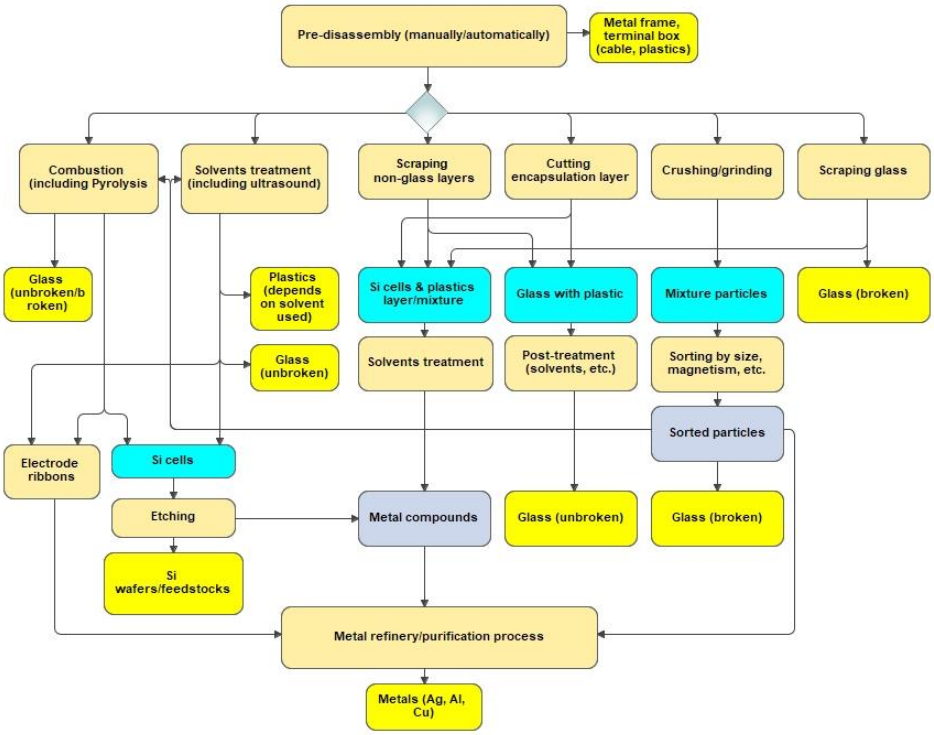

Figure 34. Process flow of silicon based PV panel recycling. Adapted by author based on End-of-life Management of Photovoltaic Panels report [42]

To the best of the author's knowledge, there are only a few industrial scale equipment builders which can supply machines together with the technology for PV module recycling: *NPC Group*, *Loser Chemie*, and *Experia*. As already mentioned in this chapter, *NPC Group* also produces equipment for inspecting PV modules in PV plants.

The process technology for EOL module recycling is different at each company; therefore, it is worth examining each of them in order to develop better understanding about the available options to treat discarded PV panels. Figure 35 presents a schematic approach of several available recycling technologies.

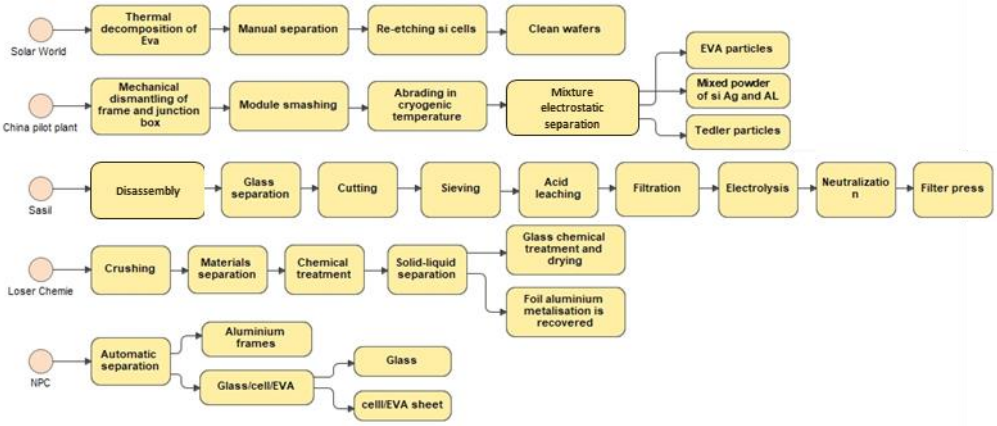

Figure 35. Various practices of silicon-based PV recycling processes (graph created by author)

Solar World AG (or *Deutsche Solar AG*) was one of the pioneers in PV recycling. Its process was based on eliminating the encapsulant material by burning, then manual separation of the metal frame and glass and etching of the recovered solar cells followed in order to recover silicon for re-use in wafer production [43].

Another recycling method was reported by (Zhang *et al*., 2013) where PV waste is treated by abrasive machining under the cryogenic condition and electrostatic separation. Due to the low purity of the recovered silicon, it cannot be reprocessed into new wafers when using this technology.

The Italian company *Sasil-life* participated in a European project FRELP in order to create a PV recycling plant as reported by Latunussa *et al*. [44]. It made a demonstration and implementation of mechanical disassembly of solar panels followed by glass separation, cutting, sieving, acid leaching, filtration, electrolysis, neutralization and filter pressing of sludge waste. Unfortunately, in April 2016, the company announced that, due to a low amount of waste and economic reasons, the full scale recycling plant will not be built.

The German based company *LuxChemtech GmbH* (previously known as *Loser Chemie*) has capabilities to recycle various electronic equipment including silicon and thin film solar modules. Their process for silicon-based panels recycling is based on water jet milling and treatment with high intensity light flashes in order to destroy adhesion of the solar module inner layers. When using this method, solar panels can be disassembled without the need to crush them, and full size solar grade glass can be recovered [45].

The Japanese company *NPC Group* developed a recycling process for silicon-based PV panels which can recover glass without damaging it. Recycling starts with the automatic separation of aluminum frames. After processing PV with hot-knife, glass and cell/EVA sheet can be used for further recycling. This process is specifically good because it is fully automated, high-value glass is recovered, and the equipment

can be purchased from NPC group along with the tools used for detecting defect(s) of installed PV panels [40].

Despite the fact that several dedicated PV panel recycling technologies are already available, there are only a few dedicated PV panel recycling plants in operation. One of them is *VEOLIA*, a French PV panel recycling enterprise which started its operation in 2018 with the recycling capacity of 1300 t/year.

An overview of the treatment strategies of End-of-life PV modules was performed in detail by Tao and Yu [43] where the three currently existing approaches were analyzed: manufacturing waste recycling, end-of-life module material recycling, and remanufacturing and reuse.

Manufacturing waste recycling in this review stresses the importance of the silicon wafer slicing step by indicating that about 40% of silicon is lost as slurry waste during this process. Lab scale recycling methods have been proposed; however, the material recovery rate of pure Si remains a challenge and needs further process developments.

End of life solar module treatment techniques were also presented in the same study. *Solarworld* was mentioned as an industrial company which was a pioneer of the end-of-life solar module treatment by using thermal, mechanical and chemical separation techniques. As reported by K. Wamback *et al*. [46], the German company *SolarMaterial AG* performed a complete recycling project of Germany's oldest PV system installed in Pellworm Island in 1983. Almost 18,000 solar modules were dismantled and recycled, and the recovered solar grade silicon was reused for the manufacturing of new PV cells and modules. The project demonstrated the possibilities of high quality production when using recycled raw materials. However, this company applied for insolvency in 2018; therefore, unfortunately, there were no further developments in this area.

A few R&D level approaches were mentioned in the same study by Tao and Yu [43], including the delamination and recovery of silicon cells when using thermal and chemical types of treatment. While several groups demonstrated possibilities to recover high purity silicon, the added costs of the delamination process still promise little commercial potential to be implemented in mass production.

On the other hand, silicon is not the only important material in PV devices, and the recovery of other useful materials like glass, aluminum, silver and copper is being considered for improving the commercial potential of recycling processes.

1.5.2 Reuse of materials in PV and other industries

One of the options to reduce the environmental impact of the solar industry at the EOL stage is to look into possibilities of material reuse in PV and other sectors. To start analyzing it, a list of options has been made in Table 2 based on the information received from two sources: the *FRELP Project* outcomes and the information provided by the *NPC Group*.

Table 2 Options of EOL PV module material reuse as proposed by companies *Sasil* and *NPC*

Material	Sasil	NPC
Aluminum	For secondary aluminum production	Sold to aluminum recycler
Copper	Sold to copper recycler	Cell sheet is sold to a refinery company
Glass	Glass culets used for packaging production, as a substitute for raw material	Sold to a glass recycler for glass wool
Silicon	Used as MG silicon metal subsidy	Cell sheet is sold to a refinery company where they extract silver
Silver	For secondary silver production	Cell sheet is sold to a refinery company where they mainly extract silver
Cables	Sold to copper recycler	Sold to copper recycler
EVA	Incinerated	Cell sheet is sold to a refinery company where they mainly extract silver
Contaminated glass	Disposal in landfill	No contaminated glass
Fly ash (hazardous waste)	Disposal in special landfill	Refinery company takes care of the hazardous waste
Liquid waste	Contains metallic residue, disposal in special landfill	No liquid waste
Sludge (hazardous waste)	Contains metallic residue, disposal in a special landfill	No sludge

It is of interest to see that various technological processes lead to possibilities for the reuse of the recovered material. After the *Sasil* recycling process, there are still materials that cannot be reused, such as fly ash, liquid waste, contaminated glass and sludge. On the other hand, *NPC Group* claims that they avoid this type of waste generation thanks to their hot knife separation method. However, the hot knife approach cannot separate such materials as silicon, silver and EVA. This has to be done externally; therefore, it can be concluded that *NPC Group* can make only partial recycling and recovery of materials from PV modules.

Another overview based on various sources and public information is presented in Table 3 where possible areas of material reuse after their recovery from EOL modules are indicated.

Table 3. Overview of possible areas of reuse of PV module materials

Module compound	possible use of output
glass	glass industry ceramic industry horticulture building industry
rear side covering	thermal treatment (polymers) plastic recycling metal industry glass industry
frame	thermal treatment (polymers) plastic recycling metal industry
junction box	thermal treatment plastic recycling
wire	metal industry wire recycler electronics industry/recycling
sealant	thermal treatment
solar cells	metallurgy
electrical connector	metal industry electronics industry

Silicon wafer contamination is one of the limiting factors of the reuse of this material in the new cycle of the production of solar cells. In addition, the purification of silicon to the solar grade quality has no economic advantage against the production of fresh material when using industrial processes. Therefore, it is important to find other niches where the purity of silicon is less demanding.

A recent study by Bendikiene *et al*. [47] presented a method to recycle and reuse industrial silicon solar scrap. In collaboration with the Lithuanian solar cell manufacturing company *Soli Tek R&D*, treatment processes of broken solar cells were suggested by creating a valuable product – metallic surface coatings.

In order to prepare silicon material for the application in coatings, solar cell scrap was milled to break the chemical and mechanical bonds between separate parts of cells followed by leaching with nitric acid (HNO_3). Particle size distribution was performed by sieve analysis, and the recovered powder was turned into a coating by using the tungsten inert gas welding (TIG) technique. The obtained results showed that silicon powder coatings made from solar cell scrap offered two times lower mass loss on average comparing to the normalized structure steel S355 substrate in rough abrasive conditions. Such an approach demonstrated the potential to re-use broken

solar cells in the production of secondary products, thus creating the value of silicon which otherwise would simply be lost. In addition, this study presents how to solve the challenge related to the recovery of intact solar wafers, material contamination and the issues related to its purification which limits the possibilities to reuse silicon in the PV industry. In some cases, it can be even more advantageous to recover high purity silicon material than the full size wafers as stated by Garvin A. Heath *et al*. [48].

Another group led by Yousef *et al*. [49] presented a lab scale experiment where a possibility to turn solar cell scrap into valuable materials in the forms of micro and nano particles was demonstrated. Silicon micro powder with the average size of 50 μm and a recycling rate of >98% from solar cell and wafer scrap was achieved. In addition, aluminum nano particles with the average size of 25 nm and a process yield of >91% was demonstrated. Another material, specifically, AgCl, was recovered at a rate of ~98% in this research.

These reported achievements on the lab scale experiments show the future potential of the recovery and reuse of valuable materials from PV equipment. Not only is it a positive achievement in terms of the environmental impact, but it also contributes from the economic point of view by opening paths to new future business models. According to IRENA [3], an estimated value of recoverable materials from EOL PV modules can reach around 450 million USD by 2030.

1.5.3 PV cell and panel design for circularity

There can be various interpretations of whatever 'Design for circular economy' is and how it can be implemented in the photovoltaic industry. Design for circularity is a complex task which often requires changing the way of thinking when creating and manufacturing various products, including solar cells and modules.

According to an overview made by Medkova *et al*. [50], the strategy for the circular product design can be explained by 6 categories:

1. Design for product attachment and trust – to create a product that the society loves and trusts;
2. Design for product durability – to create a product which is resistant to wear and tear;
3. Design for Standardization & Compatibility – to create a product which aims for multifunctional and modular use;
4. Design for ease of maintenance and repair – to create a product which is not a challenge to repair;
5. Design for upgradability and adaptability – to create a product which can be modified in order to improve its value and performance;
6. Design for dis- and reassembly – to create a product which is easy to separate for materials reuse and remanufacturing.

Some of these categories are definitely suitable to be used for designing circular PV cells and modules. However, as a solar module is an extremely durable product, it

brings many challenges to design it for an easy disassembly. As of today, the best example of such an approach being reported is the NICE (New Industrial Solar Cell Encapsulation) module technology commercialized by *Apollon Solar*, a French PV module technology and manufacturing equipment provider [37]. In contrast to the standard module technology, NICE does not use EVA or POE as encapsulants, which makes it relatively easy to be disassembled for repair or reuse.

Another approach which is explored more by standard PV technology users is related to trying to extend the durability and reduce power degradation over the lifetime of a solar module. One of the solutions recently adopted by the industry is to use glass as a rear cover in order to better protect solar cells from humidity or mechanical damage. The glass/glass technology together with alternative encapsulant materials allows the manufacturers to give power warranties exceeding 30 years [36].

What concerns other materials used in the PV industry, ITRPV reported [12] that there is a constant trend towards the reduction of the usage of silicon, silver and aluminum which is implemented by rapid developments at the levels of materials and various production processes. Moreover, the replacement of lead containing solder components, a non-recyclable encanpsulant and lamination materials by environmentally more friendly alternatives will continue to contribute towards improving the design of solar modules for the circular economy.

The ongoing European projects, e.g., CIRCUSOL [51], are looking for opportunities to unleash the full potential of circular business models in the PV industry by offering the Product-Service Systems solar power sector where power generation and storage is provided to a user as a service. This example explains that the design for circular economy should be focused not only on the technology and manufacturing level, but should also be able to see a broader picture and include the integration of power generation and storage systems, related services, data management and O&M through digitalization and similar aspects.

1.6 Summary of literature review

In total, seventy five sources including scientific articles, conference publications, market reports and websites were analyzed when preparing this literature review.

The solar energy market has been rapidly expanding during the last decade and reached more than 600 GWp of installed power capacity in 2019, 90% of which is represented by c-Si based solar cells and modules. With silicon technology being the cheapest, most reliable and cost effective technology that is available these days, it is not going to leave its strong position in terrestrial applications. Moreover, in the sunny areas of our planet, photovoltaics have already become the cheapest source of electricity when comparing newly installed power plants with different technologies, for instance, nuclear, coal, gas, wind, etc.

From the environmental impact point of view, there is still a lot of room for improvement and optimization in the whole lifecycle of PV equipment. Three areas of improvement can be addressed as the most important in tackling environmental

challenges. Firstly – the consumption reduction of raw materials as well as energy, secondly – the development of effective waste treatment methods for the recovery and reuse of raw materials at the EOL stage, and thirdly – product design for circularity, by developing PV modules which are more suitable for separation, repair and recycling.

It has been identified in our literature review that the majority of the environmental impact reduction efforts among other research groups and industrial players have been focused on the EOL stage starting from the political level (take back schemes, WEEE directive and RoHS requirements) and going down to technological developments focused on PV module recycling and material recovery technologies. On the other hand, little has been done in practice concerning the earlier stage – the manufacturing of silicon and solar cells – despite the fact that these two stages are the most energy and material intensive steps in the whole chain of the PV device lifecycle. So far, only one company – *Apollon Solar* located in France – has developed and commercialized recycling friendly solar modules based on its own NICE technology.

Recycling, material recovery and reuse from EOL solar cells and modules is technologically a highly challenging task; therefore several groups are also working on finding possibilities to reuse recovered materials not only in PV, but also in other industries where the purity requirements are less demanding. For example, there is high interest and potential for contaminated SCW to be reused as micro and nano particles in abrasive coatings and batteries.

2. METHODOLOGY

Technological experiments have been chosen as the main research methodology for testing the ideas described in the Key Thesis section of this document. The experimental work structure has been divided into three major stages according to Figure 36:

1. The **planning** phase has been dedicated for the theoretical study and preparation for experimental work. At this stage, the main focus was put on the definition of the research object and its boundaries, the understanding of the loss mechanisms in solar cells, data collection, selection of the evaluation methods and the creation of an experimental plan.

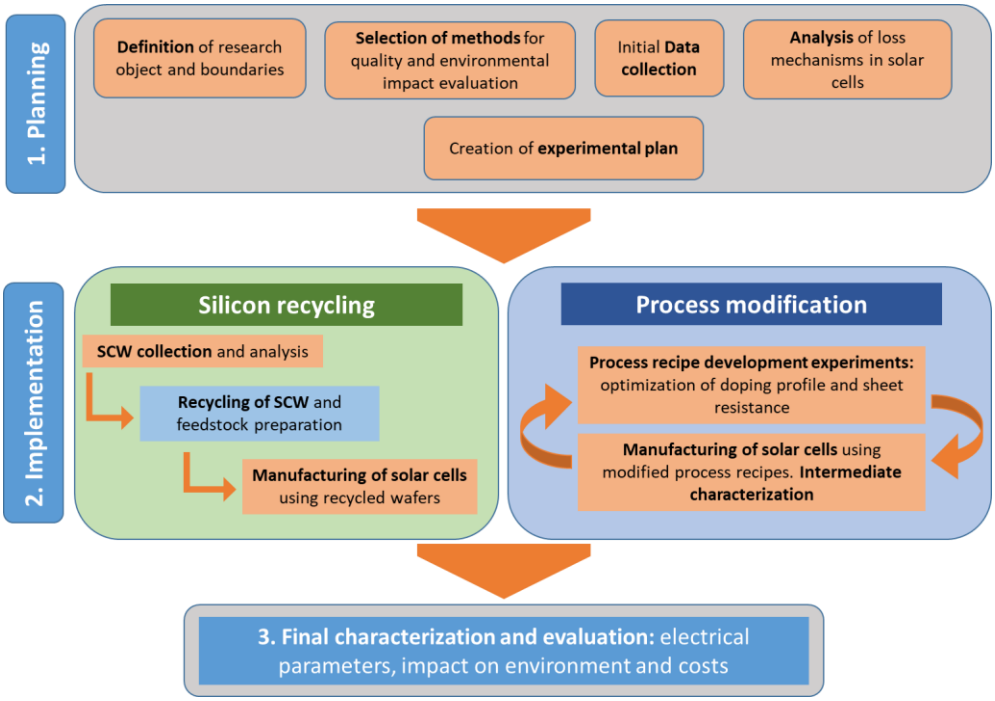

Figure 36. Schematic overview of theoretical and experimental parts of the thesis

2. At the **Implementation** phase, all the experimental work was carried out, and all related activities were divided into two separate experimental flows: silicon recycling and diffusion process modification. It should be mentioned that all the infrastructure for the experimental part was available at external companies including: JSC *Soli Tek R&D*, where 80% of work was carried out. The remaining work, including recycling of SCW and feedstock

preparation, was performed at SINTEF institute in Norway and Kaunas University of Technology (elemental composition analysis of SCW).

3. The final part – **characterization and evaluation** – was the stage of this research where all the results were collected, and all the necessary KPIs were evaluated. The environmental impact of silicon recycling and process modification was evaluated by comparing the materials and electricity consumption as well as the CO_2 footprint between the reference case and the innovative case. The electrical solar cell quality was evaluated by measuring the cell efficiency, the minority carrier lifetime by QSSPC and the diffusion length values by LBIC techniques. The latter two characterization steps were performed at CEA-INES institute in France. Cost assessment was conducted regarding the reference, recycled and modified processes by comparing Eur/Wp parameter for each case.

2.1 Functional unit

In this study, a 1 kWp of mc-Si AL-BSF (multicrystalline Aluminum Back Surface Field) solar cell was selected as the functional unit. The Kilowatt peak is a measure of the maximum electrical power which can be generated by a solar cell under standard testing conditions (STC), which means that the cell temperature of 25 °C, irradiance of 1000 W/m^2 and a light spectrum of air mass 1.5 (AM1.5) has to be ensured during the testing procedure of solar cells.

2.2 System boundary

A good description of the typical product system for solar energy generated by using PV has been provided by the Product Environmental Footprint Category Rules (PEFCR) document [52]. It consists of five main lifecycle stages: raw material acquisition and pre-processing, distribution and storage, production of the main product, use and EOL phases (Figure 37).

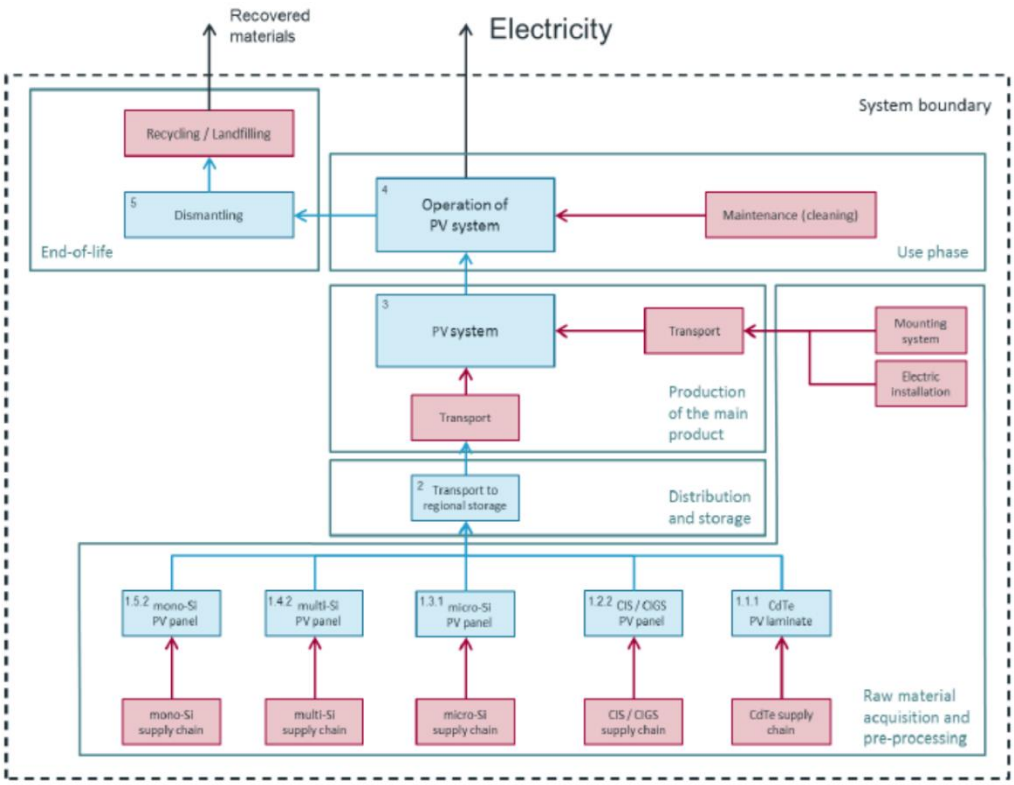

Figure 37. System diagram: Product system of electricity produced with a photovoltaic module using mono-Si, multi-Si, micro-Si, CdTe and CIS / CIGS technology [52]

The work of this thesis focuses only on the multi silicon solar cell production stage which, according to the scheme in Figure 37, is included in the 'multi-Si supply chain' stage. The system boundary which was used for the LCA study in this thesis considers the life cycle of multi-Si solar cells including all the materials and processes to produce the amount of cells which have a combined power of 1 kWp. The study does not include the transportation of the produced solar cells to the customer and therefore does not take into account the distribution and storage, the production of the PV module, the use and the End-of-life phases.

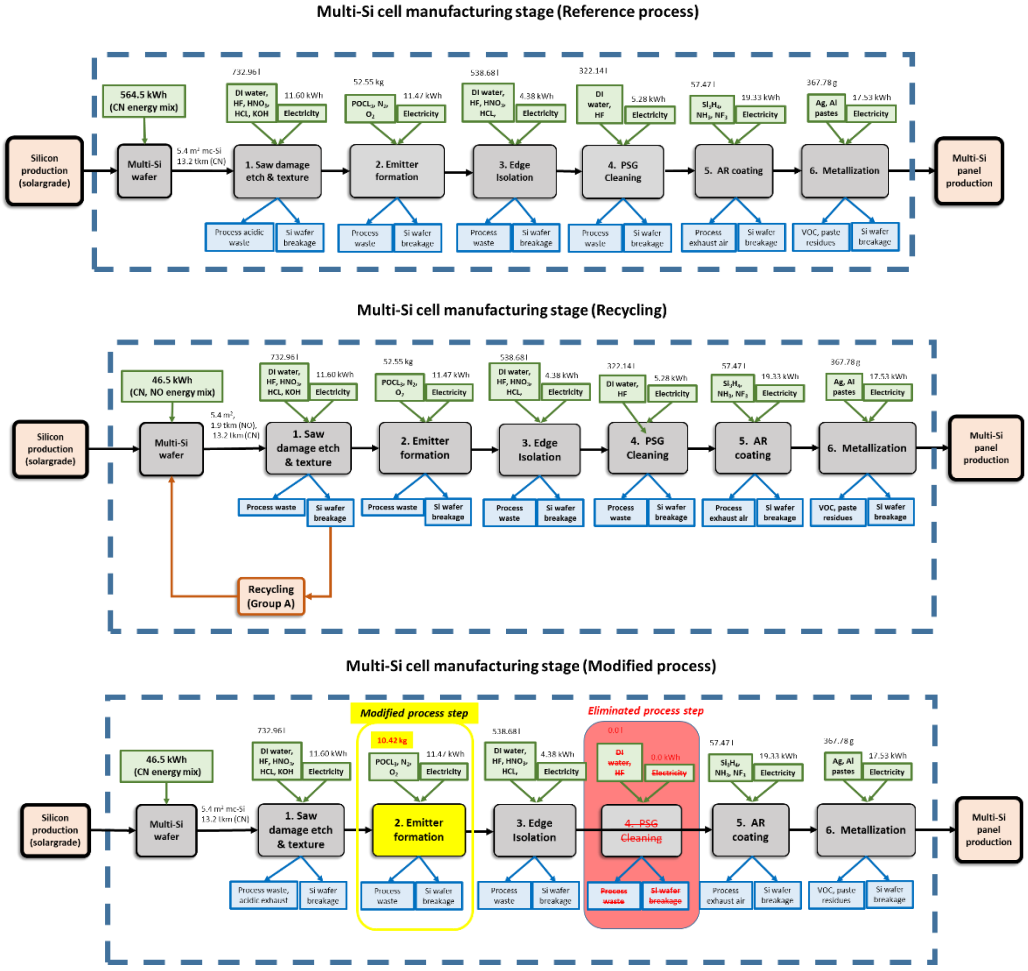

Figure 38. Explanation of system boundaries for three different cases analyzed in this thesis: standard production process, recycled silicon and modified process

For LCA evaluation, three cases were analyzed (standard, modified and recycled) of multi-Si cell manufacturing processes according to Figure 38. The blue segmented line indicates the boundaries of the system which included multi-Si wafer and cell manufacturing processes. The 'Modified' process has a different emitter formation recipe and the eliminated PSG Cleaning step, while the 'Recycling' case has standard process recipes but uses silicon wafer breakage (Group A material) as the raw material for multi silicon wafers.

2.3 Technological Experiments

This chapter explains the experimental part of this research. As already described in this document, the experimental setup for the two methods was implemented: the demonstration of the recycling and reuse of silicon in industrial solar cell production and process modification (emitter formation by the phosphorous diffusion manufacturing step), as shown in Figure 39.

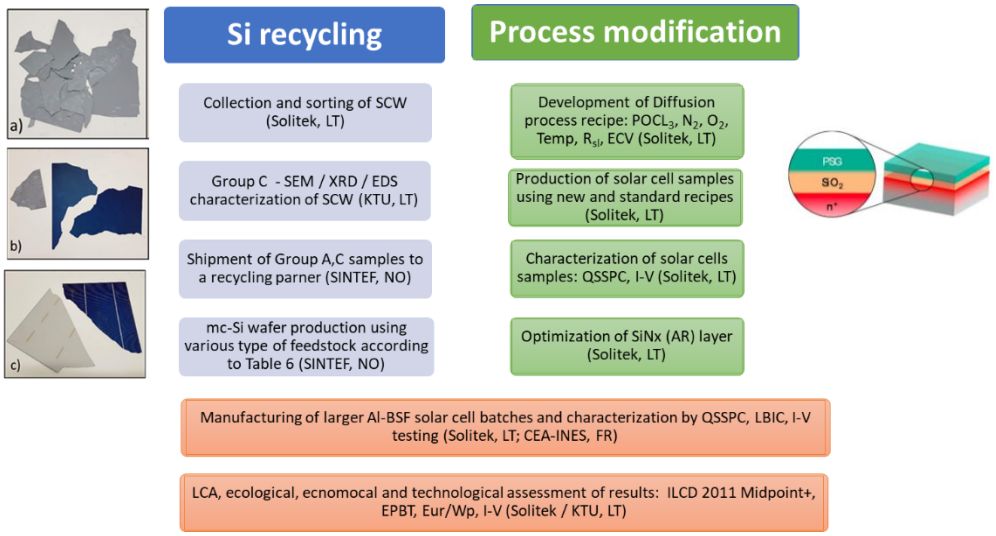

Figure 39. Explanation of experimental work flow for two methods: silicon recycling and process modification

Silicon recycling and process modification experiments were carried out in several steps and in close cooperation with external research partners. An overview of what has been performed is given in Subchapters 2.3.2 and 2.3.3, accordingly.

2.3.1 Equipment

Solar cell production and the related experiments were performed at the facilities of the *Soli Tek R&D Company* which, at the time of the work, owned an experimental manufacturing line of Al-BSF multicrystalline solar cells.

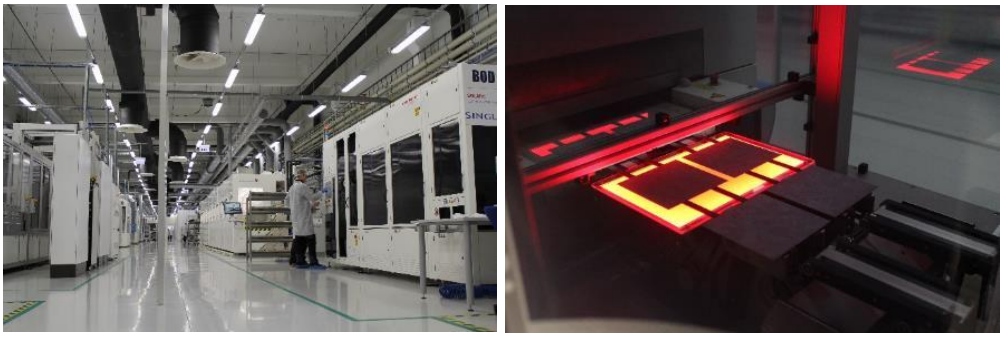

Figure 40. Manufacturing facilities of *Soli Tek R&D*: 80 MWp c-Si Al-BSF solar cell line

Table 4. Solar cell production infrastructure: list of main equipment

Function	System	Manufacturer
Stack splitter + Incoming wafer inspection	WHQ 3000	Jonas & Redmann
Wafer saw damage & texture	Silex Isotex 3000	Singulus / Stangl
Emitter formation	Lydop 6200 DF	Semco
Chemical Edge Isolation	LINEA SSE & ISOTEX 400 PILOT	Singulus / Stangl
PSG removal	Silex PSG 3000	Singulus / Stangl
Antireflective layer coating	Singular 1500	Singulus
Printing line (3 printers, 2 dryers)	JRT Mettalization line	JRT Photovoaltics
Fast Firing	RFS 500D	Rehm Thermalsystems GMBH
Optical inspection, I-V testing and sorting	Tester, Sorter	Jonas & Redmann

According to the specifications of the equipment, the total electrical power demand reaches more than 1 MW. This results in the average consumption of electricity reaching more than 250–260 MWh per month. Undoubtedly, this is an

important indicator of the potential to reduce the environmental impact and manufacturing costs if the energy consumption can be reduced.

Equipment for the characterization of the recombination losses, the diffusion profile, the sheet resistance and I-V parameters is described in detail in Chapters 1.2.2 and 2.4.

2.3.2 Silicon recycling and reuse for multi Si cell production

The main task in this experiment was to demonstrate at the industrial level a pilot production process of solar cells and modules using recycled silicon wafers. The main quality related goal set for this task was to reach a minimum cell efficiency of 17.0%. At the time of the experiments, this efficiency level was the lowest number which was still sellable in the market. Solar cells with lower performance were considered to be low grade and therefore not accepted by most of the potential customers. The expected reductions of the greenhouse gas emissions from solar cell manufacturing using recycled wafers were set to be between 25 to 30%, and the total waste reduction potential was set up to 10%. ***Table 7***Table 5 represents a general flow of the experimental steps which were planned for this activity.

Table 5. Description of silicon recycling experiment steps

Step No.	Description
1	Collection of production waste and sorting
2	Preparation of reference and experimental feedstock (recycling of broken production scrap samples and recovery of silicon)
3	Manufacturing of new silicon ingots and silicon wafers (multi crystalline)
4	Production of Al-BSF solar cells using recycled silicon wafers
5	Production of reference Al-BSF solar cells using commercial Si wafers
6	Evaluation of results: I-V testing, QSSPC lifetime measurements, LBIC mapping, GHG emission calculation

Solar cell production waste was divided into 3 main categories as shown in Figure 41.

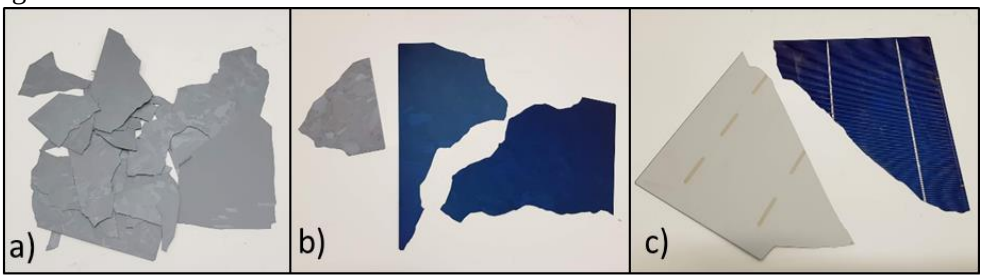

Figure 41. Several types of solar cell production waste: a) broken clean wafers (as-cut, textured), b) half processed non-metallized Si wafers (diffused and SiNx coated) and c) metallized and coated Si wafers (mainly finished broken solar cells)

Group A type of waste consists of non-contaminated broken wafer pieces because either they are already broken before the process starts (due to transport damage), or else they break after the 1st manufacturing process step which is 'Saw damage etching and texturization'. This process step modifies the surface of the silicon wafer by etching in the acidic medium, then it is rinsed and dried, therefore it leaves the silicon substrate uncontaminated, and, from the point of view of the material purity, it has the same quality as the raw material obtained directly from the manufacturers. The only problem is that it does not have the original size of 15.6 x 15.6 cm, which makes it no longer suitable for production.

Group B type of waste is collected in the intermediate manufacturing steps (process Nos. 2–5 in Figure 14) and typically has additional layers, e.g., the p-n junction and antireflective coating. During the formation of the p-n junction, phosphorus atoms are doped into the silicon wafer surface, and they diffuse to about 300–400 nm depth. The antireflective layer is made of hydrogenated silicon nitride (SiNx:H) by the low-frequency plasma-enhanced chemical vapor deposition (PECVD) process. This coating leads to efficient surface and bulk passivation of the silicon substrate and is normally about 78–80 nm thick.

The third, Group C, type of waste, is collected after manufacturing step No. 6 as shown in Figure 14. These wafers contain the p-n junction, SiNx layer and metal (silver, aluminum) contacts. Metal contacts are formed by the screen printing process with the subsequent steps of drying and fast firing in a belt furnace.

Because of the limited resource availability, only the most important Groups A and B were used in the further experiment steps. After the collection of SCW from the manufacturing line, it was sent to the research partners at SINTEF institute in Norway for the manufacturing of new silicon feedstock, ingots and wafer groups. Detailed explanation of the differences between these groups is given Table 6 below.

Table 6. List of mc-Si wafer groups manufactured by SINTEF

Group No.	Name	Ingot Casting Process	Ingot Size (Weight)	Feedstock	Resistivity – conductivity type	Solar cell samples produced
1	**Reference Lab**	P type multi Si	G1 (≈ 12 kg)	Poly Si with Boron doped	≈ 1.15 Ω.cm/p-type	80
2	**Group A**	P type multi Si	G1 (≈ 12 kg)	As-cut broken wafers	≈ 1.15 Ω.cm/p-type	37
3	**Group C**	P type multi Si	G1 (≈ 9 kg)	Solar cell scraps	≈ 1.15 Ω.cm/p-type	43
4	**Reference Industrial HQ (High Quality)**	Multi-Si	G5	Si- industrial	≈ 1.0 – 2.5 Ω.cm/p-type	100
5	**Reference Industrial MQ (Medium Quality)**	Multi-Si	G5	Si- industrial	≈ 1.0 – 3.0 Ω.cm/p-type	100

The reference and recycled mc-Si wafers were manufactured by using the process described by Syvertsen, Martin *et al*. [53] at *SINTEF*, Norway. A *Crystalox DS 250* pilot scale directional solidification furnace was used to cast G1 (9–12 kg) mc-Si ingots.

In order to determine the chemical composition of the selected samples, the samples from Group C were washed and rinsed with distilled water to remove any dust, grease, chemicals, adhesive, smudge, contamination, etc. and later dried for 24 h at room temperature. The dried samples were ground into micro-powder by using a *Planetary Ball Mill* (PM 100) at 300rpm and the varying milling time in the range between 5−20min with the 5-min interval. The optimum milling time was chosen based on the separation degree of each fraction. *Scanning Electron Microscope* (SEM) and *Energy Dispersive Spectrometry* (EDS) were used to analyze the morphology of the obtained RSCW powder, and the results showed that milling for 15 min was sufficient to break the mechanical and chemical bonds between the layers and obtain the full separation of fragments.

In order to precisely determine the concentrations of elements in the crushed RSCW samples, X-ray Diffraction (XRD) was used to determine the reflection peaks in the selected samples.

2.3.3 Diffusion process modifications

Material flow dematerialization can be defined as a principle which aims to reduce the quantity of materials in use and the waste generated in the production of a unit, which, in this case, is a mc-Si solar cell manufactured by JSC *Soli Tek R&D*. This method was applied for process steps Nos. 2, 4 and 5 (Figure 14): emitter formation, PSG cleaning and antireflective layer coating. These processes consume significant amounts of deionized water, nitrogen, oxygen, silane and ammonia gases, fluorine and hydrochloric acid as well as other hazardous and expensive chemicals, such as phosphoryl chloride ($POCl_3$). As by-products, liquid hazardous waste including diluted and concentrated acids, vapors and solid particles contaminated with various compounds are generated during the manufacturing process.

A modified diffusion recipe was developed by the *ISC-Konstanz* research institute which creates a low recombination emitter profile with in-situ oxide was implemented by using an industrial *SEMCO DF6000 – 500 LYDOP* diffusion furnace available at *Soli Tek R&D* which is capable of running at throughput of 2000 wafers/h. As reported in [54], in-situ oxidation during the thermal emitter formation was used in the manufacturing of high efficiency solar cells, but was still limited to the usage on mc-Si material due to large variations of results. The main idea of this process is to rely on diffusion from a limited dopant source. It means that a thin layer with a dopant is deposited as silicate glass on the wafer surface while using relatively low temperatures. After that, the supply of the dopant is switched off, and the temperature inside the diffusion tube is increased in order to initiate the drive-in step in the oxygen containing environment. In such a way, a high quality oxide is grown with good passivation properties, and a low surface concentration emitter profile is formed.

As a result of this new emitter, it was possible to leave out the PSG removal in diluted HF from the process chain. In addition, the subsequent SiNx coating step could be shortened, and the savings in consumption of silane and ammonia gases could be demonstrated. For the evaluation of results and the impact on the quality, price and material/waste reduction was calculated for standard and new production recipes.

The evaluation of quality was performed by measuring the I-V curve of the finished solar cells and determining such parameters as: efficiency (Eta, %), short circuit current density (J_{sc}, A), open circuit voltage ($V_{oc,}$ V) and filling factor (FF, %).

The evaluation of the manufacturing costs was done by taking into account the changed material consumption per cell and calculating the cost difference in Eur/pc and Eur/W_p.

The reduction of diluted acidic waste was calculated and compared for the two production recipes.

In took eighteen experimental rounds until the desired properties of the modified emitter were achieved. More than two hundred silicon wafers were used for manufacturing the reference and modified solar cells.

The standard process recipe schematic explanation was given in Figure 16 which indicates that the total emitter formation process consists of several parts: heat-up, deposition, drive-in and cool down. Typically, there are also several stabilization steps in between, but, as it is not relevant for the research, a closer look is needed into deposition and drive-in. During the deposition step, a dopant source is grown on the surface of a silicon wafer which is the phosphosilicate glass (PSG) layer. As shown in Figure 42, PSG is separated by a SiO_2 layer from the silicon surface. Therefore, in reality, a PSG layer is a phosphorus-rich binary P_2O_5 – SiO_2 system formed on the surface of a silicon wafer [55].

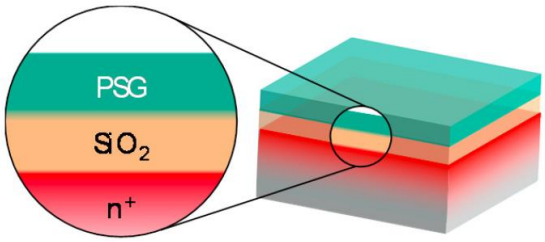

Figure 42. Schematic cross section of the solar cell surface after POCL3 diffusion [55]

If not removed, the standard PSG layer is detrimental to the efficiency of a solar cell since it contains high concentrations of unreacted phosphorus. The high concentration of phosphorus plays twofold because the ratio between active and inactive phosphorus influences the contact resistance with metal pastes and the emitter saturation current density. Therefore, it is a must to find the right balance between these two parameters in order to obtain a high efficiency solar cell. It was reported by A. Dastgheib-Shirazi *et al*. [56] that the ratio between the process gases like $POCL_3$-N_2 and O_2 plays the main role in the formation of the PSG layer.

The modified process is based on the diffusion from a limited dopant source. It means that, during the deposition step, the temperature has to be relatively low comparing to the standard process. This ensures that only a thin dopant-containing layer is deposited as silicate glass on the surface of silicon. After that, when the dopant gas flow is switched off, the temperature in the quartz tube has to be increased for the drive-in in the oxygen atmosphere. The presence of oxygen allows for growth of a high quality oxide and a low concentration emitter profile with excellent passivation properties. This process was demonstrated in a lab by the team of the *ISC-Konstanz* Solar Energy Research Institute [54]. The basis and knowledge generated during their lab scale experiments was used to transfer the process recipe to an industrial solar cell manufacturing line where it was adapted for industrial scale high throughput equipment and the manufacturing of hundreds of solar cells.

An illustration of various temperature profiles is given in Figure 43 where it is shown that the temperature has to be kept lower during the deposition phase and higher at the drive-in step. The exact temperature settings were discovered during the

experimental work carried out in this research. Another variation of the process parameters included the adjustment of the ratio between the process gases: nitrogen and oxygen.

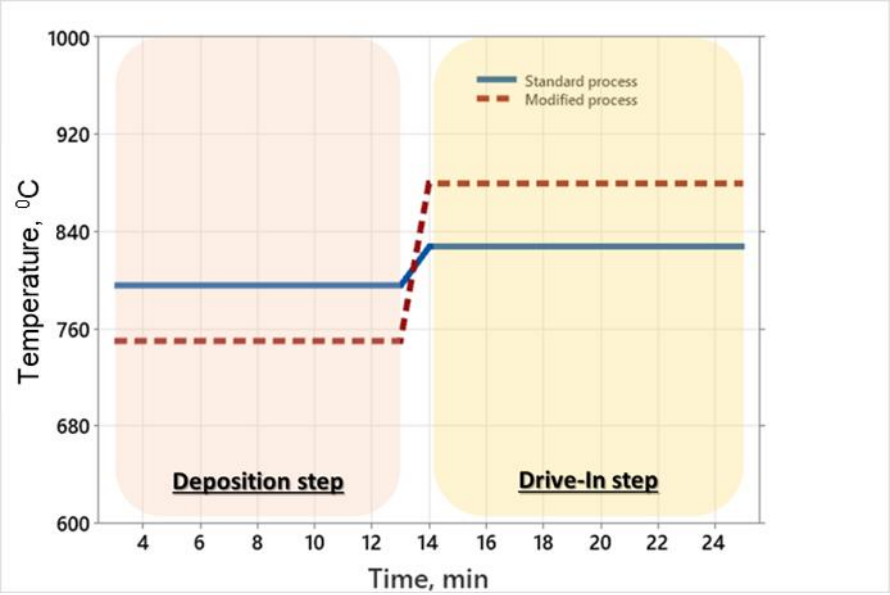

Figure 43. Schematic difference between temperature for standard and modified diffusion processes during the deposition and drive-in steps

In order to control and optimize the $POCL_3$ diffusion process, it is important to measure at least two parameters: the sheet resistance (R_{sheet}) of n diffused emitter region and the doping profile concentration (N). For the experimental part of this research, the following techniques and equipment were available:

Sheet resistance was measured by a 4-point probe method using semi-automatic *SOL Instruments* 4 point probe equipment (Figure 44).

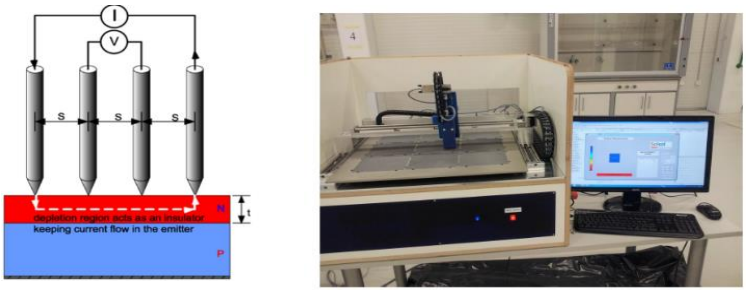

Figure 44. Measurement setup of emitter sheet resistance (image taken by author)

The 4-point probe method works in a way that the action of passing the current through the two outer probes and measuring the voltage through the inner probes allows the measurement of the substrate resistivity. As shown in Figure 44 a, the depletion region is acting as an insulator. Therefore, electrical current is flowing only through the n type region. The two outer pins are passing the current through the measurement sample while the inner two are detecting the voltage. Sheet resistance is then calculated by using the equation below:

$$\rho\left(\frac{\Omega}{cm^2}\right) = \frac{\pi}{ln(2)}\frac{V}{I} \tag{13}$$

where $\frac{\pi}{\ln(2)} = 4.53$, o ρ – sheet resistance in Ω/sq [26].

The emitter profile was measured by using *Wafer Profiler CVP 21* as developed by WEP. This tool works by the Electrochemical Capacitance Voltage Profiling (ECV) method which provides measurement of only the electrically active dopants and has a depth resolution in the sub-nm range. The technique is based on the destructive technique because the measurement sample is electrolitically etched between capacitance measurements. The depth-dependent charge carrier concentration profiles N(x) are determined by ECV measurements:

$$N = \frac{1}{q\varepsilon_0\varepsilon_r A^2}\ \frac{C^3}{dC/dV} \tag{14}$$

where q is the elementary electric charge, ε_0 – the vacuum permittivity, ε_r – the relative permittivity of silicon, A – the contact area, and C – the capacitance [57].

2.4 Description and characterization of loss mechanisms in solar cells

The implementation of the experimental part of this research is related to analyzing and improving power losses of solar cells. Therefore, it is important to briefly explain what it is in order to develop better understanding of the purpose of technological experiments.

The solar cell efficiency is limited by three main types of loss mechanisms: resistive, optical and recombination losses. It is an ongoing everyday job for many scientists and industrial players around the globe to find ways how to reduce it and to increase the maximum power of PV cells and modules.

In order to describe resistive losses, it is worth taking a look into an equivalent circuit diagram (Figure 45) which is used to present the structure and behavior of a standard photovoltaic cell.

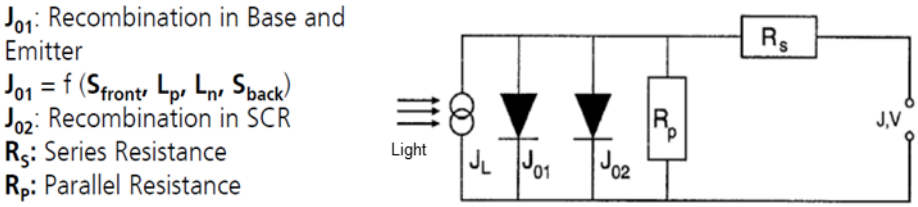

Figure 45. Equivalent circuit diagram of c-Si solar cell. Adapted by author based on publication by Sulyok *et al*. [58]

where J_L denotes the light generated current, J_{01} is the saturation current density of the 1st diode which denotes the recombination losses related to the front and rear surfaces, as well as the bulk quality determined by the diffusion length of positive and negative charge carriers. J_{02} represents the losses in the performance of a solar cell which are related to the recombination in the space charge region (SCR) [58].

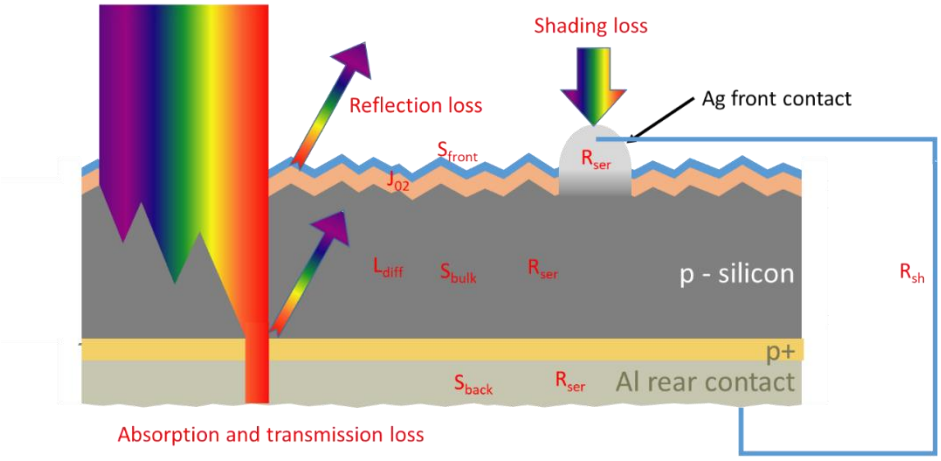

Figure 46. Typical power loss mechanisms in solar cell (see Chapter 2.4.1 for explanation of symbols)

A visual summary of all the main loss mechanisms in a c-Si solar cell is given in Figure 46 where the exact location of the occurrence of optical, resistive and

recombination losses is marked according to the internal structure of a standard Al-BSF solar cell.

2.4.1 Resistance losses

Resistive effects reduce the maximum power of the solar cell due to the power dissipation in the resistances which are divided into serial R_s and shunt R_{sh} (or parallel) types of resistances. The impact of resistance losses is typically evaluated by measuring the FF of a solar cell. The maximum current (I_{sc} – the short circuit current) is also affected if resistance losses become very high. It also highly depends on the geometry (area) and the structure of a solar cell; therefore, the common unit for resistance is Ωcm^2.

Series resistance R_{ser} is present in several parts of a solar cell: at the front and back metal contacts, the contact between the metal and silicon, the base and the emitter region, as shown in Figure 46. Parallel resistance R_{sh} is typically present due to defects generated in the structure of the solar cell during manufacturing processes. Low parallel resistance results in power losses by providing alternative current paths for the light-generated current which reduces the amount of the electrical current flowing through the PN junction. As an outcome, the voltage of the solar cell is reduced. This effect is very severe in low light conditions when there is less light-generated current.

Low shunt resistance causes power losses in solar cells by providing an alternate current path for the light-generated current. Such a diversion reduces the amount of the current flowing through the solar cell junction and reduces the voltage from the solar cell.

2.4.2 Optical losses

According to Figure 46, several optical loss mechanisms are present in a solar cell which are, first, shading due to metal contacts and the reflection on the front surface, then, there is parasitic absorption in the emitter region and the bulk of the solar cell, and, lastly, transmission losses occur due to uncaptured photons which pass through the solar cell without participating in the generation of charge carriers. Optical losses cause reduction of the current which is running through the solar cell.

2.4.3 Recombination losses

Recombination losses are one of the most detrimental and complex mechanisms. They are divided into extrinsic (surface and Shockley-Read-Hall via bulk defects) and intrinsic (Auger and radiative) categories:

$$\frac{1}{\tau_{\text{cell}}} = \frac{1}{\tau_{\text{Rad}}} + \frac{1}{\tau_{\text{SRH}}} + \frac{1}{\tau_{\text{Auger}}} \quad (15)$$

where:

- τ_{Rad} – radiative recombination is the dominating mechanism in direct band gap semiconductors and is the basis of how LED devices are working.
- τ_{SRH} – Shockley-Read-Hall (SRH) recombination is present in silicon solar cells because of material defects which create intermediate energy levels in the band gap. The SRH type of recombination is considered to be the main type of recombination for silicon semiconductor material.
- τ_{Auger} – Auger type recombination involves three charge carriers. When an electron moves from the conductive to the valence band, energy is extracted not as thermal energy or a photon, but it is transferred to another electron which is present in the conductive band. Auger recombination limits the lifetime of minority charge carriers, and it increases with the increasing doping concentration.

Recombination loss mechanisms can be solved by improving the quality of silicon, optimizing the cell manufacturing processes in order to avoid contamination, and by improving the properties of dielectric coatings which provide passivation for the surfaces and the bulk of the solar cell. In typical industrial solar cells, such layers as SiN_x, Al_2O_3 and SiOx are used for this purpose. The silicon oxide layer has been widely used in the microelectronics industry; it has also been applied in the manufacturing of first 20% efficient silicon solar cells. It has been reported that thermally grown SiO_2 passivation layers show good potential on n-type surfaces, like phosphorous emitters, which are also present in the Al-BSF solar cell structure analyzed in this research [59].

2.4.4 Characterization of recombination losses

The evaluation of recombination losses of solar cells in this research was performed by using the Quasi-Steady-State Photo conductance (OSSPC) [60] and the Light Beam Induced Current (LBIC) [61] methods. QSSPC measurement was performed by using a *WCT-120* device developed by *Sinton Instruments* (Figure 47) which is a stand-alone tool typically used by R&D labs and companies in the solar industry. This device is capable of assisting to process engineers in the monitoring and optimization of manufacturing processes by yielding valuable data about the

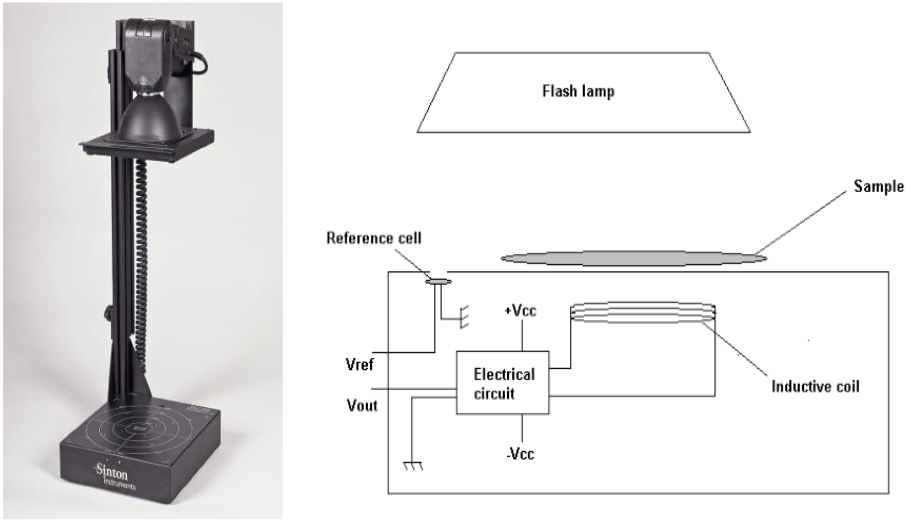

Figure 47. Schematic diagram of the WCT-120 Lifetime measurement equipment components [74] [75]

quality of the initial material, the contamination levels of heavy metals during wafer processing, evaluation of the quality of surface passivation, emitter dopant diffusion and process-induced shunting. It enables photo conductance measurements in the quasi steady state or transient modes. The main components of the system are a flash lamp, an inductive coil, a reference solar cell and electronics. When a sample is placed on the measurement chuck, the flash light is triggered, and this creates photo carriers in it. The conductivity of the sample is measured by the current induced in the coil, and the light intensity is measured by the reference cell. Both parameters are measured as a function of time. The conductivity is recalculated into the concentration of generated photo carriers, and the light intensity is recalculated into the frequency of the electron-hole pair generation. The ration between these two parameters is the lifetime minority carriers of the sample.

$$\tau_{eff} = \frac{\Delta n}{G(t)} \quad (16)$$

Two other important parameters which are measured by the QSPPC method and indicate the passivation quality of silicon wafer diffused emitters are the emitter saturation current density J_{oe} and implied V_{oc} (iV_{oc}). J_{oe} characterizes the recombination losses with the emitter region, and, for high quality passivated emitters, it should be as low as possible ($<10^{-12}$ A/cm^2) [5]. Implied V_{oc} is an alternative way to interpret the minority carrier lifetime. It allows determining the voltage of the device if contacts were applied, and it indicates the quality of the solar cell structure [62]. A big advantage of using the QSSPC method and the measurement of iV_{oc} is that there is no need to fabricate the entire solar cell, and the evaluation can be done on symmetrical samples thus allowing to save time and costs for process optimization.

$$iV_{OC} = \frac{kT}{q} ln\left(\frac{nN_A}{n_i^2}\right) \quad (17)$$

where n is the minority carrier concentration at the junction edge, n_i is the intrinsic carrier concentration, N_A is the base doping, kT/q is the thermal voltage [60] [62]. In this work, the QSSPC method was used for process optimization during the application of material flow dematerialization.

2.4.5 Light Beam Induced Current (LBIC)

In addition to the lifetime sample measurements using QSSSPC, another method was applied for the evaluation of the solar cell and silicon wafer material quality. Light Beam Induced Current (LBIC) technology based measurements are able to reveal the extended defects and their electrical properties in the silicon wafer material. LBIC (Figure 48) is based on the electrical current measurement when a laser beam is shone on the sample in one point thus creating a local electrical current.

This current represents the short circuit current at a specific location on a measurement sample.

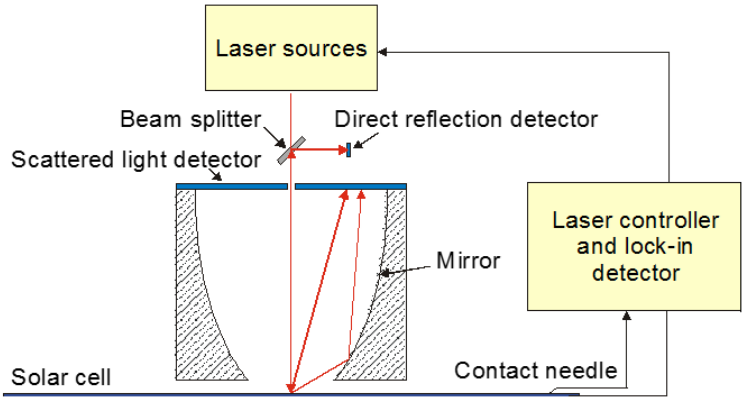

Figure 48. Explanation of LBIC method [61]

At the same time, the reflection (R) of a laser beam is measured. Having obtained these values (I_{sc} and R), the internal Quantum efficiency and other parameters can be determined [61].

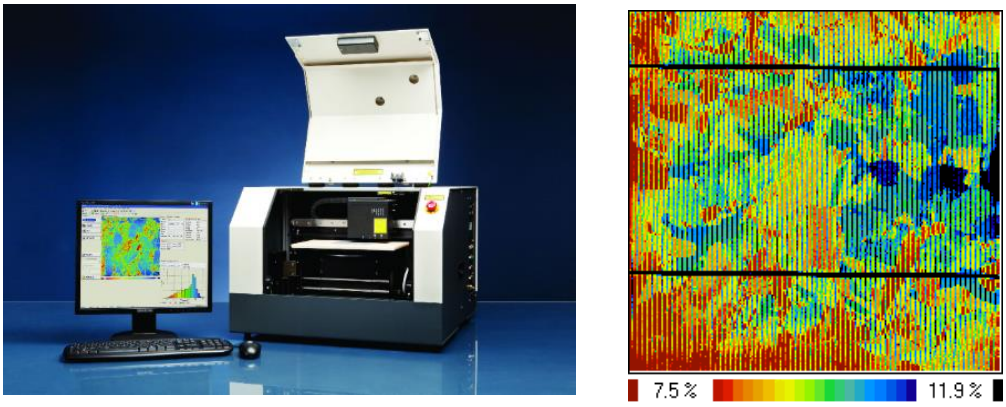

Figure 49. Illustration of *WT-2000PVN* measurement system from Semilab which was used to obtain minority carrier diffusion length of solar cells manufactured from recycled silicon [63]

LBIC results were obtained by using a *WT-2000PVN* table top measurement system from *Semilab* (Figure 49) [63]. LBIC mapping of the full solar cell area was applied in order to measure the minority carrier diffusion length of standard solar cells and samples made from recycled silicon. This parameter is important because it gives the average length that a carrier moves between generation and recombination and is highly dependent on material quality. The diffusion length can be defined as follows:

$$L_D = \sqrt{D\tau} \qquad (18)$$

where D is the diffusion coefficient and τ is the lifetime of the excited carrier.

2.4.6 Reduction of recombination losses by deposition of SiO_2 layer

In the solar cell technology, thin surface layers are used for two purposes – to improve the antireflection properties of incident light in order to reduce optical losses and to provide surface passivation so that to reduce recombination losses at the surface. Dielectric layers of SiO_2 (silicon dioxide), Si_3N_4 (silicon nitride), TiO_2 (titanium dioxide) or Al_2O_3 (aluminum oxide) are used to serve for these functions in various solar cell structures [24]. What is relevant for this research is the stack of SiO_2 and Si_3N_4 layers.

SiO_2 is normally grown at high temperatures (800–1200 ^{0}C) in a tube furnace where Si is oxidized in the presence of Oxygen gas. This is the so-called dry process which can be briefly explained by using the following equation:

$$Si(s) + O_2(g) \rightarrow SiO_2(s) \qquad (19)$$

The thickness of SiO_2 is controlled by temperature and time, and tenths of nm is typically enough to provide the necessary passivation properties. As SiO_2 is a dielectric, it also provides good surface passivation properties. This is a must for solar cells because silicon, as a crystalline material, has discontinuity of the crystal structure arrangement which leads to the formation of the so-called dangling (unfinished) bonds. These crystal defects act as recombination centers for charge carriers. SiO_2 is able to passivate the dangling bonds, which results in the reduction of surface recombination velocity.

As shown by Valentin D. Mihailetchi *et al*. [64] SiO_2 can be grown in situ without the need for investment into new production equipment by merely utilizing the already available diffusion furnaces. It also shows excellent passivation properties in combination with SiNx.

The goal of this research was to adapt in situ silicon oxide growth process for the p type multicrystalline wafer based solar cell industrial process, and the theoretical part of this task is further explained in Chapter 3.2.

2.5 Evaluation of environmental impact

Two basic and yet widely accepted indicators were used in this thesis to assess the environmental impact of recycling and process modification innovations in the solar cell manufacturing stage.

The first is the energy payback time (EPBT) which shows what is the period of time for an energy system to generate as much energy as it was consumed to produce that system.

$$EPBT = \frac{Energy\ used\ for\ production}{Energy\ generated\ in\ one\ year} \quad (20)$$

EPBT is a parameter which heavily depends on the geographical location because it takes into account the average energy yield generated by a 1 kWp system in one year, or, in other words, the photovoltaic power potential. This number obviously depends on the solar irradiation level and can vary a lot depending on the location.

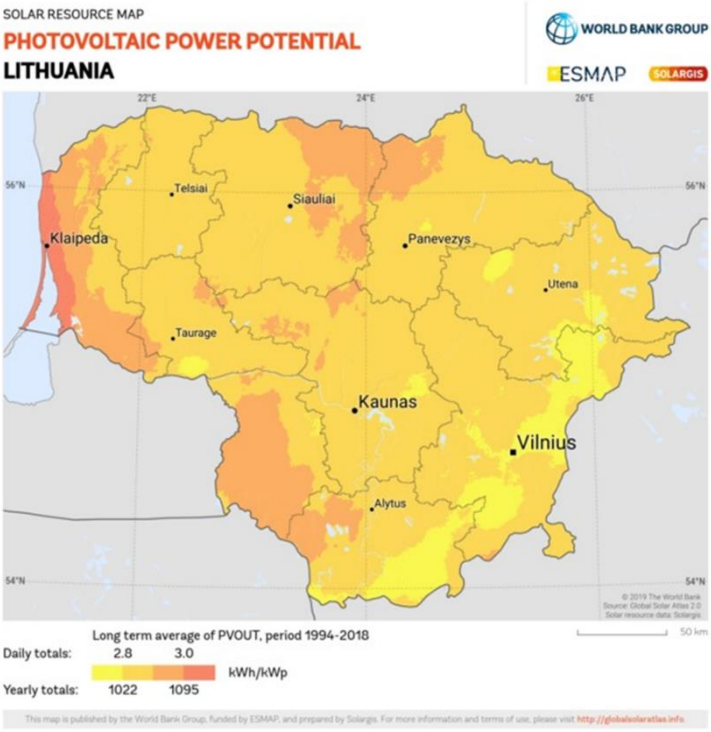

Figure 50. Photovoltaic power potential for Lithuania [65]

For example, the PV power potential for Lithuania (Figure 50) is about 1050 kWh/kWp, whereas, for a much sunnier region, such as southern Spain, it reaches more than 1600 kWh/kWp. In this thesis, Lithuania was chosen as a region for the evaluation of EPBT.

The second most basic LCA indicator is the greenhouse gas (GHG) emissions (GHG) during the lifecycle of the product(s). GHG emissions expressed as the carbon footprint are a widely accepted measure of the product or service impact to climate

change in many industries, including photovoltaics as well. PV manufacturers have to take it into account if they want to sell their products in such countries as France which applies strict carbon footprint rules to solar power project development.

LCA analysis was performed by using the *ILCD 2011 Midpoint+ V1.11* [66] and *ReCiPe 2016 Endpoint H* [67] methods. The calculations were performed by using the *SimaPro* software version 9.1.0.8 with the *ecoinvent 3.6* database.

The system boundaries of the environmental impact evaluation have already been presented in Chapter 2.2. The data which was used for LCA and EPBT was taken from Tables 6, 7 and 8 presented in Chapter 2.7.

2.6 Assessment of cost savings

Modified processes and the usage of recycled silicon in the production of mc-Si solar cells have an impact not only on the environment and product quality, but also on the manufacturing costs. Savings due to the reduction of material consumption are also expected. The following mathematical formulas were used for evaluation:

$$X_i = P_i \times (M_{Std} - M_{Mod}) \qquad (20)$$

$$X_{cell} = \frac{\sum_{i=m}^{n} X_i}{W_p} \qquad (21)$$

where:

X_i – cost difference of materials in Eur/cell
P_i – price of material *i* in Eur/kg or Eur/l
M_{Std} – quantity of material kg or l per cell for the standard process
M_{mod} – quantity of material kg or l per cell for the modified process
Wp – power of a solar cell in watts.

In order to simulate cost savings for the real manufacturing environment, it was assumed that a solar cell factory is running at the 80 MW_p annual capacity, which, depending on the solar cell efficiency, is about 15 million solar cells.

The final cost assessment results were recalculated for a functional unit of 1 kWp, and the actual values were expressed in % (instead of Eur/Wp) due to confidentiality restrictions.

2.7 Data sources

The cell and module production data including values for materials and energy consumption, waste generation, production yield and quality parameters were kindly

provided by the manufacturing company *Soli Tek R&D* (Lithuania) whose facilities were used for the experiments performed in this research. *Soli Tek* has been running the Al-BSF solar cell production since 2013 with the 80 MW annual capacity and a 100 MW module line. These numbers clearly indicate that our hypothesis has been tested on the real industrial level, which allows generating industry-relevant results.

The lifecycle inventory for a functional unit of 1kWp mc-Si Al-BSF solar cell is given in Table 7, Table 8 and Table 9.

Table 7. List of consumables and their quantities used for standard and modified production processes of Al-BSF solar cells

Process step	Consumable	Standard	Modified	Unit
Saw damage etch & Texture	**DI water**	731.10	731.10	l/kW_p
	HNO_3	0.38	0.38	l/kW_p
	HF	1.20	1.20	l/kW_p
	AcAc	0.15	0.15	l/kW_p
	HCl	0.04	0.04	l/kW_p
	KOH	0.07	0.07	l/kW_p
Emitter formation	**Nitrogen gas**	4.45	2.64	kg/kW_p
	Oxygen gas	47.77	7.79	kg/kW_p
	$POCL_3$	0.0009	0.0003	kg/kW_p
Chemical Edge Isolation	**DI water**	537.78	537.78	l/kW_p
	HNO_3 acid	0.50	0.50	l/kW_p
	HF acid	0.14	0.14	l/kW_p
Phosphorous Glass Cleaning	**DI water**	1.45	0.00	l/kW_p
	HF	0.0006	0.00	l/kW_p
Antireflective layer coating	**SiH_4 gas**	10.80	10.80	l/kW_p
	NH_3 gas	27.11	27.11	l/kW_p
	NF_3 gas	19.56	19.56	l/kW_p
Metallization	**Ag/Al paste**	24.44	24.44	g / kW_p
	Al paste	333.33	333.33	g / kW_p
	Ag paste	10.00	10.00	g / kW_p

Table 8. Consumption of electricity in manufacturing of silicon feedstock and solar cell processes

Process step	Standard cell	Modified Emitter	Modified Emitter + recycled Si feedstock
	kWh/kWp	kWh/kWp	kWh/kWp
Metalurgical grade silicon	34.67	34.67	0.00
Solar grade silicon	577.78	577.78	0.00
Ingot casting	54.65	54.65	54.65
Saw damage etch & Texture	11.6	11.6	11.6
Emitter formation	11.47	11.47	11.47
Chemical Edge Isolation	4.38	4.38	4.38
Phosphorous Glass Cleaning	5.28	0.00	0.00
Antireflective layer coating	19.33	19.33	19.33
Metallization (printing)	12.37	12.37	12.37
Metallization (drying and firing)	5.16	5.16	5.16
Technical exhaust	10.74	10.74	10.74
Total	747.42	742.14	129.70

As reported by F. Chigondo [68], production of the main raw material for photovoltaics industry – metallurgical grade silicon – consumes approximately 12 kWh/kg of electrical energy because it is manufactured by the reduction of silicon dioxide with carbon at very high temperatures (>1900 °C). There are several methods (metallurgical and chemical ones) to make solar grade silicon, but the most common one is the Siemens^{TM} process which is toxic, produces corrosive compounds, and requires about 200 kWh/kg of energy to reach the purity level which is suitable for cell manufacturing.

Table 9. Average quantities of various kinds of process waste generated during manufacturing of Al-BSF solar cells

Process step	Silicon wafer breakage (kg/kWp)	Liquid VOC waste (kg/kWp)	Inorganic dust after burner-washer scrubber (kg/kWp)	HF/HNO_3 waste (l/kWp)	CaF_2 sludge (kg/kWp)
Saw damage etch & Texture	0.007			1.65	1.21
Emitter formation	0.003				
Chemical Edge Isolation	0.005				
Phosphorous Glass Cleaning	0.000				

Antireflective layer coating	0.002		0.0091		
Metallization	0.019	0.052			
Technical exhaust	0.000				

2.8 Statistical data analysis

For the statistical evaluation of the experimental results, mainly the electrical parameters of the experimental groups, the boxplot method was used. Boxplots are very useful because of a very convenient way to understand the spread and detect the outliers of the data set [69]. Box plots visualize the distribution of the data based on the five number summary as explained below in Figure 51.

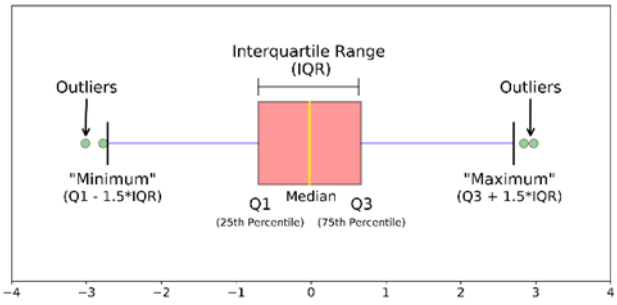

Figure 51. Example and explanation how to understand a box plot [69]

The five numbers which are calculated by using the box plot method are the following:

- Minimum Score – it is the lower score excluding the outliers.
- Lower Quartile (or Q1) – 25% of scores fall below its value.
- Median – the median marks the mid-point of the data and is shown by the line that divides the box into two parts. 50% of the scores are greater than or equal to this value, and 50% are lower.
- Upper Quartile (or Q3) – seventy-five percent of the scores fall below the upper quartile value, and 25% of the data are above it.
- Maximum Score – gives a value of the highest score, excluding the outliers.
- Whiskers – the upper and lower whiskers represent the scores outside the middle 50% (i.e., the lower 25% of scores and the upper 25% of scores).
- The Interquartile Range (or IQR) is the box plot which shows the range between Q1 and Q3, or, in other words, the middle 50% of scores.

In order to develop better understanding of the significance of the experimental results, statistical analysis, including data point spread analysis, probability plots using Normal and Weibull fits and Kruskal-Wallis Tests, was performed with the statistical package available in *Minitab 20.2* software [70].

3 EXPERIMENTAL RESULTS

3.1 Silicon recycling

In this chapter, a detailed overview of the experimental results is provided including elemental composition analysis of the solar cell waste, recycling of silicon, and manufacturing of Al-BSF solar cells using this material, application of dematerialization and the related diffusion process modification results. The achievements are evaluated by looking into the qualitative, economic and environmental impact related KPIs.

3.1.1 Elemental composition of untreated solar cell waste

As already explained in Chapter 2.3.2, three types of SCW were collected from an operational production line. For the elemental composition analysis, Group C (breakage of fully processed solar cells) was used. At the beginning, the primary content of the investigated SCW was evaluated by the XRD method. The XRD spectrum is undoubtedly dominated by silicon peaks (the violet color) and aluminum peaks (the blue color) which are visible. Trace amounts of quartz SiO_2 (the very small green peaks) were recorded as a product of slight oxidation of silicon. Minor Ag peaks (the red color) are also weakly observable (see Figure 52).

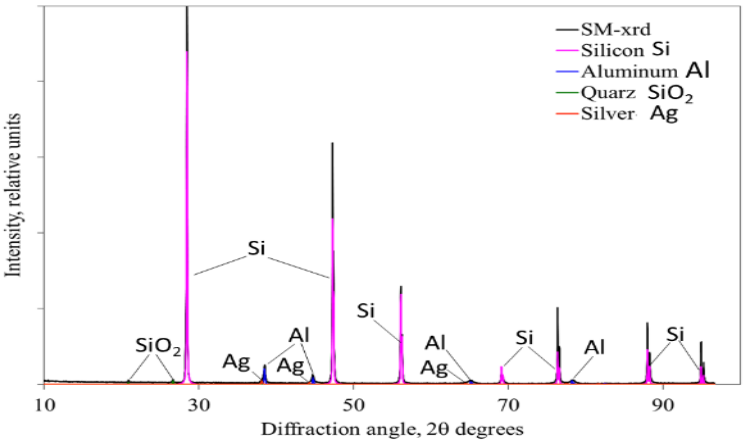

Figure 52. XRD spectrum of SCW Group C

In Figure 53 and Figure 54, the SEM images and EDS spectrums of untreated SCW are presented. Figure 53 shows the results for milled SCW, whereas Figure 54 depicts crushed SCW. For the crushed sample, the average size of SCW particles is 200–500 µm, for the milled sample, the result was 10–50 µm.

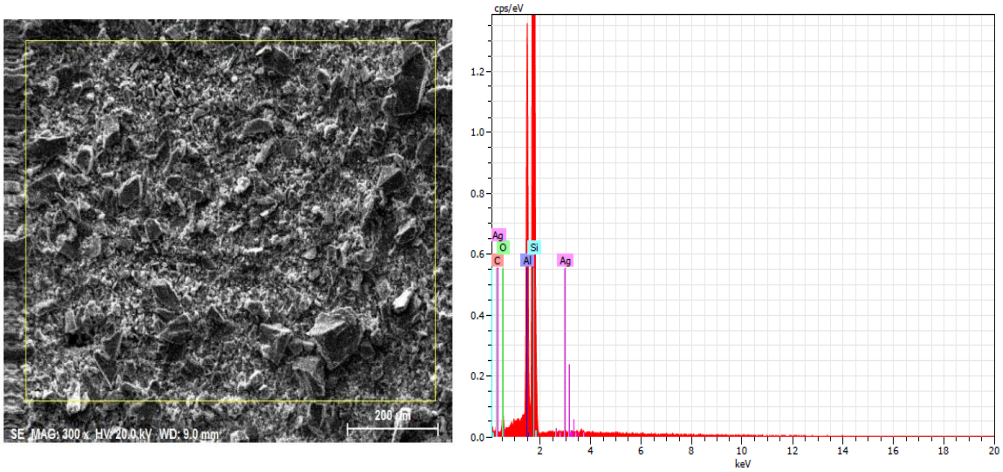

Figure 53. SEM image and EDS spectrum for milled SCW samples

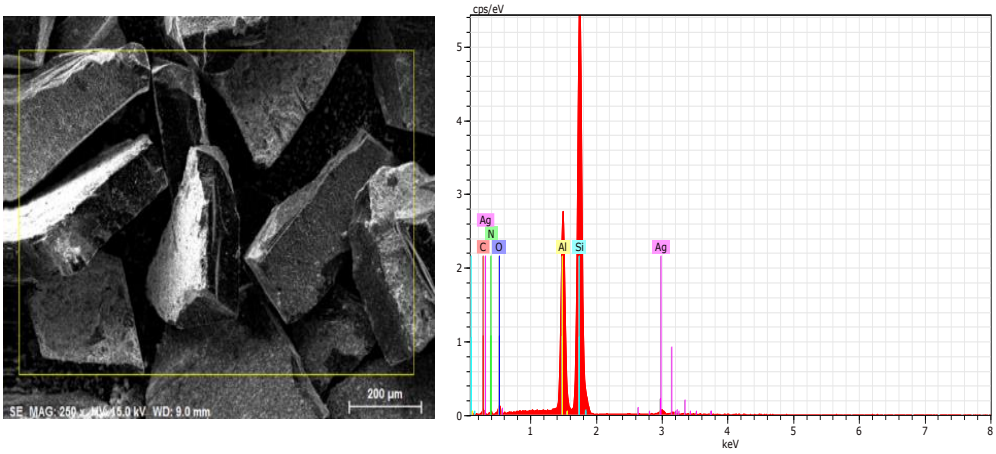

Figure 54. SEM image and EDS spectrum for crushed SCW samples

XRD and EDS measurements confirm the type of elements which can be found in SCW, and this information is very important so that to choose the further treatment methods of SCW, since the composition and concentration of impurities will impact the purity and value of the recycled silicon material and will determine the potential area of reuse after recovery.

3.1.2 Quality evaluation of silicon solar cell scrap Recycling

There were 5 groups of wafer material including the lab scale and two industrial reference groups, as well as two experimental groups of wafers manufactured from SCW. Silicon wafers of all groups were processed at the industrial *Soli Tek R&D* cell production line while keeping the process recipe stable for all groups. A summary of the achieved results, including the batch size and the main solar cell electrical parameters, are shown in Table 10.

Table 10. Results of reference and experimental solar cell groups

Group No.	Name	Number of solar cells produced	Eta, %	V_{oc}, mV	Js_c , mA/cm^2	FF, %
1	**Reference Lab**	80	17.26	627.36	34.69	79.22
2	**Group A**	37	17.38	627.06	35.43	78.20
3	**Group C**	43	9.97	571.56	22.81	76.87
4	**Reference Industrial HQ**	100	17.86	631.32	35.88	78.87
5	**Reference Industrial MQ**	100	17.50	623.21	35.80	78.47

The obtained results show that Group A (feedstock from a mixture including as-cut and textured broken wafers) achieved a threshold efficiency value of 17.0%, which concludes that such a type of production waste can be reused in production without any loss in quality. In a typical 80 MW capacity production line, 1–1.5% of silicon wafers are broken in various stages of production. Group A type scraps make up about 50% of this volume, which is about 160,000 units/year, or, if we count at year 2016 (the period of our experiments) level prices – about 100,000 Eur annualy. The solar cell plant, having implemented such cooperation with the manufacturers of silicon wafers, would potentially reduce the amount of generated waste by 0.5–0.75% because of getting a possibility to produce new solar cells from the scraps.

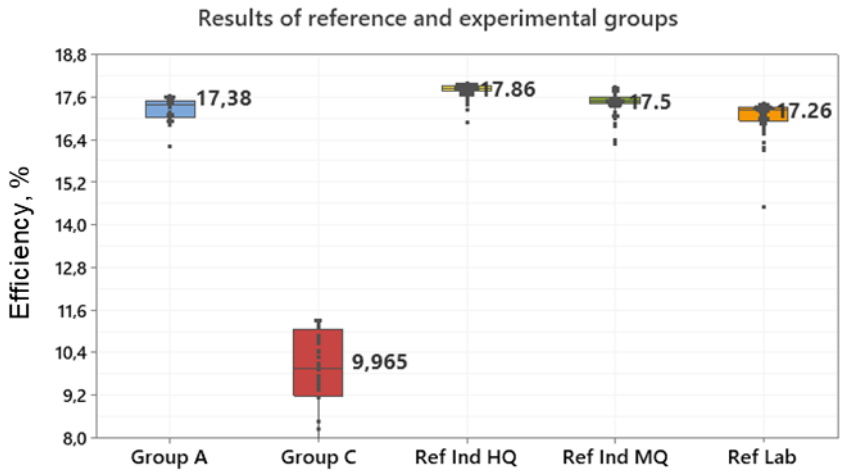

Figure 55. Comparison of efficiency medians for reference (Industrial High quality, Industrial Medium Quality, Reference laboratory) and recycled (Group A and Group C) solar cells

A more detailed look into the distribution of the solar cell efficiency for various groups is shown by the box plot graphs (Figure 55). It can be seen that the higher is the material quality, the more narrow spread of results can be achieved. Some basic statistical analysis was also performed for better understanding and interpretation of the measured results. In Figure 56, the shape and spread of the data points for each experimental group is shown.

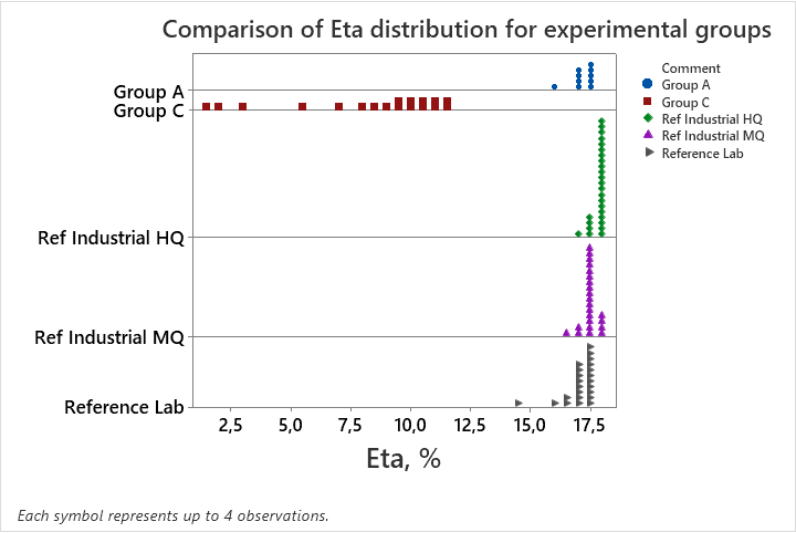

Figure 56. Efficiency data point distribution comparison for silicon recycling experimental groups

Clearly, Group C (a low quality solar cell) has a much larger spread of data comparing to the other groups. The scale and shape of the data points from the remaining groups looks to be comparable and threfore is worth being analyzed a bit further.

A test whether the data sets follow Normal or Weibull distributions was performed. Group C in both probability plots (Figure 57 and Figure 58) has a significant difference comparing to the other groups, which is shown by the calculated parameters: standard deviation, AD and P values, shape and scale.

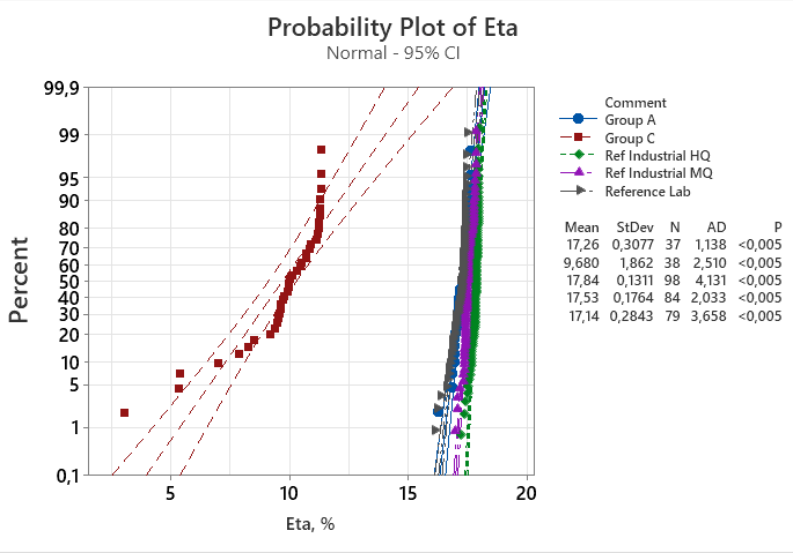

Figure 57. Probability plots to test whether the data follows the normal distribution

Results of the normal distribution test show that the p-values are well below the significance level of 0.05, and therefore the hypothesis that our data is following the normal distribution has to be rejected (Figure 57).

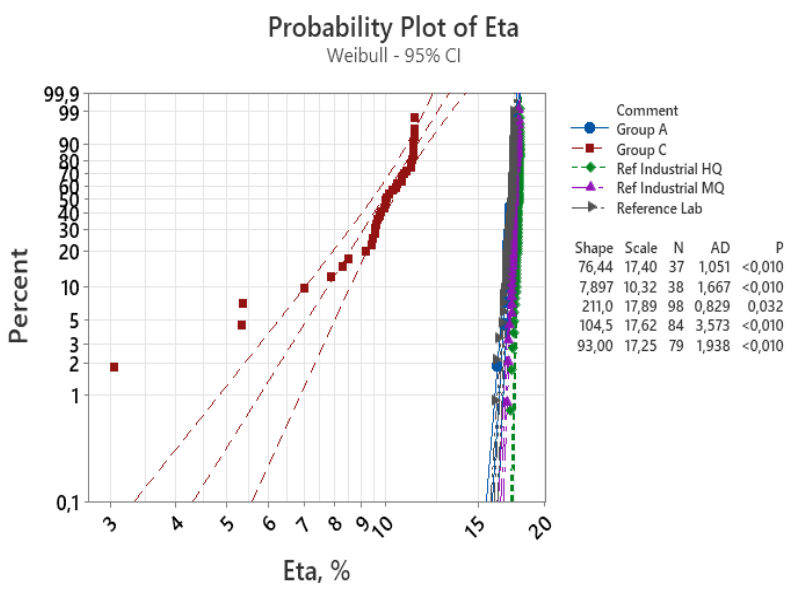

Figure 58. Probability plot to test whether the data follows Weibull distribution

The results of the Weibull distribution test show that most of the p-values are as well below the significance level of 0.05 except for the Red Industrial HQ group which has a p-value of 0.032 and the lowest AD value of 0.829. It indicates that the data distribution of this particular group has the closest match to the Weibull type among others (Figure 58). This group also has the highest shape factor, which indicates that it is the left-skewed type of distribution. From the technical point of view, this (Weibull) type is a desired shape of the solar cell efficiency data distribution because it allows to have a bigger concentration of good quality (high efficiency) solar cells and minimize the number of low quality (low efficiency) cells in the manufacturing.

A closer analysis of Group C (feedstock from finished solar cell scraps) samples was made in order to understand better the loss of efficiency. The LBIC mapping technique was applied in order to determine the minority carrier diffusion length. As

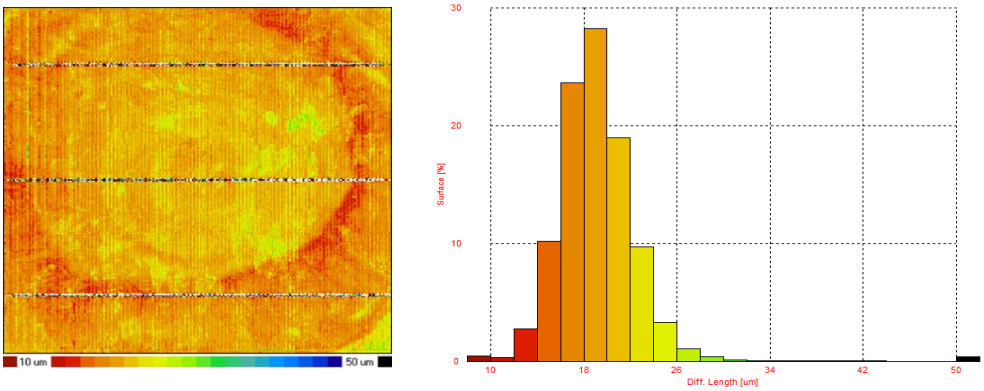

Figure 59. Results of LBIC measurements for low performing Group C solar cells

shown in Figure 59, the diffusion length is extremely low, and it is in the range of 10–30 μm. In addition, in the left image, where the LBIC mapping of the solar cell surface is given, a clear circular pattern of the low diffusion length region is visible, which indicates a contaminated silicon wafer region. As reported in literature, the average minority carrier diffusion length values for a high quality silicon material should be in the range of 400 to 600 μm [71]. There are three main parameters which are limiting the diffusion length: doping concentration, impurity concentration, and solar cell process parameters. The solar processing parameters in this experiment were kept constant for all wafer groups, including the reference and recycled samples. Therefore, it is possible to neglect the influence on low diffusion length of manufacturing process instability. Impurity concentration is likely to be the main reason because a clear circular pattern is visible in the LBIC map of Group C low efficiency solar cell samples. One can think about contamination during the preparation of feedstock and/or ingot casting. When taking into account that the

silicon feedstock for this group of solar cells was manufactured from recycled fully processed silicon cell scraps, which means that the material contained several type of elements, LBIC measurement results proved that these elements reduced the purity of silicon dramatically.

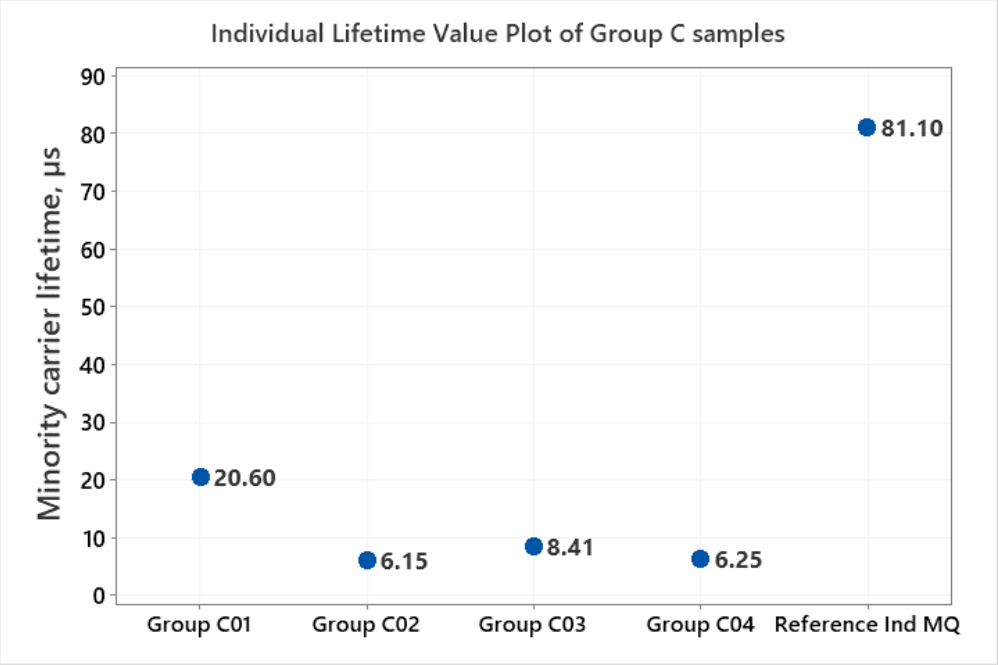

Figure 60. Results of QSSPC minority carrier lifetime measurements for samples of Group C solar cells

The minority carrier lifetime of several Group C wafer samples was measured by using the QSSPC method. For this characterization step, symmetrically (both sides) diffused and passivated wafer samples were manufactured. The extremely low level of the lifetime values indicates issues with the material quality. The medium quality reference industrial silicon material, which was used for comparison in this experiment, showed the average lifetime values of 81.10 µs. The results in Figure 60 largely correspond to what was already shown by LBIC mapping. With polysilicon (a standard feedstock material) costs being around 10 Eur/kg [72], it makes the purification of contaminated SCW a highly unattractive option from the economic point of view.

To the best of the author's knowledge, a similar experiment has never been performed before by other research groups at the time of writing this thesis; therefore, it can be stated that new results have been generated which can be used as a reference for future experimental work in this field.

3.2 Process modification

As described in Section 3.3.3, process modification was implemented by applying the modified emitter formation process step in order to form an in situ grown silicon oxide passivation layer on the surface of multicrystalline silicon solar cells. The main changes made to the process were:

• Reduction of the flow of $POCl_3$ material.

• Increase of the drive-in step temperature by ≈ 100 °C. At the same time, the reduction of the deposition step temperature by ≈ 50 °C was made.

• The optimization of the ratio between oxygen and nitrogen gas flows in order to ensure the homogeneity of the emitter formation across the silicon wafer surface and along the process quartz tube was made.

For better understanding of the combination of all the process parameter modifications, a graph has been created which shows the most important steps in the diffusion process: deposition and drive-in (Figure 61).

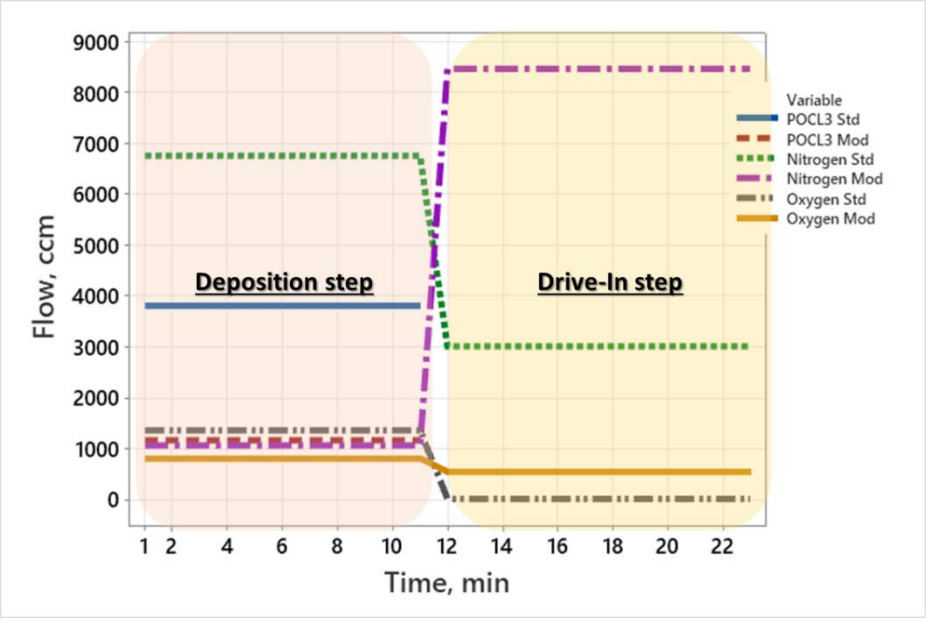

Figure 61. Graphical summary of main differences between standard (STD) and modified (Mod) diffusion process recipes

In the modified recipe, a flow of $POCL_3$ material, which is the source of phosphorus, was reduced more than 3 times during the deposition step. The nitrogen gas consumption trends show that a flow of this consumable was reduced dramatically during the deposition step, but increased almost 3 times for the drive-in. Oxygen gas consumption was lowered for the deposition, but increased slightly for the drive-in as compared to the standard process recipe.

The impact of process modifications was first analyzed on the quality parameters. Symmetrical lifetime samples were produced, and two parameters were measured by using the QSSPC technique: implied V_{oc} and minority carrier lifetime. These two parameters indicate the quality of the emitter and passivation properties.

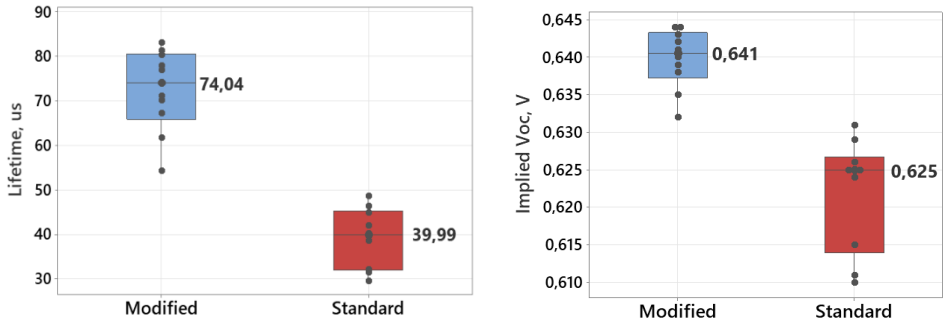

Figure 62. Minority carrier lifetime (left) and implied V_{oc} (right) measurements by QSSPC method of samples with different emitter recipes

As seen in Figure 62, a modified emitter shows a better performance comparing to the standard recipe. This indicates that the modified diffusion recipe is performing as expected, and an in-site grown SiO_2 layer provides excellent passivation properties.

Next, standard and modified emitters were characterized by employing the Electrochemical Capacitance-Voltage (ECV) profiling technique which is capable to measure active carrier concentration profiles in semi-conductor layers.

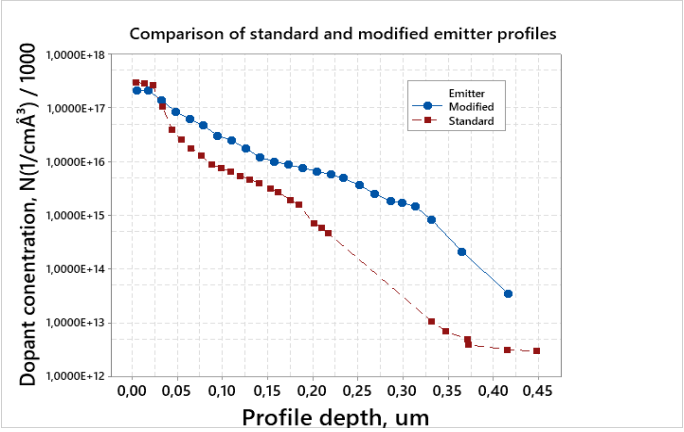

Figure 63. ECV profile measurements of standard and modified emitters

As shown in the graph in Figure 63, the modified diffusion process creates a profile which has a higher and deeper concentration of active carriers in the bulk comparing to the standard emitter profile. That is a result of the modified temperatures and carrier gas flow during the deposition and drive-in steps of the diffusion process. The lower surface concentration and the slower drop near the surface indicates that the new emitter profile will have a much smaller 'dead' region which is full of electrically inactive phosphorus. ECV measurements confirmed that the modified process parameters were chosen properly and delivered a desired emitter profile. The next step in the experiments related to dematerialization was the optimization of the SiNx antireflective coating. This became necessary because the in-situ grown SiO_2 layer increased the total thickness of the front side coatings and affected negatively the antireflection properties. In order to understand how to optimize it, front surface light reflection curves were obtained by performing measurements on the sample cells with standard and modified emitters.

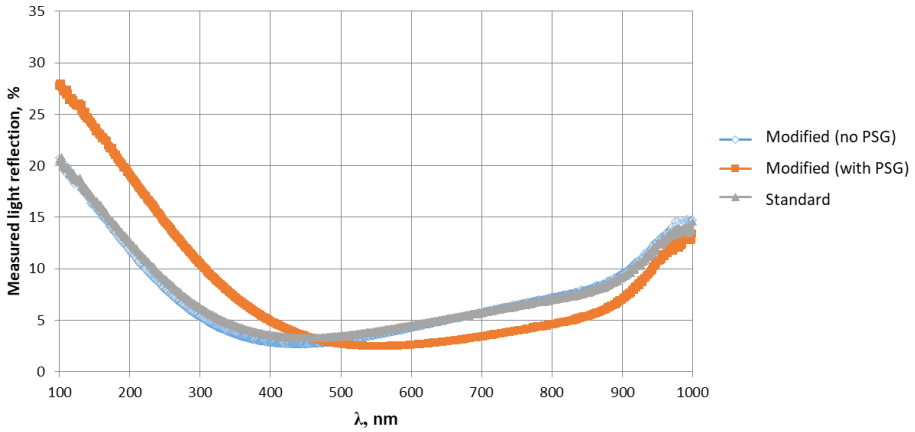

Figure 64. Reflection curves of standard and modified (with and without PSG) solar cells. The orange curve (modified emitter with PSG) shows that there is a shift of minimum reflection towards the longer wavelength region

The results given in Figure 64 show that those modified solar cells in which the PSG layer is present give the reflection curve whose minimum is shifted towards the longer wavelength region compared to the cells which do not have the PSG layer in between the silicon surface and SiNx AR coating. This mismatch was compensated by slightly reducing the thickness of the SiNx layer for the solar cells with a modified emitter without the PSG layer being removed. The reduction of SiNx thickness was in the range of 10–15 nm.

The data of all the process and AR layer modifications was gathered into one graph shown in Figure 65. The efficiency of solar cells with the modified emitter profile without the PSG layer being removed is at the same level as that of the reference group and is equal to 16.84% and 16.80%, respectively. The 0.04% absolute lower efficiency is within the measurement accuracy tolerance range, therefore, it is negligible in this particular case.

The second parameter, the short circuit current (I_{sc}), is lower by 0.21 A for a the modified emitter (Modified 1st run) with the PSG solar cells comparing to the standard solar cells. This corresponds to the results obtained while measuring AR properties where a shift in the minimum reflection position was detected. In order to improve Isc for the modified emitter solar cells, the SiNx layer thickness optimization by reducing it was performed.

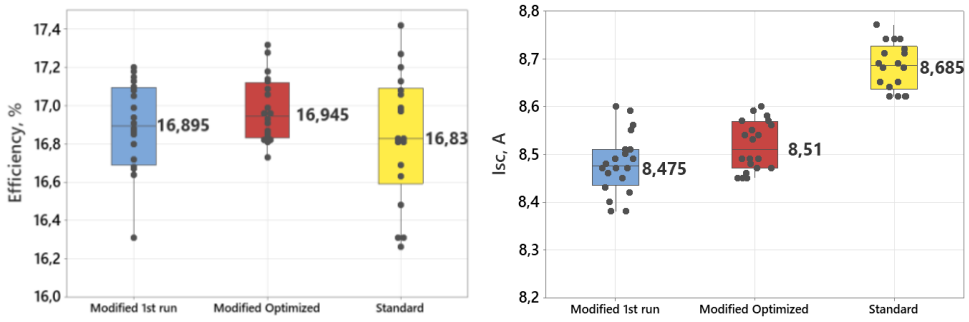

Figure 65. Boxplots of the main electrical parameters – efficiency and short circuit current (Isc) of solar cells manufactured with standard and modified emitters

The 'Modified Optimized' group showed a slight increase in the short circuit current of 0.035 A comparing to the 'Modified 1st run' group. This leads to the higher overall efficiency by 0.115% abs comparing to the standard group. In addition, the reduction of the SiNx layer thickness means a shorter process time and a lower silane and ammonia gas consumption level.

The spread of the data points of the process modification experiment is shown in Figure 66.

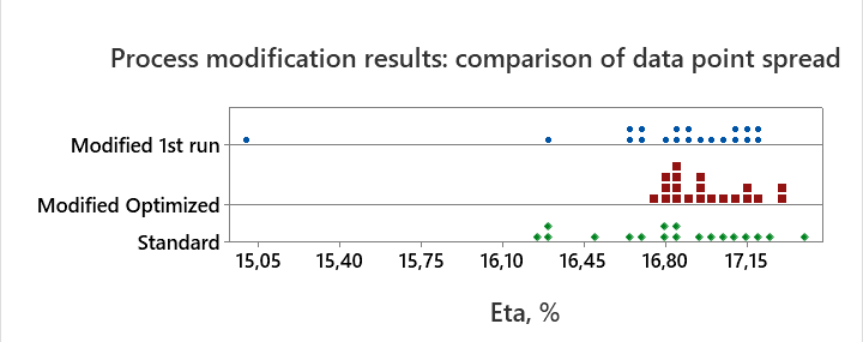

Figure 66. Comparison of cell efficiency measurement datapoint distribution for different groups of process modification experiment

Unfortunately, there is a big spread of the measured solar cell efficiency values for all groups; therefore, it is important to understand whether the difference between the medians of the three process modification experiment groups are significant from the technical and statistical point of view. To answer this question, a statistical test using the Kruskal-Wallis method was performed; it is represented by Figure 67.

Descriptive Statistics

Comment	N	Median	Mean Rank	Z-Value
Modified 1st run	20	16,895	28,2	-0,43
Modified Optimized	20	16,945	33,5	1,33
Standard	18	16,830	26,5	-0,92
Overall	58		29,5	

Test

Null hypothesis	H_0: All medians are equal
Alternative hypothesis	H_1: At least one median is different

Method	DF	H-Value	P-Value
Not adjusted for ties	2	1,85	0,396
Adjusted for ties	2	1,85	0,396

Figure 67. Kruskal-Wallis test results for diffusion process modification measurement results

In order to determine whether any of the differences between the medians are statistically significant, the p-values were compared to the significance level (equal to 0.05). From the calculated test results, the p-value of 0.396 was received, which suggests that the differences between the medians are not statistically significant.

Table 11. Main statistical parameters for process modification experimental groups

Variable	Comment	Total Count	StDev	Minimum	Median	Maximum	Range
Eta	Modified 1st run	20	0,481	15,000	16,895	17,200	2,200
	Modified Optimized	20	0,168	16,730	16,945	17,320	0,590
	Standard	18	0,341	16,260	16,830	17,420	1,160

Looking from the technical point of view, the medians are also not significantly different. However, when analyzing the values in Table 11, it can be clearly seen that the ‘Modified Optimized’ solar cell group not only had the highest median value, but also featured the smallest StDev and Range numbers, which is a positive overall result of the process modification experiment and a preferred situation in the solar cell production because the narrow range and small standard deviation indicate a better controlled process, and therefore more stable manufacturing conditions.

As a result of the above described process modifications, a significant reduction of materials consumption in the emitter formation step has been achieved (Figure 68).

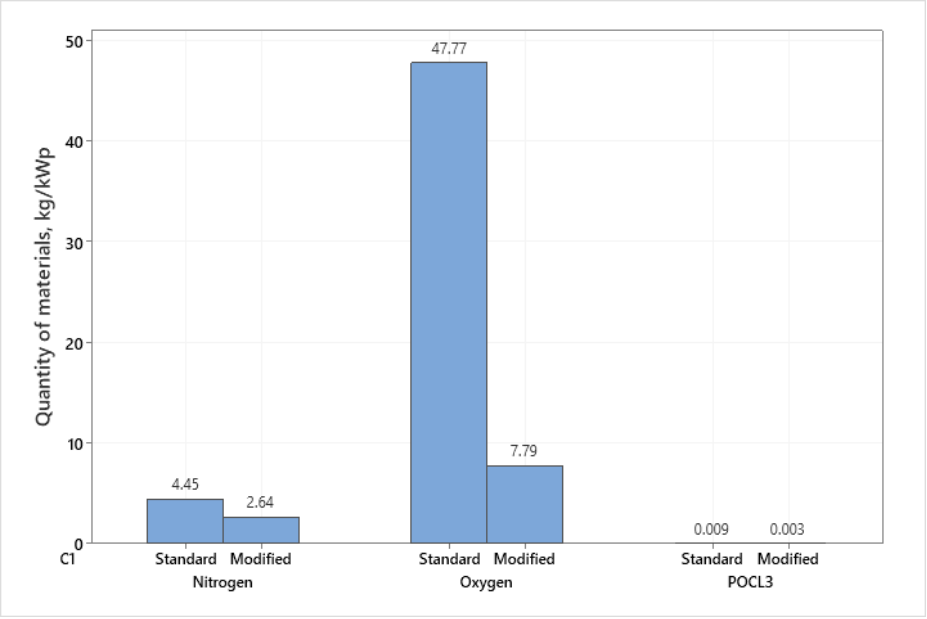

Figure 68. Difference between standard and modified emitter formation production process recipes

The consumption of Nitrogen, Oxygen and $POCL_3$ was reduced by 41%, 84% and 71%, accordingly, if calculating in kg/kWp units.

It can be concluded that these positive results (the efficiency gain and material savings with the modified process) have confirmed the theory that with the optimized in-situ grown SiO_2, PSG layer removal is not needed for solar cells; therefore, the PSG cleaning step can be eliminated from the manufacturing flow of Al-BSF solar cells thus allowing further savings of about 0.0006 l/kWp of HF, 1.45 l/kWp of DI water, 3.5% consumption of special gases (silane and ammonia) and electrical energy. The consumption of electricity was calculated based on the information provided by the *Soli Tek R&D Company*.

Table 12. Comparison between electrical energy consumption of standard and modified processes

Process step	Standard	Modified	Unit
Saw damage etch & Texture	11.60	11.60	kWh/kWp
Emitter formation	11.47	11.47	
Chemical Edge Isolation	4.38	4.38	

Phosphorous Glass Cleaning	5.28	0.00	
Antireflective layer coating	19.33	19.33	
Metallization (printing)	12.37	12.37	
Metallization (drying and firing)	5.15	5.15	
Technical exhaust	10.74	10.74	
Total	**80.33**	**75.05**	

As given in Table 12, the total consumption for the standard process technology is 80.33 kWh/kWp. With the modifications implemented while using the material flow dematerialization method (the process of elimination of PSG), the demand is reduced down to 75.05 kWh/kWp, which is about 7% of savings on energy.

To the best of the author's knowledge, a similar experiment has not been performed by other research groups at the industrial solar cell production level at the time of writing this thesis. Therefore, it can be stated that new results have been generated which can be used as a reference for future experimental work in this field.

3.3 Assessment of the environmental impact reduction potential

As discussed above in Chapter 2.5, LCA analysis and additional two basic KPIs were chosen for the evaluation of the environmental impact: Energy Pay Back Time (EPBT), calculated in months, and Green House Gas (GHG) emissions, calculated in kg CO_2 Eq/kWp.

For a more convenient estimation of EPBT for all the three types of solar cells (standard, modified process and recycled Si), the same PV production potential equal to 1050 kWh/kWp was assumed. The data of electricity consumption for cell production was taken from Table 8 and was 747.42, 742.14 and 134.98 kWh/kWp, respectively. Based on the experiments that were performed in this study, it was estimated that about 212 kWh/kg of electrical energy in case of silicon recycling and another 5 kWh/kWp could be saved in the solar cell production when the modified diffusion process is used.

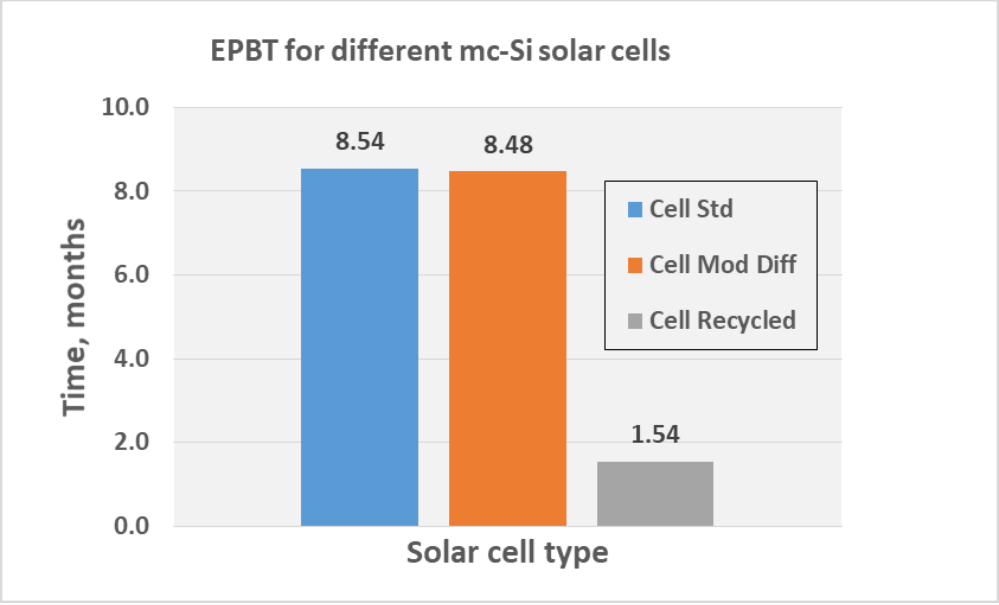

Figure 69. Energy payback time as calculated for 1 kWp of standard mc-Si cell technology, modified processes and for solar cells made by using recycled silicon

The combined results show that a significant reduction of EPBT can be achieved when using recycled silicon as the feedstock for silicon ingot and wafer production comparing to the standard case: 1.54 months instead of 8.54 months, which is a period shorter by 82%. Only 1% shorter EPBT period was achieved when comparing the standard and modified process solar cells (Figure 69).

GHG evaluation was performed by the *ILCD 2011 Midpoint+* method, and the results are given in Figure 70.

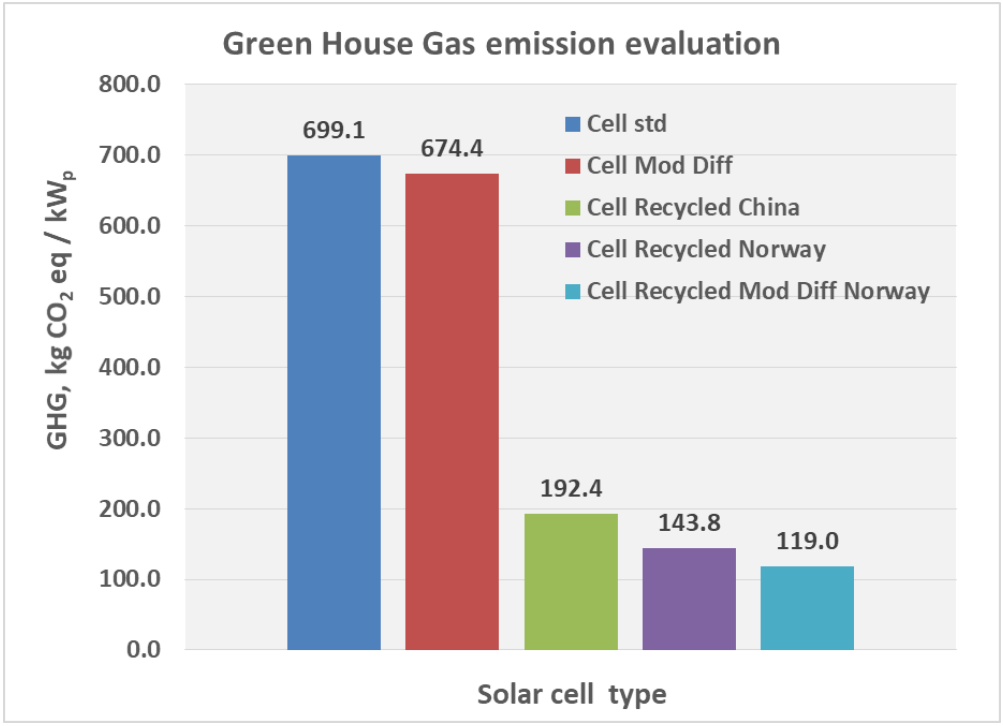

Figure 70. Evaluation results of climate change impact for three types of solar cell production processes: standard, modified diffusion, recycled Si (including Norwegian and Chinese energy mixes)

The process modification (marked as 'Cell Mod Diff') experiment resulted in about 4% lower carbon footprint (674.4 kg CO_2 eq/kW_p) comparing to the standard ('Cell std') case – 699.1 kg CO_2 eq/kW_p (Figure 70). However, when silicon feedstock manufactured from broken clean wafers is used in the solar cell production, the reduction of the GHG parameter becomes much more evident: 72% (Chinese energy mix) and 79% (Norwegian energy mix) lower carbon emission levels for the same functional unit were calculated. That corresponds to 192.4 and 143.8 kg CO_2 eq/kW_p, accordingly. A theoretical combined case (recycling + process modification) could potentially allow reaching a carbon footprint level even below 120 kg CO_2 eq/kW_p level.

The *ILCD 2011 Midpoint+ LCA Impact* assessment method allows evaluating whichever of the sixteen categories has the highest impact by yielding normalized results.

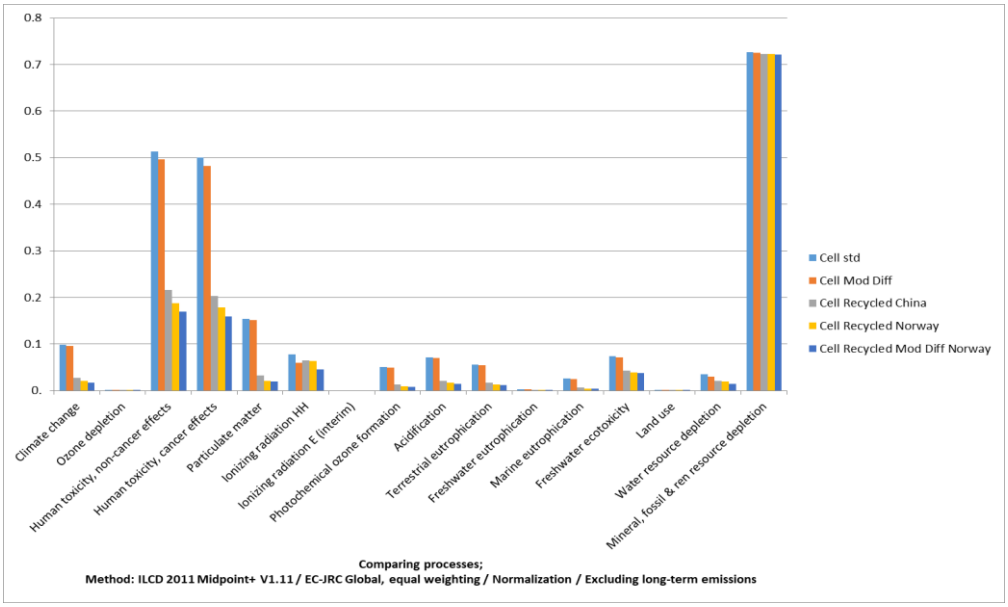

Figure 71. Comparison of characterization factors for several solar cell types using ILCD *2011 Midpoint+* method

The results in Figure 71 show that the biggest impact is in the categories of Human toxicity (cancer and non-cancer effects) and mineral, fossil & renewable resource depletion. On the other hand, it is important to determine other categories which have the biggest impact reduction for every type of the solar cell.

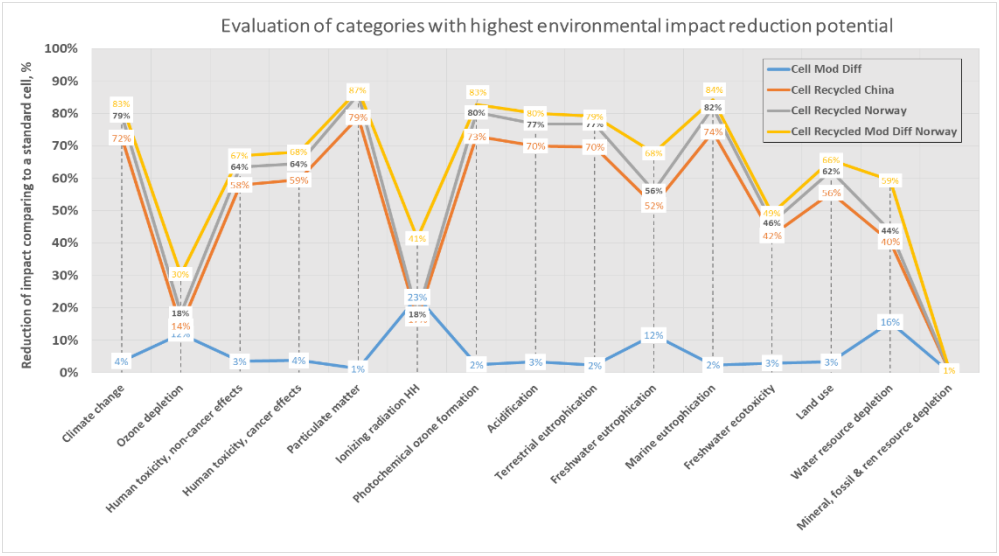

Figure 72. Evaluation of factors with highest environmental impact reduction potential for every type of solar cell

Following the blue line in Figure 72 which represents a solar cell with the modified diffusion process, it can be seen that the highest reduction was achieved for Ionizing radiation (23%), water resource depletion (16%), fresh water eutrophication and ozone depletion (12% for either) categories. For recycled solar cells, more than 70% reduction was achieved for several categories including the climate change, particulate matter, photochemical ozone formation, marine eutrophication and a few others. Clearly, the recycling and reuse of silicon has the most significant potential in an attempt to reduce the environmental impact in all the categories. It is of interest to see that, even with the assumption that silicon is recycled in China, the results are only slightly worse when all the recycling activities take part in Norway.

ReCiPe 2016 Endpoint H calculations (Figure 73) show that the human health category has both the highest impact and the highest reduction potential when such innovations as process modifications and recycling are implemented in the production of c-Si solar cells.

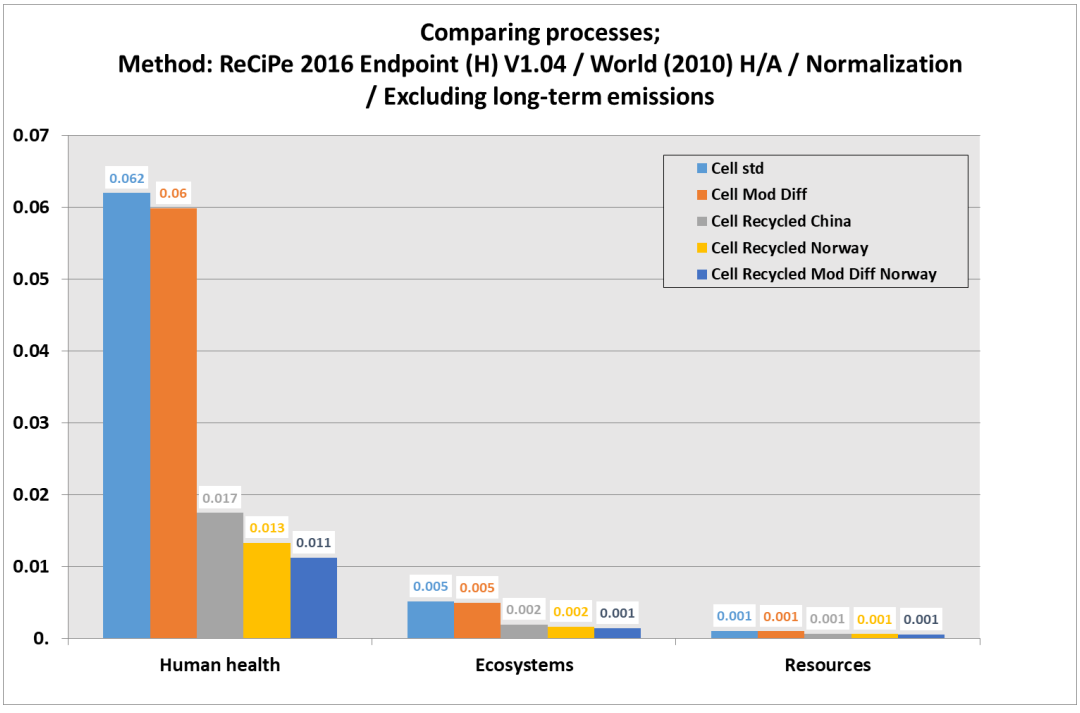

Figure 73. Results of normalized LCIA using *ReCiPe 2016 Endpoint (H)* method

It results in the reduction of the impact by 72–82% in the human health, 62–72% in the ecosystem and 36–46% in the resources categories.

3.4 Evaluation of cost savings

In order to perform analysis of cost savings related to the experimental results of this research, it is important to take a look into the distributed costs of Al-BSF solar cell manufacturing (Figure 74) first. Due to confidentiality requirements, the costs of each component in Eur/Wp unit had to be recalculated into percentages. Even though this is not the ideal situation, but it still represents the real picture and the distribution of cost elements. It can be seen that silicon wafer is responsible for about 47% of the total cell costs. The second major component is process consumables (16%), followed by equipment depreciation, personnel and operating costs. The cost of electricity is responsible for about 4% of cell manufacturing costs.

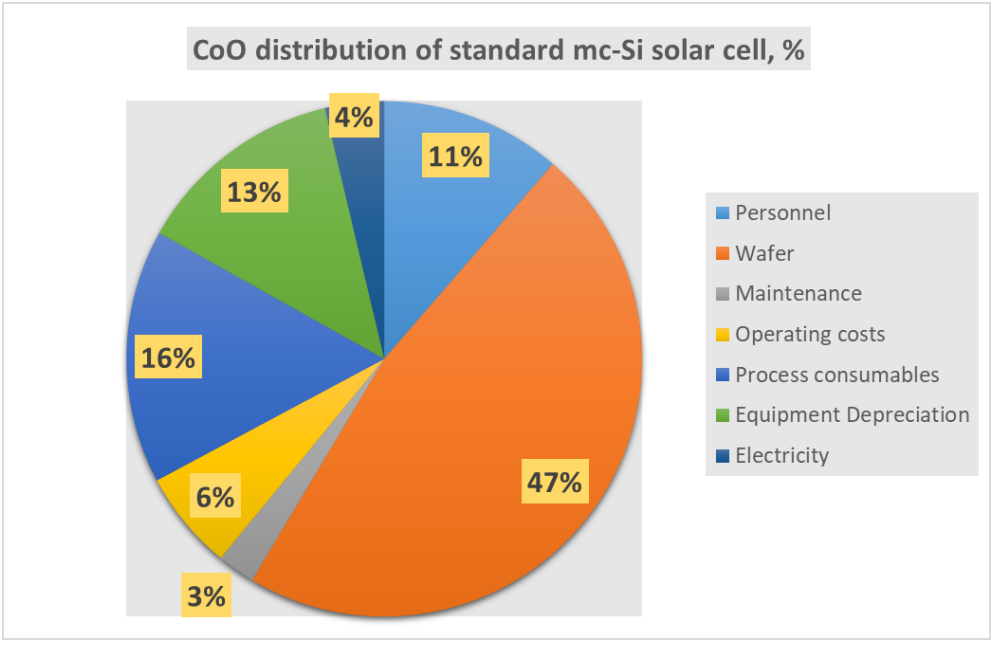

Figure 74. Cost of Ownership distribution of Al-BSF mc-Si solar cell manufacturing

Clearly, these numbers reflect the importance of focusing on the optimization of silicon wafer costs and the usage of process consumables during the evaluation process of cost savings related to the results achieved by the technological

experiments which were performed in this thesis.

In Section 3.1, it was presented that only Group A type of silicon wafer production scrap can be successfully reused in the manufacturing of good quality wafers without any additional purification steps. For cost evaluation, several assumptions were made:

- Group A material can deliver 0.7% abs higher cell efficiency comparing to standard silicon wafers.
- Industrial polysilicon, which is the main raw material for wafer production, is completely replaced by feedstock manufactured from Group A production scrap (as-cut and textured broken, non-contaminated wafers).
- The price of polysilicon is responsible for about 30% of the total mc-Si wafer cost, which means that it should be theoretically possible to reduce the wafer price by the same magnitude when using Group A type of material.
- The average industrial price of silicon wafer is 0.45 Eur/pcs (the industrial price in 2017 according to data provided by *Soli Tek R&D*).
- Production losses of Group A wafers are equal to 1.4% (the average combined value for solar cell production factory in year 2016/2017).

Based on these assumptions, the following cost saving calculation results were achieved. Figure 75 gives a comparison of three cases: 'standard' – which is the 'business as usual' case (standard, non-recycled silicon), 'ideal' case – when the cell production would be using entirely 100% recycled and therefore 30% cheaper silicon wafers, and the third case – the 'realistic' case, when only a small part of wafers (equal to 1.4% – the amount of Group A type production scrap) is used in the manufacturing of solar cells from recycled silicon.

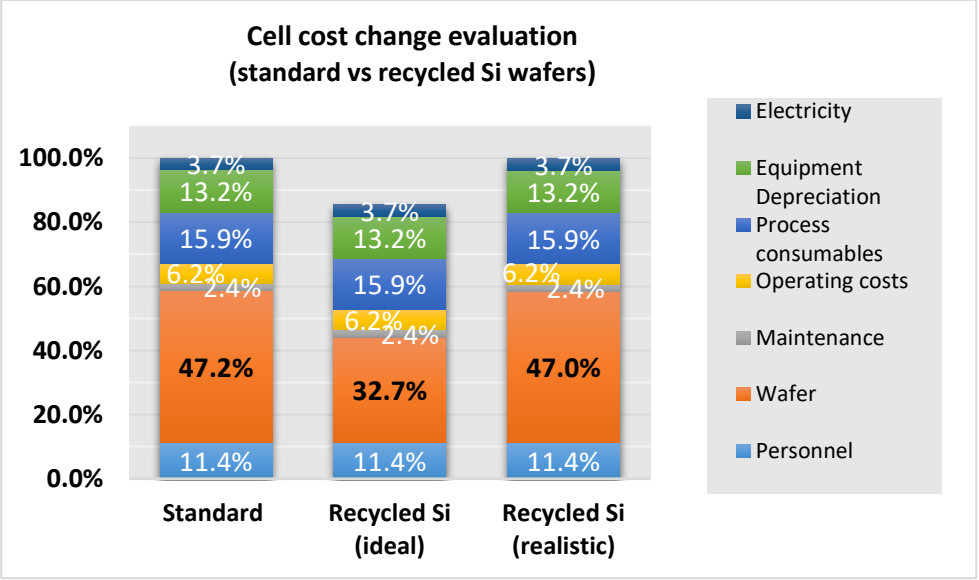

Figure 75. Evaluation of cell production manufacturing costs representing three different approaches: standard, recycled ideal and realistic

The cost saving in the ideal case would be equal to almost 14.5%, while in a more realistic scenario a much smaller 0.2% reduction of the cell price was estimated.

Furthermore, the cost reduction potential was evaluated for the modified process based on the experimental results presented in Chapter 3.2. It was discovered that the consumption of nitrogen, oxygen, POCL3, silane, ammonia and electrical energy can be reduced by 41%, 84%, 71%, 3.5% and 7%, respectively.

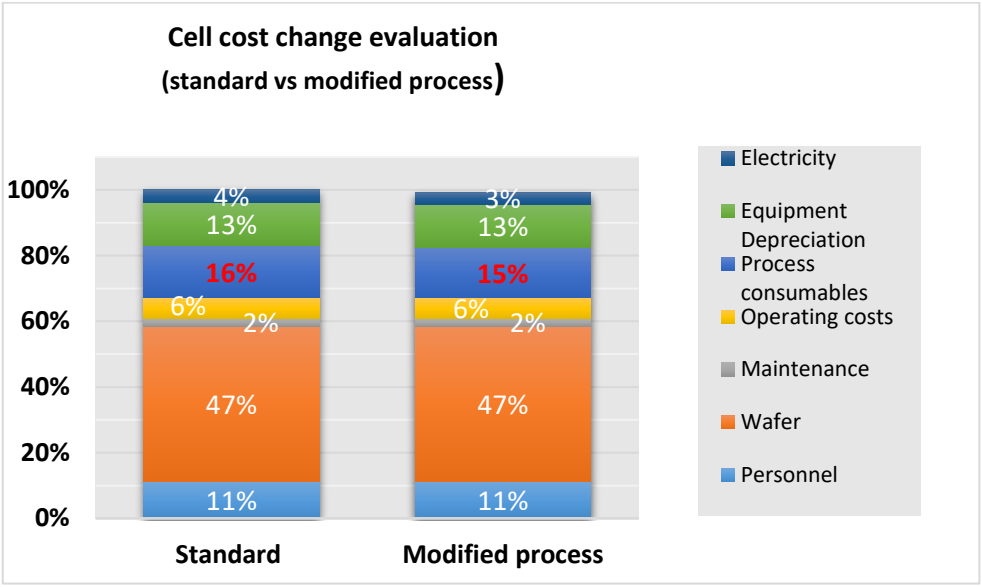

Figure 76. Evaluation of cell production manufacturing costs representing two cases: standard and modified technology using a new diffusion process, eliminated PSG cleaning and shortened antireflective layer coating process steps

The savings in these process steps were included in the calculation of the total cell production costs (Figure 76). However, it was estimated that the impact to the accumulated total cell production cost reduction is around 1%, mainly because such process steps as diffusion and PSG are among the cheapest processes comparing to other solar cell components, specifically, silicon wafer or metallization pastes containing materials, e.g., silver and aluminum.

So far, the costs in terms of the materials price and quantity per manufactured cell have been evaluated. It is equally important to take into account the changes in the solar cell quality after the implementation of the experiments. Figure 77 summarizes what was presented in Sections 3.2 and 3.3 with respect to changes in the solar cell efficiency. Both innovations (recycling and process modifications) resulted in about 0.7% abs gain in the solar cell efficiency.

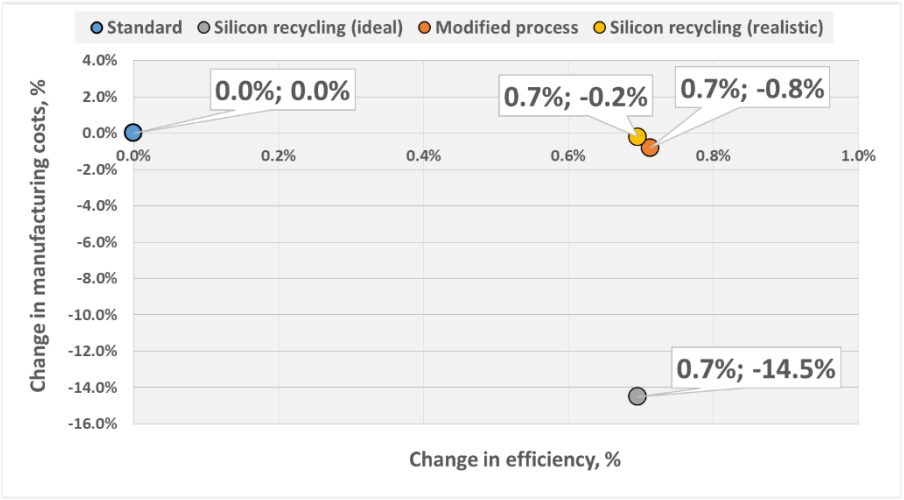

Figure 77. Combined results with respect to impact on costs and efficiency – the main electrical parameter determining the quality of PV devices

In the case when the ideal model of silicon recycling and reuse in production could be applied, it could lead to 14.5% cheaper and 0.7% more powerful solar cells. As the final step in the economic evaluation, simple theoretical modeling of how the reduction in costs and the increase in the solar cell efficiency change the financial results (the yearly revenue) of a small scale (80 MW maximum capacity) c-Si solar cell manufacturing facility. It was assumed that the selling price is 0.25 Eur/Wp, the manufacturing costs of standard cells are 0.245 Eur/Wp, and the sales margin for other solar cell categories (recycled ideal, recycled realistic and modified process) varies according to the results presented in Figure 77.

Table 13. Theoretical modeling of experimental result impact on the financial income of a solar cell manufacturing company

	A. CoO in Eur/Wp	**B. Yearly capacity, MW**	**C. Price margin, Eur/Wp. (0.25-A)**	**Estimation of profit, Eur. (C*B)**	**Profit difference (vs. standard), %**
Standard	0.245	80.00	0.005	368 000.00 €	-
Silicon recycling (ideal)	0.210	80.00	0.040	3 200 000.00 €	870%
Silicon recycling (realistic)	0.245	80.00	0.005	408 000.00 €	11%
Modified process	0.243	80.00	0.007	560 000.00 €	52%

The solar cell market has been known to be a ‘single digit margin’ industry; therefore, even a slight reduction in the manufacturing costs or a small increase in the cell efficiency results in highly noticeable changes in the incomes from sales activities (Table 13). The process modifications applied and demonstrated in this thesis have the potential to increase the profit of companies by up to 52%, the silicon recycling (realistic) approach – by up to 11%, and silicon recycling (the ideal scenario) – almost 9 times. Despite the fact that, in practice, only a small fraction of silicon could be reused, this still indicates that both selected approaches could allow companies to benefit from both the environmental and commercial points of view.

4 CONCLUSIONS

1. It has been discovered that as much as 90% of the total solar energy market (which in year 2019 exceeded the 600 GWp threshold) consists of solutions based on the crystalline silicon technology. Moreover, in sunny regions (such as the Middle East), electricity generated from the sun has already become the cheapest source of energy. Such rapid developments and expansion of the photovoltaic industry also means that the society has already begun to face environmental problems due to the amount of EoL photovoltaic device waste which will reach more than 1 million tons in total by 2030. There are three main possible ways to tackle the EoL waste challenge: reduction of raw materials and energy consumption, efficient treatment of waste in order to recover and reuse raw materials, and development of new products based on the principles of the circular economy.

2. Silicon wafer production has been identified as a major contributor of GHG emissions which is responsible for 70% of emissions at the manufacturing stage of c-Si solar cells and modules. Such a high number clearly indicates that silicon feedstock preparation and ingot casting steps have the biggest potential of environmental impact reduction in the manufacturing chain of PV devices. It has been reported that the production of silicon feedstock is responsible for approximately 212 kWh/kg of electricity consumption. Three leading EOL treatment methods have been identified as the most promising for silicon-based module recycling: thermal (combustion including pyrolysis), mechanical (scraping non-glass layers, cutting the encapsulation layer, crushing/grinding and scraping glass) and chemical (solvent treatment including ultrasound).

3. Two experimental methods have been chosen for testing the optimization of PV equipment environmental impact at the manufacturing stage:

- Recycling of broken solar cells and reuse of different quality recycled silicon as the feedstock for solar cell manufacturing. Experimental results have shown that

uncontaminated (broken wafers collected before and after the texturing process step SCW have good potential to be reused as the feedstock for silicon wafer production without any substantial degradation in material quality. However, fully processed, therefore, contaminated SCW is not suitable as a feedstock material due to quality related issues as shown by the lifetime and LBIC measurements. This type of SCW needs additional purification steps which have a limited potential to be used in the real life because of additional costs being involved.

- The process modification method allows reducing the consumption of materials in the solar cell production and making it shorter by eliminating one of the chemical process steps – phosphorous glass cleaning.

4. It has been demonstrated that the proposed methods (SCW recycling and diffusion process modifications) offer good potential to reduce the negative environmental impact and high manufacturing costs of c-Si solar cell production without the loss in the product quality. Both methods can be implemented on the industrial level and are an economically attractive solution as well.

- The highest negative environmental impact reduction (of more than 70%) has been achieved for the categories including climate change, particulate matter, photochemical ozone formation, marine eutrophication and a few other aspects.
- When silicon recycling and reuse in the mc-Si solar cell production chain is implemented, it can reduce GHG emissions (measured in kg CO_2 eq/kWp) by up to 79% comparing to the standard mc-Si solar cells manufacturing process.
- The diffusion process modification method offers the potential to reduce GHG emissions (measured in kg CO_2 eq/kWp) by 4% comparing to the standard mc-Si solar cells which are processed by using the standard emitter diffusion process recipe.
- EPBT for solar cells made from recycled silicon has potential to be reduced by 82%, whereas, for the cells manufactured by using the modified diffusion process – by 1% comparing to the standard mc-Si solar cells.
- A slight increase in the solar cell efficiency (≈ 0.12% abs when comparing Group A and Laboratory reference groups from the list in Table 6) has been demonstrated in pilot production by using recycled silicon. Group A solar cells had a lower average efficiency comparing to the industrial reference material, which indicates that there is potential for further improvements of the recycled silicon material.
- For the process modification case, a slight increase of efficiency by 0.12% has also been demonstrated, which indicates that a new recipe with in-situ grown oxide is working as expected even with a significant reduction of material consumption.
- The manufacturing costs of solar cells can be reduced by up to 14.5% when the ideal silicon recycling method (100% recycled and therefore 30% cheaper silicon

wafers) is applied in the solar cell manufacturing. The process modification method offers the potential to lower the manufacturing costs by a further 1%.

5 Acknowledgments

Experimental work was performed in cooperation with the European solar cell manufacturer *Soli Tek R&D* and was partially funded by EU H2020 projects *CABRISS* (Grant agreement No. 641972), *ECO SOLAR* (Grant agreement No. 679692) and *CIRCUSOL* (Grant agreement No. 776680).

6 References

[1] H. Wirth, “Recent Facts about Photovoltaics in Germany,” 2021.

[2] M. J. (Mariska) de Wild-Scholten, “Energy payback time and carbon footprint of commercial photovoltaic systems,” *Sol. Energy Mater. Sol. Cells*, vol. 119, no. December 2013, pp. 296–305, 2013, doi: 10.1016/j.solmat.2013.08.037.

[3] IRENA and IEA-PVPS, “End of Life Management Solar Photovoltaic Panels,” 2016.

[4] Vasilis Fthenakis, H. C. Kim, R. Frischknecht, M. Raugei, P. Sinha, and M. Stuck, “Life Cycle Inventories and Life Cycle Assessment of Photovoltaic Systems, International Energy Agency (IEA) PVPS Task 12, Report T12-04:2015.,” 2011.

[5] L. McEvoy, A. J., Markvart, Tom, Castaner and T. M. Augustin McEvoy, L. Castaner, *Solar Cells: Materials, Manufacture and Operation*. Academic Press, 2013.

[6] M. a Green, “Third generation photovoltaics: comparative evaluation of advanced solar conversion options,” in *Conference Record of the Twenty-Ninth IEEE Photovoltaic Specialists Conference*, 2002, pp. 1330–1334, doi: 10.1109/PVSC.2002.1190855.

[7] Fraunhofer-ISE, “Photovoltaics report,” Freiburg, 2020.

[8] B. S. Xakalashe and M. Tangstad, “Silicon processing : from quartz to crystalline silicon solar cells,” *Chem. Technol.*, no. April, pp. 83–100, 2012.

[9] M. A. Green, “Silicon solar cells : state of the art Subject Areas : Author for correspondence :,” *Philos. Trans. R. Soc. A Math. Phys. Eng. Sci.*, vol. 371, no. 1996, 2013, doi: http://dx.doi.org/10.1098/rsta.2011.0413.

[10] G. Bye and B. Ceccaroli, “Solar grade silicon: Technology status and industrial trends,” *Sol. Energy Mater. Sol. Cells*, vol. 130, pp. 634–646, 2014, doi: 10.1016/j.solmat.2014.06.019.

[11] VDMA, “International Technology Roadmap for Photovoltaic (ITRPV) 7th Eedition,” 2016.

[12] VDMA, “International Technology Roadmap for Photovoltaic (ITRPV) 11th edition,” 2020.

[13] H. Seigneur *et al.*, “Manufacturing metrology for c-Si photovoltaic module reliability and durability , Part I : Feedstock , crystallization and wafering,” *Renew. Sustain. Energy Rev.*, vol. 59, pp. 84–106, 2016, doi: 10.1016/j.rser.2015.12.343.

[14] Z. Zhang, Z. Xiong, H. Ye, S. Fu, Z. Feng, and P. J. Verlinden, “Two Methods for High Performance Mc-Si Ingot Growth,” in *31st European Photovoltaic Solar Energy Conference and Exhibition*, 2015, pp. 304–306, doi: 10.4229/EUPVSEC20152015-2BO.2.3.

[15] “Eco-Solar Factory: 40%plus Eco-Efficiency Gains in the Photovoltaic Value Chain with Minimised Resource and Energy Consumption by Closed Loop Systems.” [Online]. Available: http://ecosolar.eu.com/.
[16] VDMA, “International Technology Roadmap for Photovoltaic (ITRPV) 8th Edition,” 2017.
[17] H. Wu, “Wire sawing technology : A state-of-the-art review,” *Precis. Eng.*, vol. 43, pp. 1–9, 2016, doi: 10.1016/j.precisioneng.2015.08.008.
[18] A. Kumar and S. N. Melkote, “Diamond Wire Sawing of Solar Silicon Wafers: A Sustainable Manufacturing Alternative to Loose Abrasive Slurry Sawing,” *Procedia Manuf.*, vol. 21, no. 2017, pp. 549–566, 2018, doi: 10.1016/j.promfg.2018.02.156.
[19] M. De Sousa, A. Vardelle, G. Mariaux, M. Vardelle, U. Michon, and V. Beudin, “Use of a thermal plasma process to recycle silicon kerf loss to solar-grade silicon feedstock,” *Sep. Purif. Technol.*, vol. 161, pp. 187–192, 2016, doi: 10.1016/j.seppur.2016.02.005.
[20] N. P. Wagner, A. Tron, J. R. Tolchard, G. Noia, and M. P. Bellmann, “Silicon anodes for lithium-ion batteries produced from recovered kerf powders,” *J. Power Sources*, vol. 414, no. September 2018, pp. 486–494, 2019, doi: 10.1016/j.jpowsour.2019.01.035.
[21] “NexWafe GmbH - Growing Power.” [Online]. Available: https://www.nexwafe.com/#about-us.
[22] M. A. Green, “Forty Years of Photovoltaic Research at UNSW,” *J. Proc. R. Soc. New South Wales*, vol. 148, pp. 2–14, 2015.
[23] J. Denafas *et al.*, “Implementation and Optimization of an Industrial Mc-Si PERC Process for Mass Production,” in *31st European Photovoltaic Solar Energy Conference and Exhibition*, 2015, doi: 10.4229/EUPVSEC20152015-2DO.16.2.
[24] MicroChemicals GmbH, “Wet-Chemical Etching of Silicon and SiO2,” 2013. [Online]. Available: www.microchemicals.com/downloads/application_notes.html%0Ahttps://www.microchemicals.eu/technical_information/silicon_etching.pdf.
[25] K. O. Davis *et al.*, “Manufacturing metrology for c-Si module reliability and durability Part II: Cell manufacturing,” *Renew. Sustain. Energy Rev.*, vol. 59, pp. 225–252, 2016, doi: 10.1016/j.rser.2015.12.217.
[26] “www.pveducation.org.” [Online]. Available: https://www.pveducation.org/.
[27] E. J. Schneller *et al.*, “Manufacturing metrology for c-Si module reliability and durability Part III : Module manufacturing,” *Renew. Sustain. Energy Rev.*, vol. 59, pp. 992–1016, 2016, doi: 10.1016/j.rser.2015.12.215.
[28] E. Bellini, “World now has 583.5 GW of operational PV,” 2020. [Online]. Available: https://www.pv-magazine.com/2020/04/06/world-now-has-583-5-gw-of-operational-pv/.
[29] W. Hemetsberger, M. Schmela, and G. Chianetta, “Global Market Outlook For Solar Power / 2020 - 2024,” 2020.
[30] Europos Komisija, “Komisijos komunikatas Europos Parlamentui, Tarybai,

Europos Ekonomikos ir Socialinių Reikalų Komitetui ir Regionų Komitetui. 2030 m. klimato politikos tikslo įgyvendinimo planas.” 2020.
[31] “PV Cycle.” [Online]. Available: http://www.pvcycle.org/homepage/.
[32] “The RoHS Directive.” [Online]. Available: https://ec.europa.eu/environment/waste/rohs_eee/index_en.htm.
[33] E.A. Alsema and M. J. de Wild-Scholten, “Reduction of the environmental impacts in crystalline silicon module manufacturing,” in *22nd European Photovoltaic Solar Energy Conference*, 2007.
[34] M. P. Bellmann, G. Stokkan, A. Ciftja, J. Denafas, and T. Kaden, “Crystallization of multicrystalline silicon from reusable silicon nitride crucibles: Material properties and solar cell efficiency,” *J. Cryst. Growth*, vol. 504, no. July, pp. 51–55, 2018, doi: 10.1016/j.jcrysgro.2018.09.026.
[35] W. Nam, Y. Hahn, and S. Baik, “Local optimization of graphite heater to save a power consumption of Czochralski Si ingot grower for PV application,” *Energy Procedia*, vol. 124, pp. 767–776, 2017, doi: 10.1016/j.egypro.2017.09.083.
[36] “Soli Tek - Leadership Through Innovation.” [Online]. Available: https://www.solitek.eu/en/company.
[37] V. C. and B. D. F.Madon, O. Nichiporuk, R. Einhaus, L. Crampette, B. Semmache, L. Valette, “NICE Module Technology Using Industrial n-Type Solar Cells without Front and Rear Busbars,” in *28th European Photovoltaic Solar Energy Conference and Exhibition*, 2013, pp. 3149–3153, doi: 10.4229/28thEUPVSEC2013-4AV.4.43.
[38] European Parliament, “Directive 2012/19/EU of the European Parliament and of the Council of 4 July 2012 on waste electrical and electronic equipment (WEEE) (recast),” *Off. J. Eur. Union*, no. June, pp. 1009–1017, 2012.
[39] A. T. Vekony, “The Opportunities of Solar Panel Recycling.” [Online]. Available: https://www.greenmatch.co.uk/blog/2017/10/the-opportunities-of-solar-panel-recycling.
[40] “NPC incorporated | Global leader of solar module manufacturing equipment.” [Online]. Available: https://www.npcgroup.net/eng/.
[41] “h.a.l.m. elektronik gmbh.” [Online]. Available: http://www.halm.de/.
[42] K. Komoto and J. S. Lee, “End-of-Life Management of Photovoltaic Panels: Trends in PV Module Recycling Technologies,” 2018.
[43] J. Tao and S. Yu, “Review on feasible recycling pathways and technologies of solar photovoltaic modules,” *Sol. Energy Mater. Sol. Cells*, vol. 141, pp. 108–124, 2015, doi: 10.1016/j.solmat.2015.05.005.
[44] C. Latunussa, L. Mancini, G. Blengini, F. Ardente, and D. Pennington, *Analysis of Material Recovery from Silicon Photovoltaic Panels*, no. March. 2016.
[45] W. Palitzsch, A. Killenberg, P. Schonherr, and U. Loser, “Photovoltaic Recycling with the help of Water and Light - It does not get greener,” *2018 IEEE 7th World Conf. Photovolt. Energy Conversion, WCPEC 2018 - A Jt.*

Conf. 45th IEEE PVSC, 28th PVSEC 34th EU PVSEC, pp. 2465–2466, 2018, doi: 10.1109/PVSC.2018.8548095.
[46] E. W. K. Wambach, S. Schlenker, A. Müller, M. Klenk, S. Wallat, R. Kopecek, "The second life of a 300 kW PV generator manufactured with recycled wafers from the oldest german pv power plant," in *21st European Photovoltaic Solar Energy Conference.*, 2006.
[47] R. Bendikiene *et al.*, "Utilization of Industrial Solar Cells' Scrap as the Base Material to Form Coatings," *Waste and Biomass Valorization*, vol. 12, no. 5, pp. 2757–2767, 2020, doi: 10.1007/s12649-020-01153-8.
[48] G. A. Heath *et al.*, "Research and development priorities for silicon photovoltaic module recycling to support a circular economy," *Nat. Energy*, vol. 5, no. 5, pp. 502–510, 2020.
[49] S. Yousef, M. Tatariants, J. Denafas, V. Makarevicius, S. I. Lukošiūtė, and J. Kruopienė, "Sustainable industrial technology for recovery of Al nanocrystals, Si micro-particles and Ag from solar cell wafer production waste," *Sol. Energy Mater. Sol. Cells*, vol. 191, no. December 2018, pp. 493–501, 2019, doi: 10.1016/j.solmat.2018.12.008.
[50] K. Medkova and B. Fifield, "Circular Design - Design for Circular Economy," *Lahti Cleantech Annu. Rev. 2016*, no. February, pp. 32–47, 2016.
[51] "CIRCUSOL - Circular business models for the solar power industry." [Online]. Available: https://www.circusol.eu/en.
[52] "Product Environmental Footprint Category Rules (PEFCR) Photovoltaic modules used in photovoltaic power systems for electricity generation," no. December. European Comission, 2020.
[53] M. Syvertsen, M. Juel, and M. P. Bellmann, "Effect of Better Insulation in a CRYSTALOX DS 250 Furnace During Melting and Solidification on the Furnace Operation," in *25th European Photovoltaic Solar Energy Conference and Exhibition / 5th World Conference on Photovoltaic Energy Conversion*, 2010, pp. 1543–1545, doi: 10.4229/25thEUPVSEC2010-2CV.1.21.
[54] F. Buchholz *et al.*, "Low Recombination Emitter Profile with In-Situ Oxide Passivation for Multi-Crystalline Solar Cells," in *33rd European Photovoltaic Solar Energy Conference and Exhibition*, 2017, pp. 963–966, doi: 10.4229/EUPVSEC20172017-2CV.2.77.
[55] S. Werner, S. Mourad, W. Hasan, and A. Wolf, "Structure and composition of phosphosilicate glass systems formed by POCl3 diffusion," *Energy Procedia*, vol. 124, pp. 455–463, 2017, doi: 10.1016/j.egypro.2017.09.280.
[56] A. Dastgheib-Shirazi, M. Steyer, G. Micard, H. Wagner, P. P. Altermatt, and G. Hahn, "Relationships between diffusion parameters and phosphorus precipitation during the POCl3 diffusion process," *Energy Procedia*, vol. 38, pp. 254–262, 2013, doi: 10.1016/j.egypro.2013.07.275.
[57] S. Werner, E. Lohmüller, S. Maier, S. Mourad, and Andreas Wolf, "Challenges for lowly-doped phosphorus emitters in silicon solar cells with screen-printed silver contacts," *Energy Procedia*, vol. 124, pp. 936–946,

2017, doi: 10.1016/j.egypro.2017.09.274.
[58] G. Sulyok and J. Summhammer, “Extraction of a photovoltaic cell ’ s double- - diode model parameters from data sheet values,” *Energy Sci. Eng.*, vol. 6, no. 5, pp. 424–436, 2018, doi: 10.1002/ese3.216.
[59] S. W. Glunz and F. Feldmann, “SiO2 surface passivation layers – a key technology for silicon solar cells,” *Sol. Energy Mater. Sol. Cells*, vol. 185, no. April, pp. 260–269, 2018, doi: 10.1016/j.solmat.2018.04.029.
[60] R. A. Sinton, A. Cuevas, and M. Stuckings, “Quasi-steady-state photoconductance, a new method for solar cell material and device characterization,” in *25th IEEE Photovoltaic Specialists Conference*, 1996, pp. 457–460, doi: 10.1109/PVSC.1996.564042.
[61] A. Kaminski, O. Breitenstein, J. P. Boyeaux, P. Rakotoniaina, and A. Laugier, “Light beam induced current and infrared thermography studies of multicrystalline silicon solar cells,” *J. Phys. Condens. Matter*, vol. 16, no. 2, 2004, doi: 10.1088/0953-8984/16/2/002.
[62] S. Bowden, V. Yelundur, and A. Rohatgi, “Implied-Voc and Suns-Voc measurements in multicrystalline solar cells,” *Conf. Rec. IEEE Photovolt. Spec. Conf.*, vol. 3, pp. 371–374, 2002, doi: 10.1109/pvsc.2002.1190536.
[63] “Semilab products - Light Beam Induced current.” [Online]. Available: https://semilab.com/category/products/light-beam-induced-current.
[64] V. D. Mihailetchi, H. Chu, J. Lossen, and R. Kopecek, “Surface Passivation of Boron-Diffused Junctions by a Borosilicate Glass and in Situ Grown Silicon Dioxide Interface Layer,” *IEEE J. Photovoltaics*, vol. 8, no. 2, pp. 435–440, 2018, doi: 10.1109/JPHOTOV.2018.2792422.
[65] “Solar resource maps and GIS data for 200+ countries | Solargis.” [Online]. Available: https://solargis.com/maps-and-gis-data/download.
[66] E. C.-J. R. C.-I. for E. and Sustainability, *The International Reference Life Cycle Data System (ILCD) Handbook*. 2012.
[67] “LCIA: the ReCiPe model.” [Online]. Available: https://www.rivm.nl/en/life-cycle-assessment-lca/recipe.
[68] F. Chigondo, “From Metallurgical-Grade to Solar-Grade Silicon: An Overview,” *Silicon*, vol. 10, no. 3, pp. 789–798, 2018, doi: 10.1007/s12633-016-9532-7.
[69] S. McLeod, “StatisticsBox and Whisker Plot,” 2019. [Online]. Available: https://www.simplypsychology.org/boxplots.html.
[70] “Interpret all statistics for a probability plot with normal fit,” 2020. [Online]. Available: https://support.minitab.com/en-us/minitab-express/1/help-and-how-to/graphs/probability-plot/interpret-the-results/all-statistics/probability-plot-with-normal-fit/.
[71] B. Michl *et al.*, “Excellent average diffusion lengths of 600 μm of N-type multicrystalline silicon wafers after the full solar cell process including boron diffusion,” *Energy Procedia*, vol. 33, no. 0, pp. 41–49, 2013, doi: 10.1016/j.egypro.2013.05.038.
[72] “PV Insights.” [Online]. Available: http://pvinsights.com/.

[73] “SENTECH: Home of thin film measurement.” [Online]. Available: https://www.sentech.com/en/Home__2235/.
[74] “WCT-120 - the standard offline wafer-lifetime tool.” [Online]. Available: https://www.sintoninstruments.com/products/wct-120/.
[75] W. Favre *et al.*, “Coil-to-Sample Distance Influence on Contactless QSSPC Effective Lifetime Measurements : Application to Silicon Wafers Passivated with Thin Amorphous Silicon Layers,” *26th Eur. Photovolt. Sol. Energy Conf. Exhib.*, no. March 2015, pp. 1563–1568, 2011, doi: 10.4229/26thEUPVSEC2011-2BV.2.49.

SL344. 2021-*-*, * leidyb. apsk. l. Tiražas 14 egz. Užsakymas * .
Išleido Kauno technologijos universitetas, K. Donelaičio g. 73, 44249 Kaunas
Spausdino leidyklos „Technologija“ spaustuvė, Studentų g. 54, 51424 Kaunas